CHAPTER IV
RESULTS AND DISCUSSION

4.1 Uncompatibilized PC/PMMA Alloys

4.1.1 Physical properties

4.1.1.1 Rheological properties

The rheological properties have been characterized in term of the Melt Flow Index (MFI) in accordance with ASTM D1238. MFI measurement is used to simplify the flowability of the polymer melt. It is determined by the weight of the melted polymers, in grams, flowing through an orifice at prescribed temperature and load in 10 minutes. The MFI of PC, PMMA and uncompatibilized PC/PMMA alloys were measured at 250°C with 2.16 kg hammer. The increment of PMMA content led the MFI of alloys to increase as shown in Figure 4.1. Due to the stronger bonds between PC, the higher energy was required to move the chains. It can imply that PC has higher thermal resistance than PMMA. Conversely, the polymer chain of PMMA is more sensitive to thermal than PC which makes it flow easier than PC at 250°C.

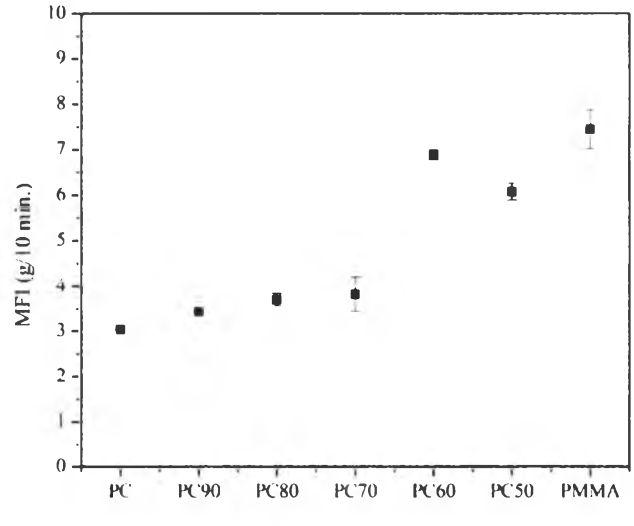

Figure 4.1 Melt Flow Index of PC, PMMA, and uncompatibilized PC/PMMA alloys.

4.1.2 Thermal properties

4.1.2.1 Temperature decomposition characterization

The decomposition temperature (T_d) of polymer can point to its thermal stability which was investigated by TGA. The results suggested that T_d of PC was higher than that of PMMA, in contrast, weight loss percentage of PC was lower than PMMA as given in Figure 4.3. Because the presence of phenyl rings in PC chains formed the intermolecular attraction with other phenyl rings in other PC chains resulting in the higher T_d. Therefore, PC has much higher thermal stability than PMMA at the same operating temperature and also low melt flow rate as mentioned before.

T_d of uncompatibilized PC/PMMA blends was observed between 504.5 °C and 356.5 °C, which belong to PC and PMMA, respectively. As the amount of PMMA increase, T_d of PC/PMMA alloys decreased resulting from PMMA phase. Additionally, PMMA phase can induce the degradation in the blend being the reason that the weight loss percentage of PC/PMMA alloys increased with increasing of PMMA content.

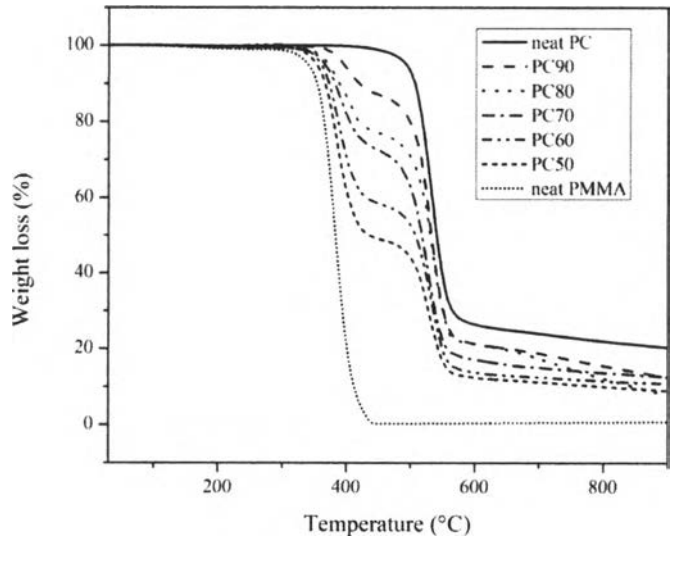

Figure 4.2 TGA plots of PC, PMMA, and uncompatibilized PC/PMMA alloys.

4.1.3 Miscibility

4.1.3.1 Glass transition temperature observation

The glass transition temperature (T_g) of polymers was determined by using DSC. Figure 4.2 shows DSC thermograms at the second heating of PC, PMMA and uncompatibilized PC/PMMA. PC and PMMA exhibit no such peak owing to their glassy nature, which was the basic property of amorphous polymers with the T_g around 139.14 °C and 107.07 °C, respectively. Uncompatibilized PC/PMMA, PC90 and PC80 showed single T_g of each that T_g of PC90 and PC80 slightly decreased comparing with T_g of neat PC. The alloys containing PMMA between 30-50 wt.%, show two distinct T_g and they are shifted inward as shown in Figure 4.3. It may be possible that increase in disperse phase (PMMA), the clearer in T_g of PMMA was observed. The lower T_g of alloys can cause by the PMMA rich phase, on the other hand, the higher T_g of alloys may come from PC rich phase. The shift of T_g of alloys was probable due to some weak interaction between the phenyl rings of PC and carbonyl groups of PMMA.

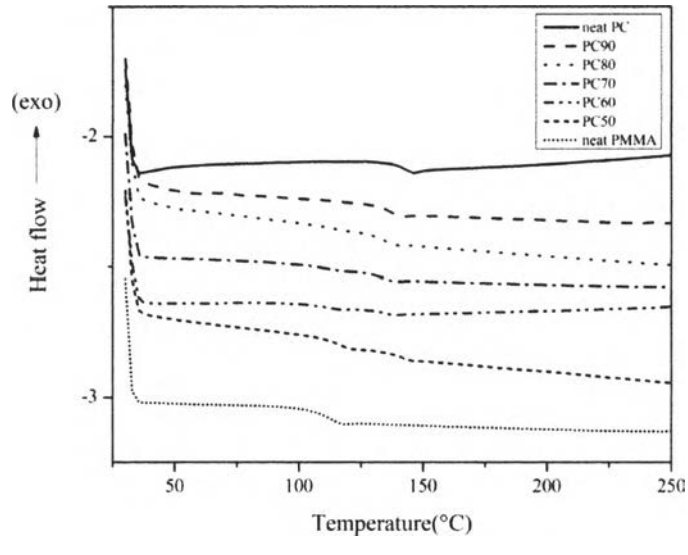

Figure 4.3 DSC plots (second heating) of PC, PMMA, and uncompatibilized PC/PMMA alloys.

DMA is the technique used to measuring stiffness and damping of the material based on mechanical properties change with time, temperature and frequency, then reported as modulus (storage and loss modulus) and tan delta (the ratio of loss to storage modulus). While, DSC measures the differential energy or heat flow between the sample and reference which associated with the transitions of the materials as a function of time and temperature under the controlled atmosphere. These two techniques measure T_g in different process resulting in the possibility of the slight difference in T_g value. T_g in DMA is the peak of tan delta as can be seen in Figure 4.4. Both of neat components and all uncompatibilized PC/PMMA alloys showed single T_g. The T_g from DMA was dissimilar from T_g obtained from DSC, which can detect two distinct T_g at some composition of PC/PMMA alloys. The reason is the low content of minor phase was limited the detection. It is possible due to the entrapment of minor phase in major phase hence T_g shown in the diagram was belonged to the major phase.

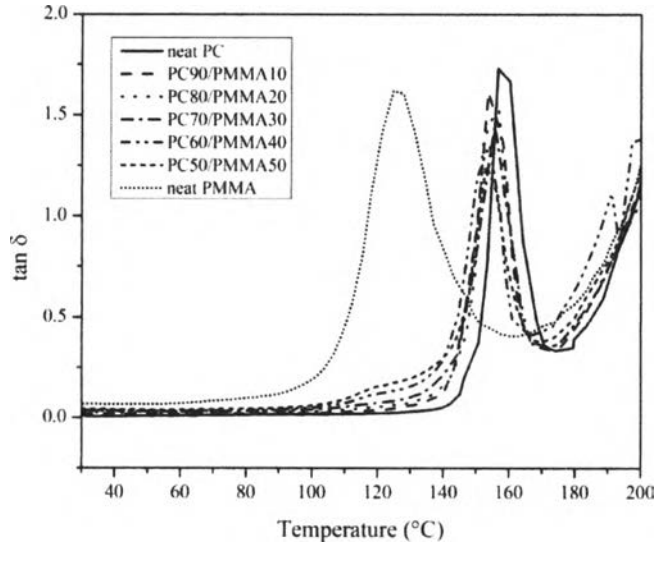

Figure 4.4 DMA plots of PC, PMMA, and uncompatibilized PC/PMMA alloys.

4.1.3.2 Glass transition temperature observation

SEM was conducted to observe the morphology of the impact-fractured surface of the PC/PMMA alloys with and without etching as shown in Figure 4.5. Dimethylacetamide was used as a solvent to etch out PC domain and the surface was immersed in solvent for 3 minutes. All images revealed the phase separation of PC phase and PMMA phase. The PC domains (the etched component) were showed in irregular shape with random dispersion. For the case of PC10, the dispersion was regular because PC was a minor phase. This observation can be concluded that the minor phase was not homogeneously dispersed in the matrix phase. The toughness properties of PC/PMMA blends at all compositions can be confirmed by the unetched images. Although they showed the roughness surface, the shear yielding or shear bands did not appear. It was well known that the shear band could absorb large amount of energy during being impact. Therefore, it can be indicated that PC/PMMA alloys were not ductile materials.

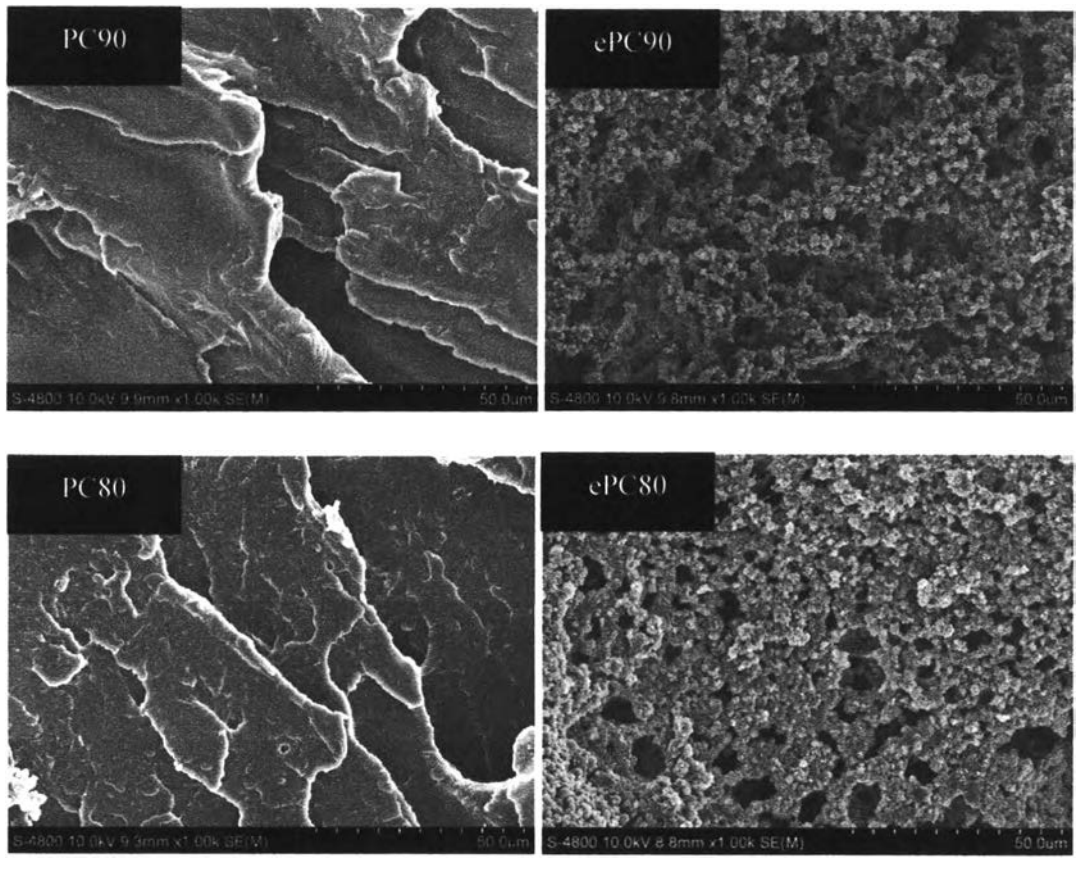

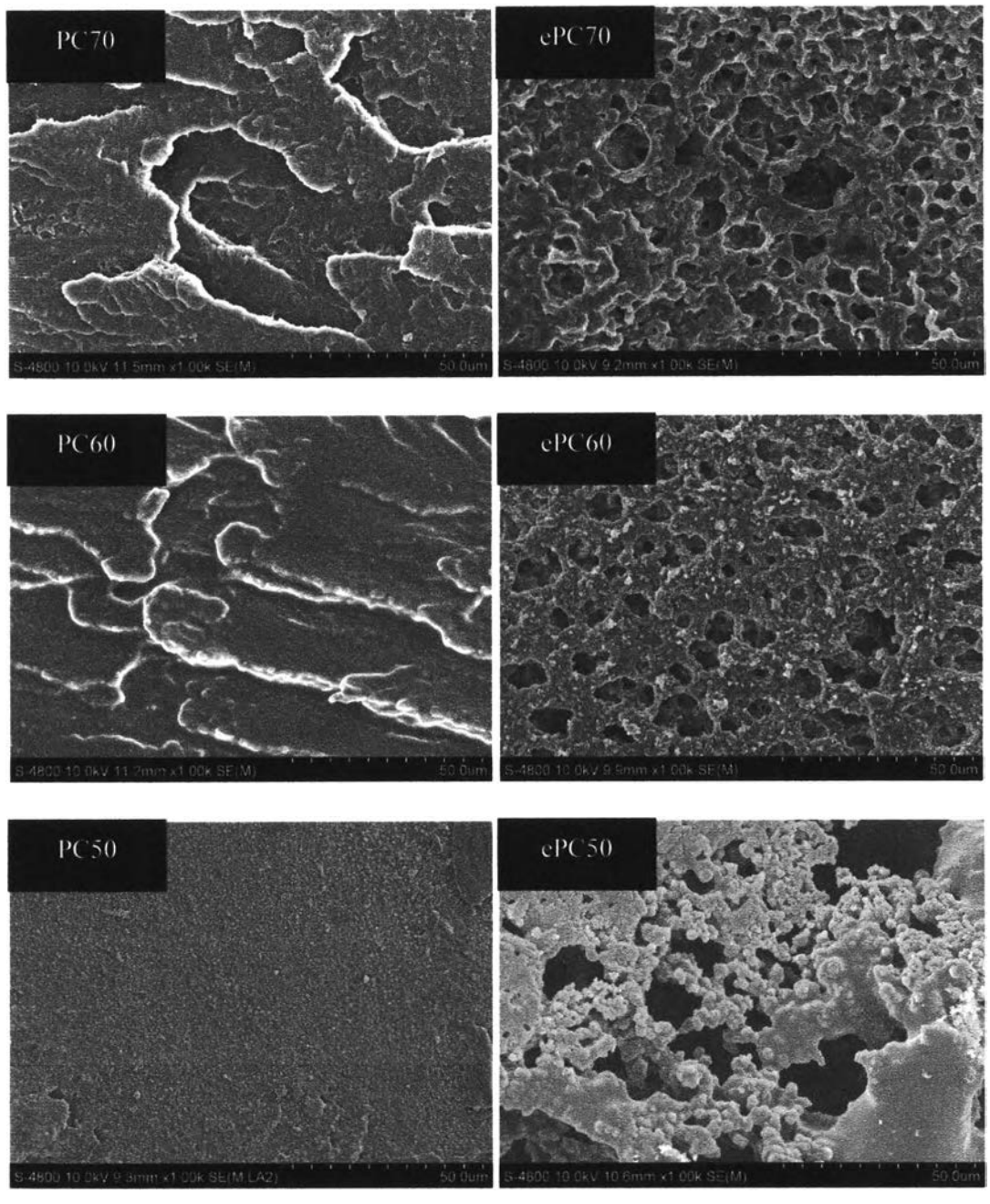

Figure 4.5 SEM micrographs of fractural impact surface of PC90, PC80, PC70, PC60 and PC50 (etching (ePCXX) and no etching (PCXX)).

4.1.4 Mechanical properties

4.1.4.1 Tensile properties

Figure 4.6-4.8 show tensile strength at yield, elongation at yield and young's modulus of PC, PMMA and uncompatibilized PC/PMMA alloys. The tensile strength of uncompatibilized PC/PMMA alloys resembles to linearly increase. It is because the nature of PC and PMMA is strong material and there are some interactions between PC and PMMA as described in DSC discussion resulting in synergism in tensile strength. While the inclination of elongation of alloys diminishes when increase the amount of PMMA. PMMA is stiff and brittle so the higher in PMMA content, the lower in elongation. In the case of young's modulus, the trend, however, is non-linear due to the non-homogeneous PC/PMMA alloys. From these results, it can be noted that blending of PC and PMMA will give the stronger but more brittle materials. The results of tensile strength at yield, elongation at yield and young's modulus of PC, PMMA and uncompatibilized PC/PMMA alloys

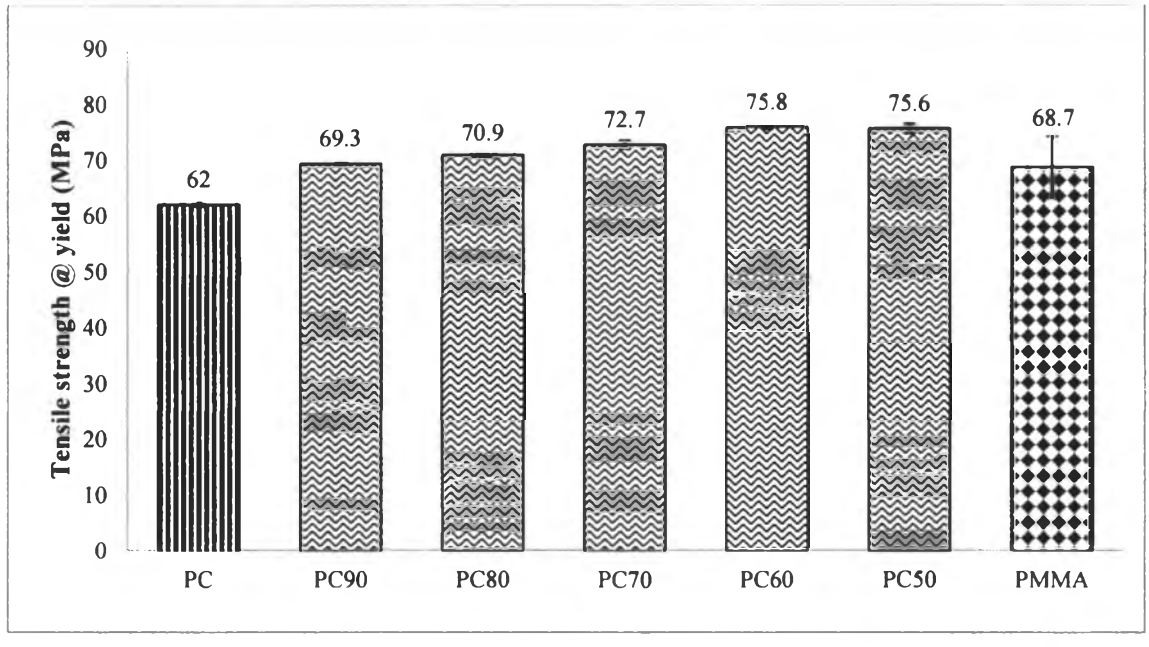

Figure 4.6 Tensile strength at yield of PC, PMMA, and uncompatibilized PC/PMMA alloys.

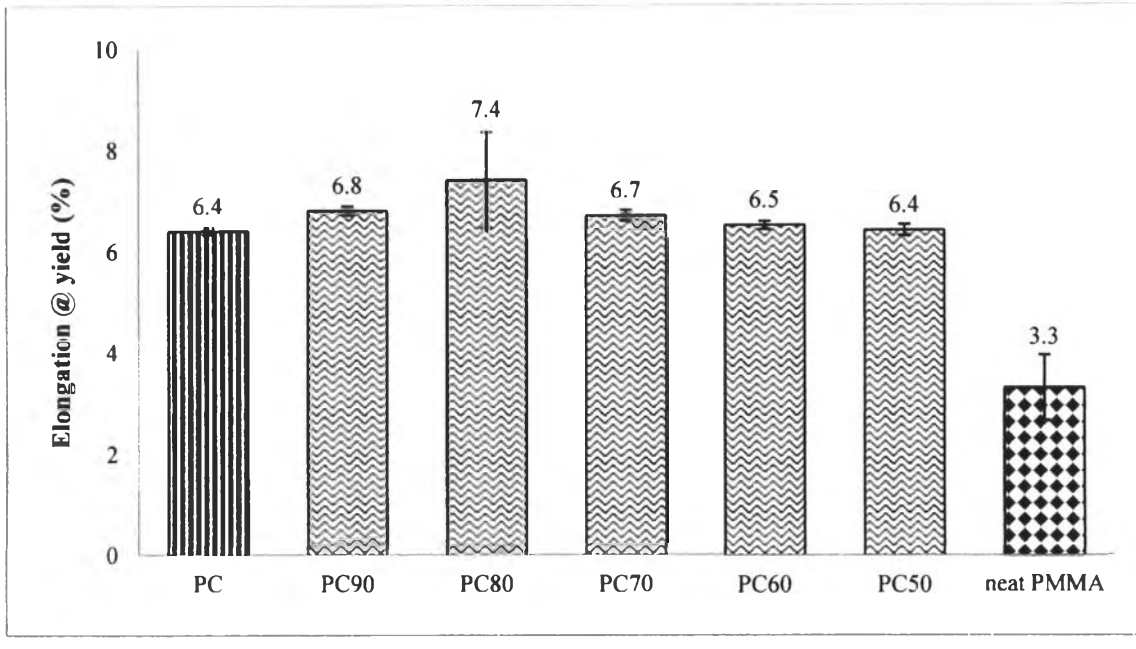

Figure 4.7 Elongation at yield of PC, PMMA, and uncompatibilized PC/PMMA alloys.

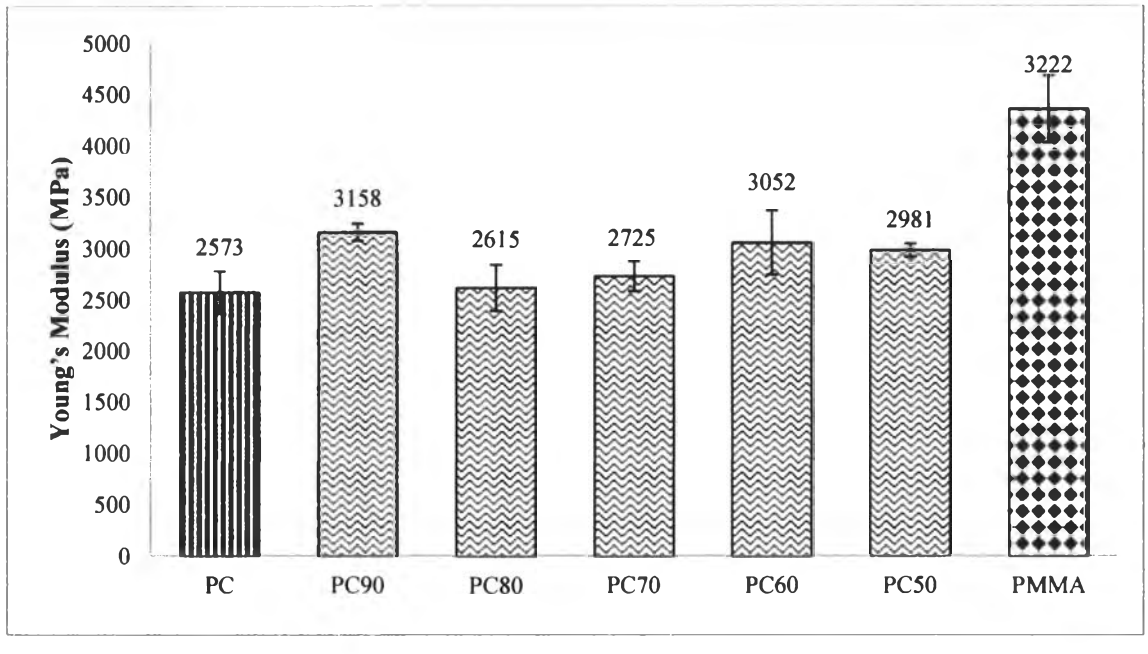

Figure 4.8 Young's modulus of PC, PMMA, and uncompatibilized PC/PMMA alloys.

4.1.4.2 Flexural properties

Figure 4.9-4.10 present flexural strength and flexural modulus of PC, PMMA and uncompatibilized PC/PMMA alloys. The flexural strength of PC was higher than that of PMMA, however, it seemed to be equally in flexural modulus. The trend of flexural strength and flexural modulus of uncompatibilied PC/PMMA alloys were the same as exhibited in tensile test. This may be because of the partly interaction between PC and PMMA which resulted from the phenyl rings of PC and carbonyl groups of PMMA.

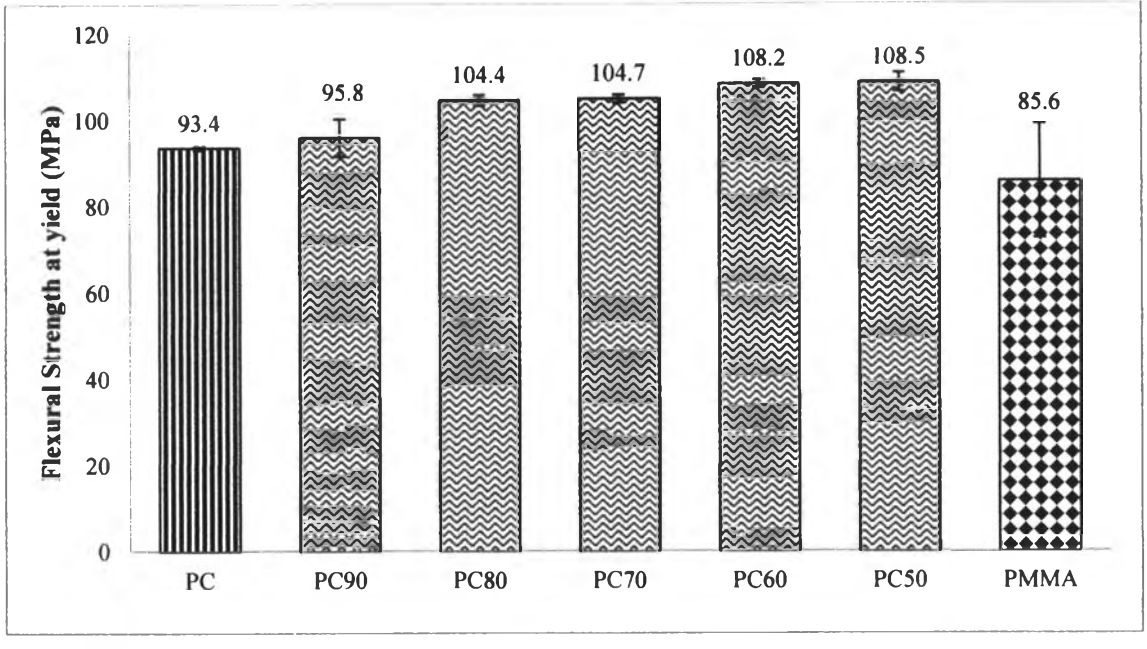

Figure 4.9 Flexural strength of PC, PMMA, and uncompatibilized PC/PMMA alloys.

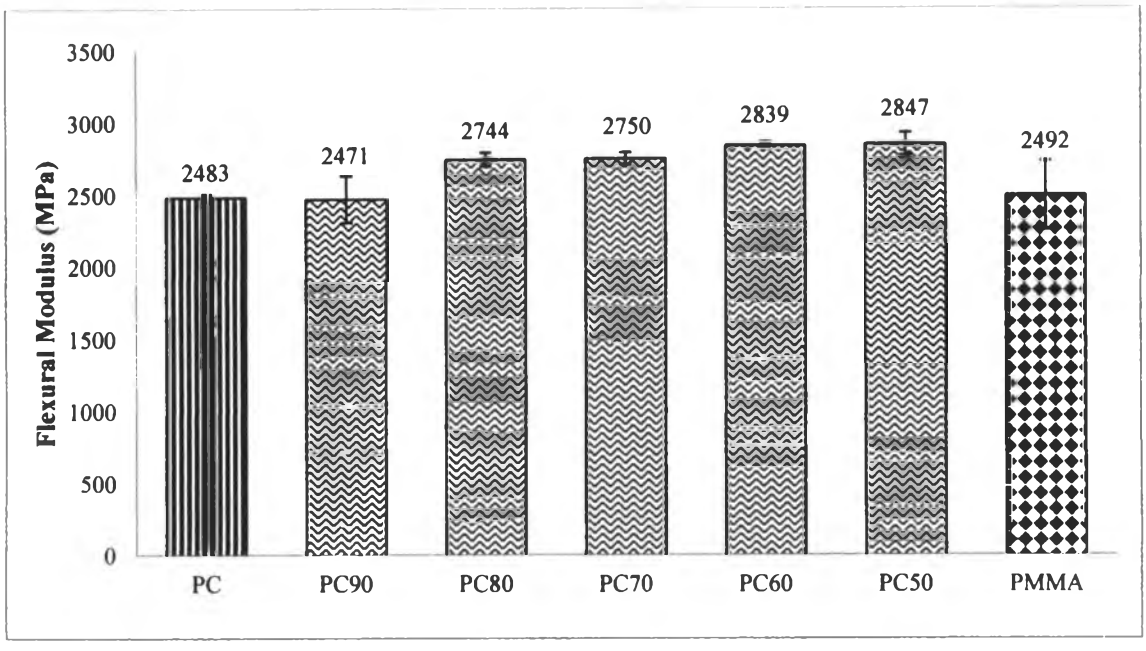

Figure 4.10 Flexural modulus of PC, PMMA, and uncompatibilized PC/PMMA alloys.

4.1.4.3 Notched Izod Impact properties

As can be seen from Figure 4.11, the impact strength of uncompatibilized PC/PMMA alloys decreased drastically when compared with PC owing to the addition of PMMA. In general, PC has oxygen atom in the main chain, which makes the chain become flexible. Incidentally, its structure also has benzene ring and two methyl side group which contribute to molecular stiffness. Both of those two reasons made PC were tough and stiffness. When blend PC with PMMA, it seemed to introduce rigid parts into the system. Then, the elastic part, oxygen atoms in PC, was not adequate to absorb energy and stop craze propagation, resulting in dramatic fall in impact strength. This phenomenon will be carefully investigated in compatibilized PC/PMMA syetem.

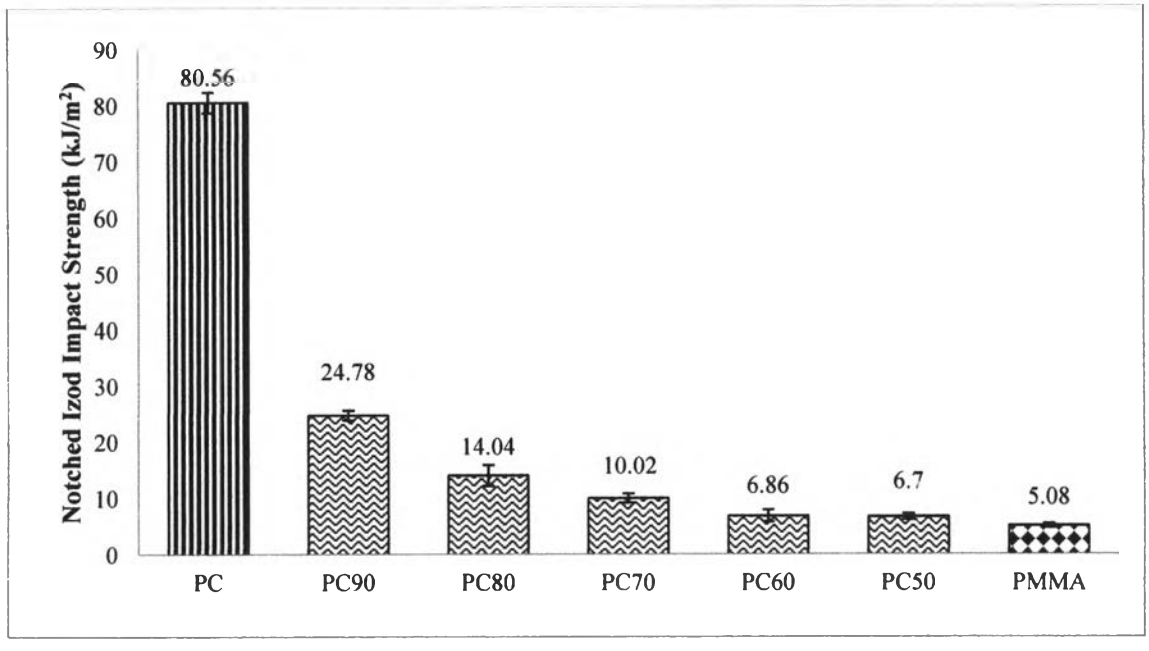

Figure 4.11 Notched izod impact strength of PC, PMMA, and uncompatibilized PC/PMMA alloys.

4.2 Compatibilized PC/PMMA Alloys with Poly(ethylene-*co*-methacrylic acid (EMAA)

4.2.1 Physical properties

4.2.1.1 Rheological properties

The melt flow index (MFI) was determined at 250°C with the hammer weighted 2.16 kg. For uncompatibilized system, MFI of alloys increased with increasing PMMA content. The addition of EMAA into PC/PMMA system affected to the flowability of the compounds particularly in compatibilized PC80/PMMA20 with EMAA, which led to higher. The higher the amount of EMAA gradually increased the MFI of PC50 system as shown in Figure 4.13. In contrast with PC80, the larger improvement of MFI was obtained by adding EMAA as seen in Figure 4.12. It was possible that the effect of EMAA on the flowability of alloys relied on the amount of PC.

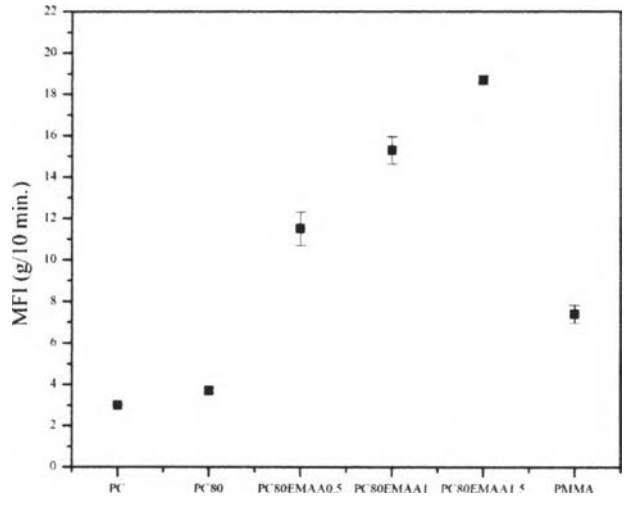

Figure 4.12 Melt Flow Index of PC, PMMA and PC80/EMAA alloys.

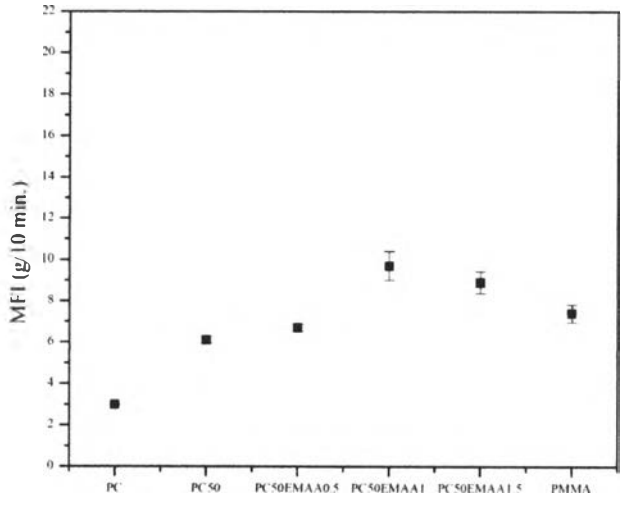

Figure 4.13 Melt Flow Index of PC, PMMA and PC50/EMAA alloys.

4.2.2 Thermal properties

4.2.2.1 Temperature decomposition characterization

The thermal resistance was evaluated by the onset decomposition temperature (T_d) from TGA technique. The results showed that the composition of PC80, EMAA did not affect to the T_d significantly (Figure 4.14). On the other hand, the addition of EMAA into PC50 decreased the onset T_d around 20°C with respect to uncompatibilized PC50 and neat PMMA (Figure 4.15). Due to the degradation caused by EMAA consisting of ethylene part in the molecular chain that was degraded at lower temperature than of PC. The onset T_d of EMAA was around 446°C. Both of PMMA and EMAA had lower thermal stability when compared with PC so the degradation of PC/PMMA alloys containing EMAA occurred at lower temperature than PC/PMMA without EMAA. In addition, it may be because PMMA and EMAA can induce the degradation of the system and the induced degradation favorably depended on the amount of EMAA more than PMMA as can be clearly seen in the composition of PC50. The T_d value after adding EMAA was less than T_d of PMMA but that was not in the composition of PC80. These were the reason that weight loss percentage of PC/PMMA alloys increased after adding EMAA.

The PC/PMMA alloys in the absence of EMAA exhibited two separate thermal degradation steps corresponding to PC and PMMA. However, the thermal degradation of these alloys seemed to be the single step after adding EMAA. It was suggested that the addition of EMAA could increase the homogeneity of the system that resulted in the phases of PC and PMMA were likely compatible with each other

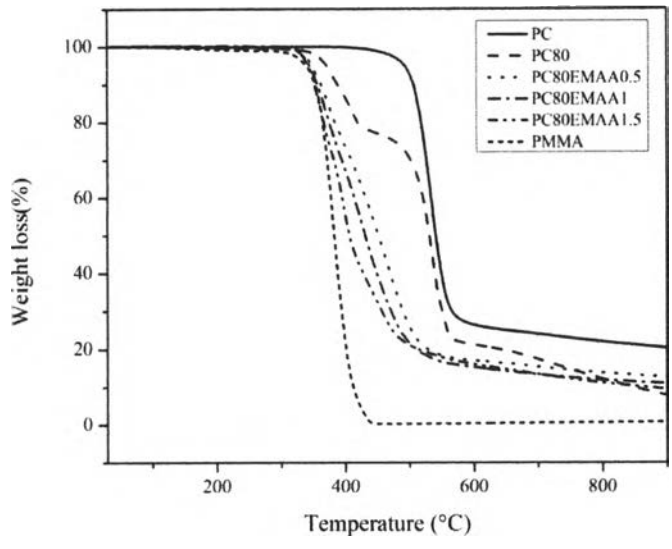

Figure 4.14 TGA plots of PC, PMMA and PC80/EMAA alloys.

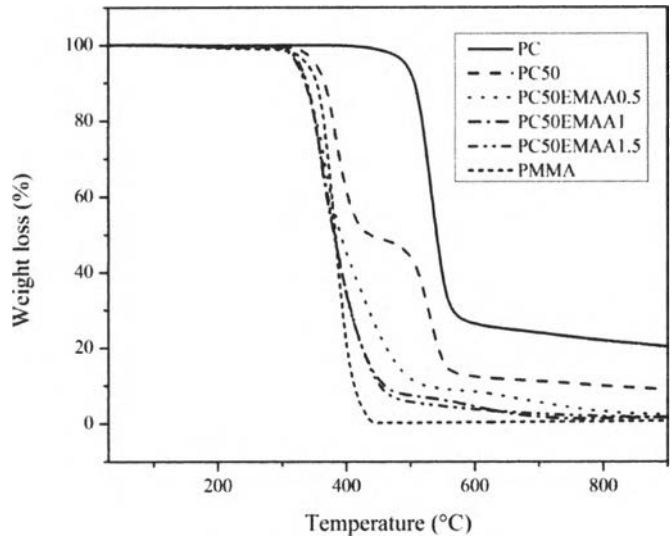

Figure 4.15 TGA plots of PC, PMMA and PC50/EMAA alloys.

4.2.3 Miscibility

4.2.3.1 Glass transition temperature observation

Blending of PC and PMMA, the two distinct glass transition temperatures (2 T_gs) were clearly observed with increasing PMMA content. Then, the combination of PC and PMMA showed the immiscible PC/PMMA alloys. In order to enhance the miscibility of these alloys, the compatibilizer was needed. For this section, EMAA was use as a compatibilizer. From DSC results (Figure 4.16 and 4.17) showed the single glass transition temperature (T_g) of alloys which shift to lower temperature after adding EMAA. The reason is EMAA is an ionomer that has different components. It is a random copolymer of polyethylene and methacrylic acid which acid is partially neutralized by sodium ions. The carbonate group of PC is sensitive to interact with other functional groups like carboxyl acid carboxylate group. For PMMA parts, it is possible to compatibilize with EMAA due to the intermolecular chemical reaction between ester side groups of PMMA and acid groups of EMAA. Even though the reaction between PC, PMMA and EMAA was occurred, the degradation reaction was possible to take place at high temperature which was catalyzed by sodium carboxylate group of EMAA. This is the reason that T_g of alloys is pretty low.

The chemical reaction between PC and EMAA

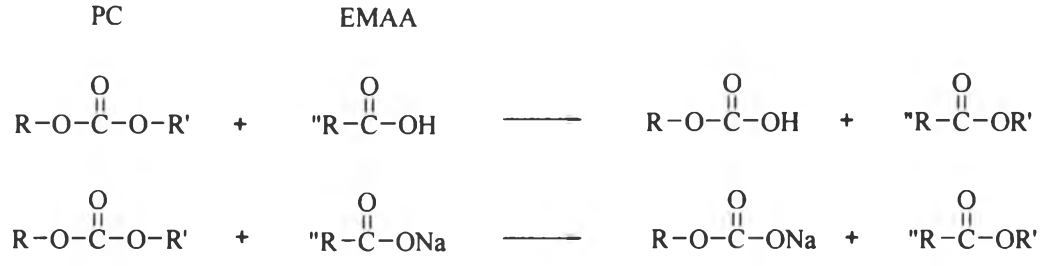

The chemical reaction between PMMA and EMAA

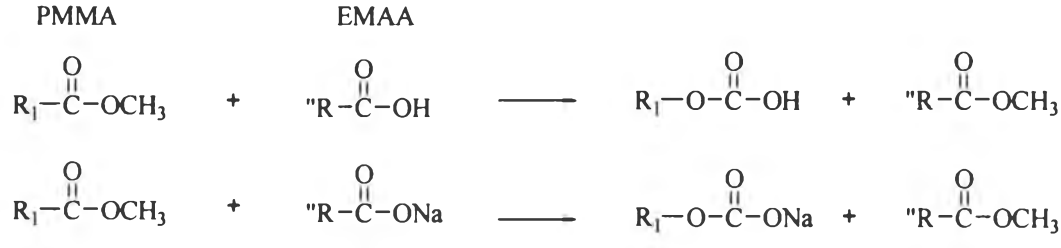

Scheme 1. The chemical reaction of PC, PMMA and EMAA.

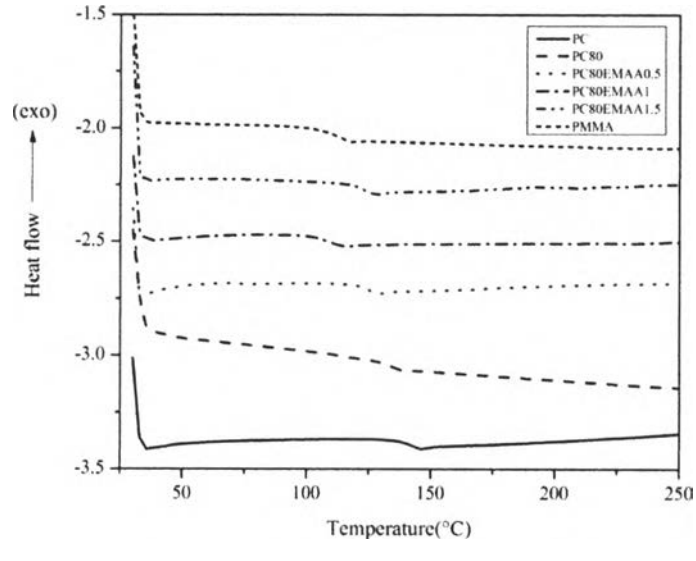

Figure 4.16 DSC plots (second heating) of PC, PMMA and PC80/EMAA alloys.

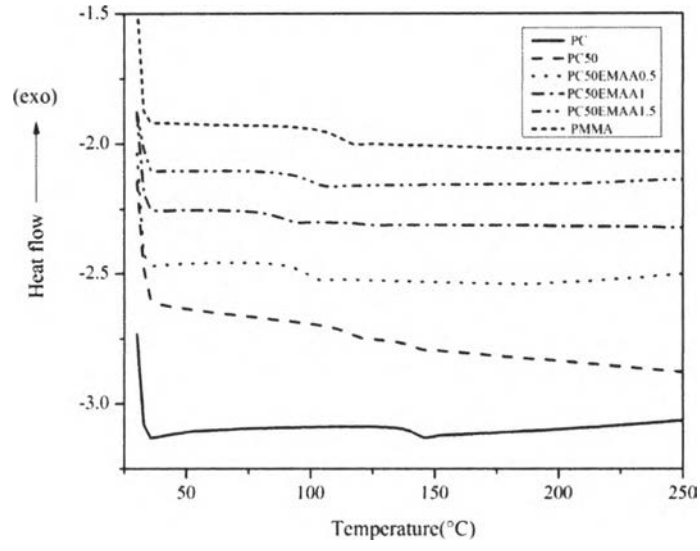

Figure 4.17 DSC plots (second heating) of PC, PMMA and PC50/EMAA alloys.

DMA is one of the most techniques, which is generally used to measure the glass transition temperature or to follow the changes in mechanical that caused by chemical reaction. The glass transition temperature (T_g) can determine from the transition onset or inflection point in the storage modulus, the peak of loss modulus or tan δ. The difference in T_g value between the onset of the storage modulus drop and the peak of tan delta could be as high as 40°C. In this case, the tan delta peak was used to define T_g of the alloys. From DMA measurement, the single glass transition temperature of the alloys in the presence of EMAA was observed. The T_g of the alloys was in the range between PC and PMMA but it seemed to close up with T_g of uncompatibilized PC/PMMA. It was suggested that the compatibility of alloys was better after adding EMAA. The T_g value of alloys with EMAA, however, decreased insignificantly that meant the energy use for the chain motion was equal to uncompatibilized system. If the alloys became more ductile after adding EMAA, the energy use for the molecular motion should be lower than uncompatibilized alloys,

which resulted in the decrement of T_g. the DMA plots of PC80 and PC50 with EMAA were shown in Figure 7.18 and 7.19, respectively.

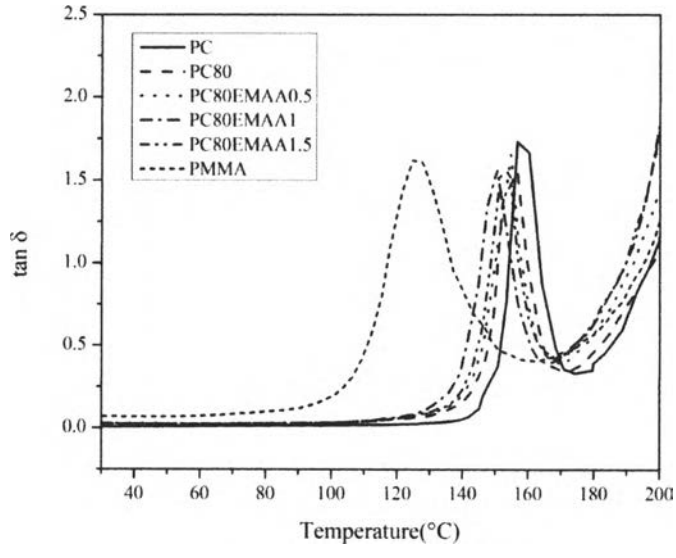

Figure 4.18 DMA plots of PC, PMMA and PC80/EMAA alloys.

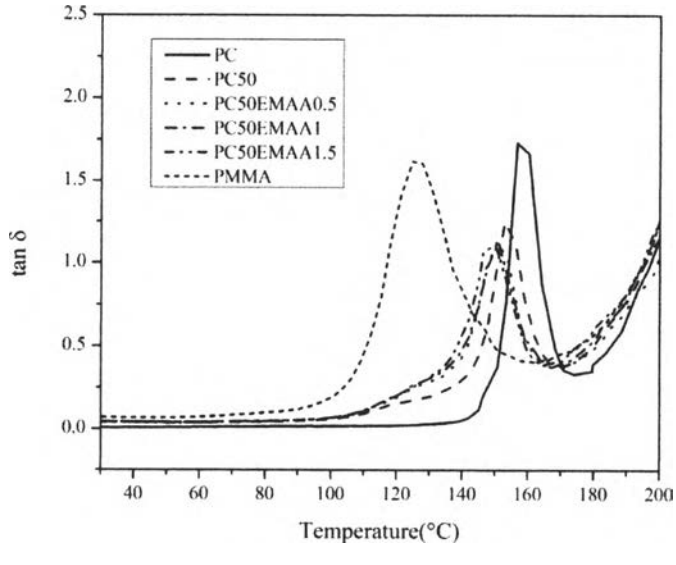

Figure 4.19 DMA plots of PC, PMMA and PC50/EMAA alloys.

4.2.3.2 Morphological temperature observation

SEM was conducted to observe the morphology of the impact-fractured surface of the PC/PMMA alloys with and without etching as shown in Figure 4.20 and 4.21. Dimethylacetamide was used as a solvent to etch out PC domain and the surface was immersed in solvent for 3 minutes. For uncompatibilized system, The PC domains (the etched component) were showed in irregular shape with random dispersion. On the other hand, the PC phase rather decreased and the dispersion was quite regular after adding EMAA. Then, it can be indicated that EMAA can enhance the miscibility of PC/PMMA alloys. Additionally, the toughness of the alloys can be confirmed from the unetched images. In the presence of EMAA in the system, they showed the rough surface but the shear yielding still did not appear. That was the reason that the addition of EMAA did not improve the toughness of the alloys, which corresponded to the impact strength.

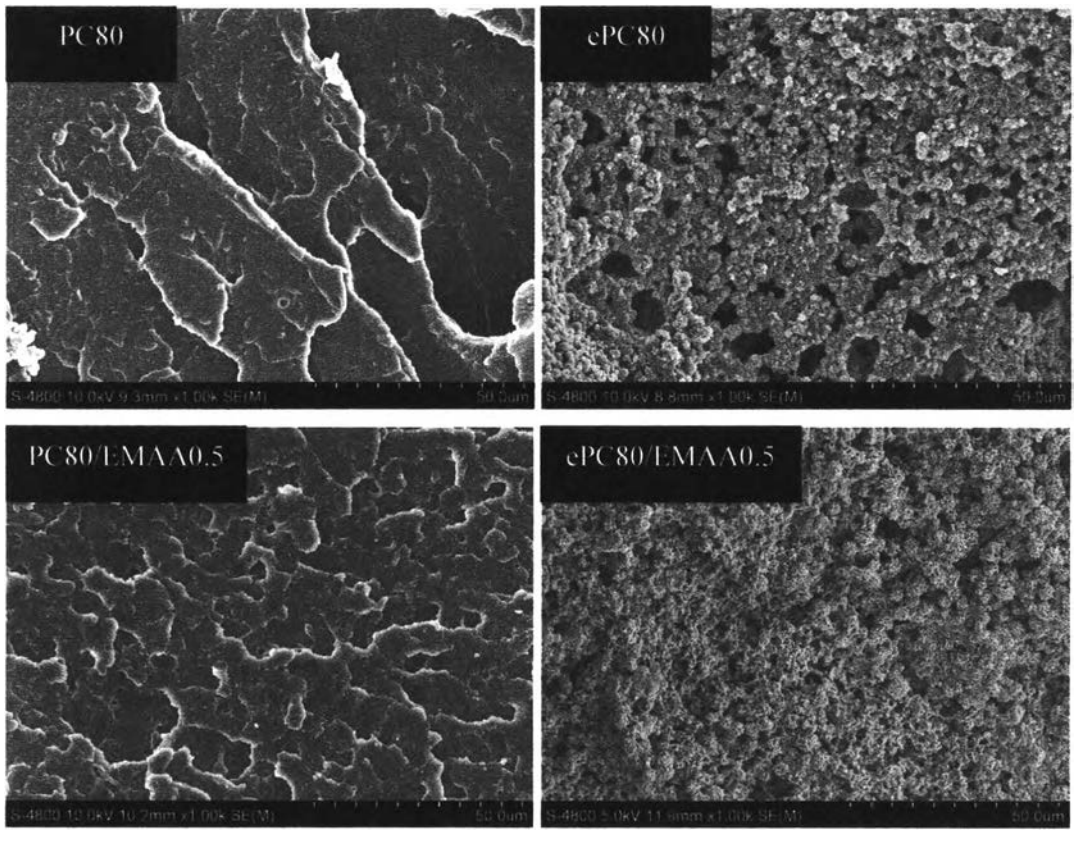

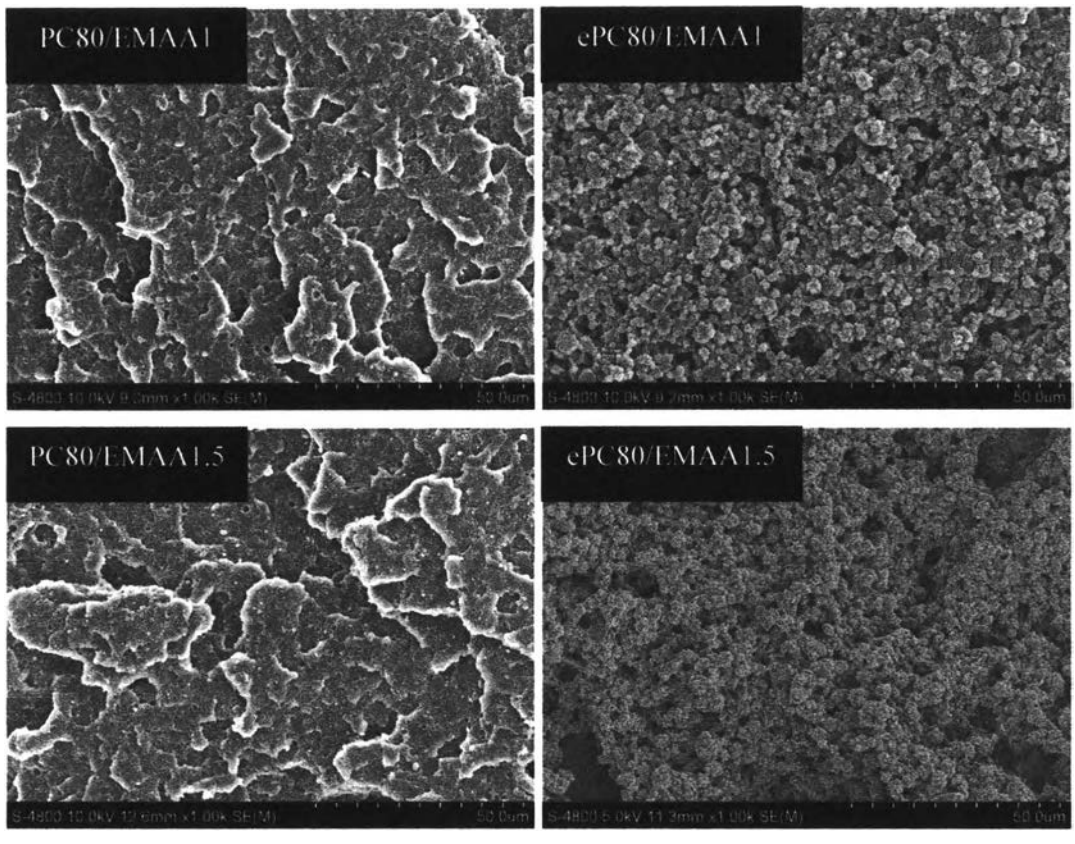

Figure 4.20 SEM micrographs of fracture surface of PC80/EMAA alloys (etching (ePCXX) and no etching (PCXX)).

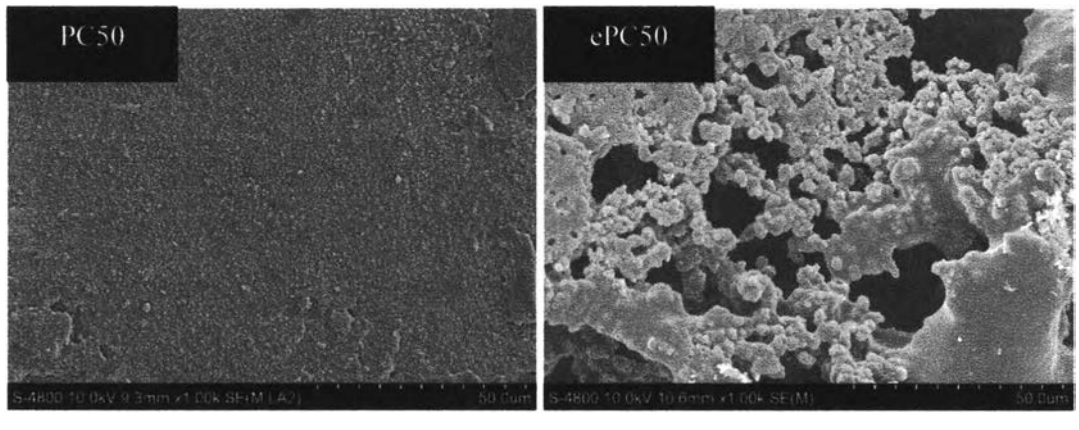

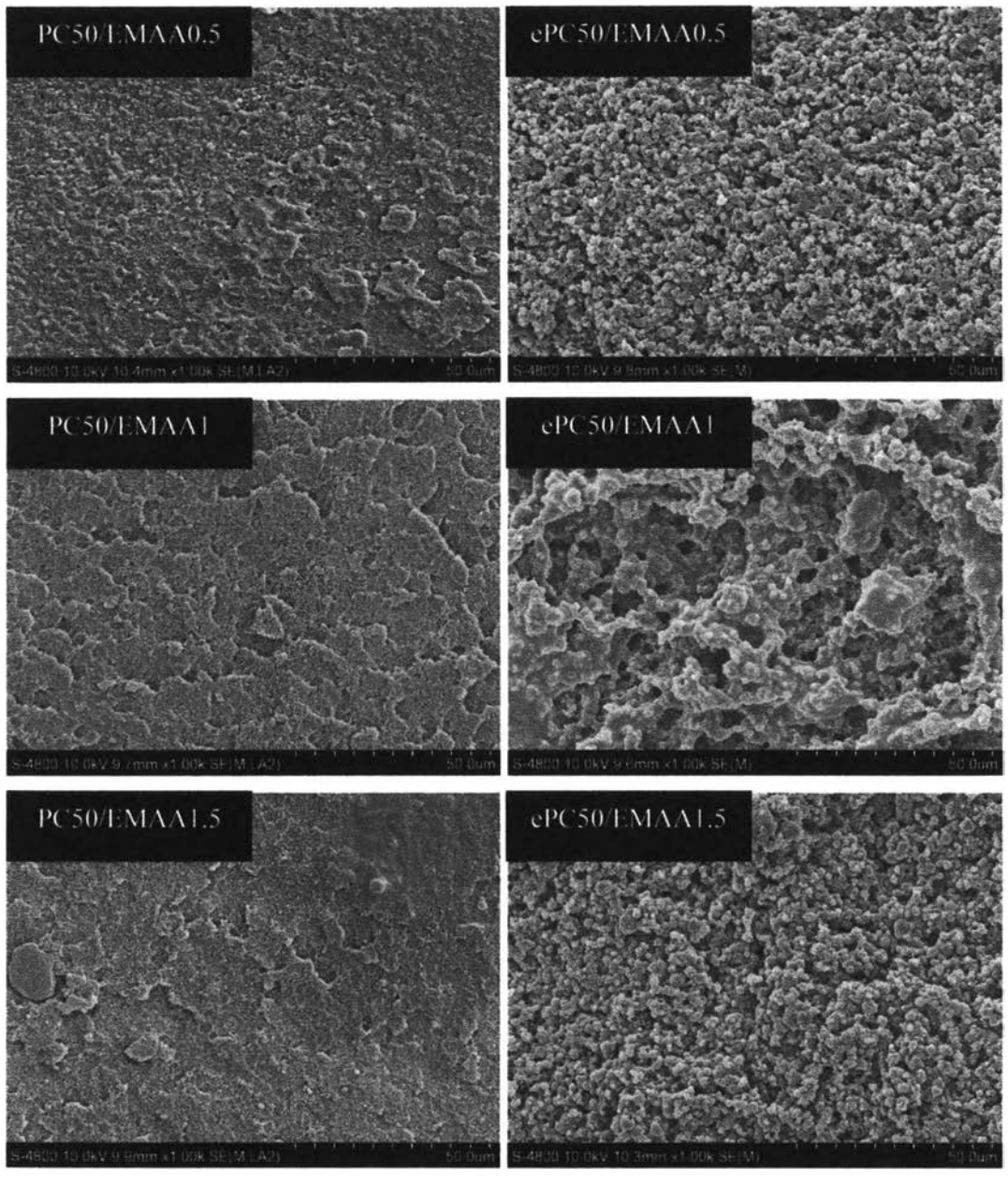

Figure 4.21 SEM micrographs of fracture surface of PC50/EMAA alloys (etching (ePCXX) and no etching (PCXX)).

4.2.4 Mechanical properties

4.2.4.1 Tensile properties

The tensile strength at yield, elongation at yield and Young's modulus of PC/PMMA alloys with EMAA is shown in Figure 4.22-4.27 The addition of

EMAA into PC/PMMA alloys affected to the tensile properties especially in the composition of PC50. For the composition of PC50, the tensile stress at yield slightly increased while the elongation at yield did not change when compared with PC50 and it seemed to decreased after adding EMAA more than 1 phr. Young's modulus is calculated by dividing tensile stress by tensile strain (elongation) so this is the reason that Young's modulus of PC50 in the presence of EMAA increased. Since the acid group of EMAA can react with carbonate group of PC and ester side groups of PMMA, the specific interaction between of each component in the system increased which lead to the compatibility between phases of PC and PMMA while the molecular and segmental motion was restrict causing the reduction of elongation of the alloys. However, the effect of EMAA on tensile properties of composition of PC80 was insignificant. The tensile properties of PC80 with EMAA were similar to these of uncompatibilized PC80. It was because the ratio of PC to EMAA in the case of PC80 was not properly which resulted in the similar tensile properties.

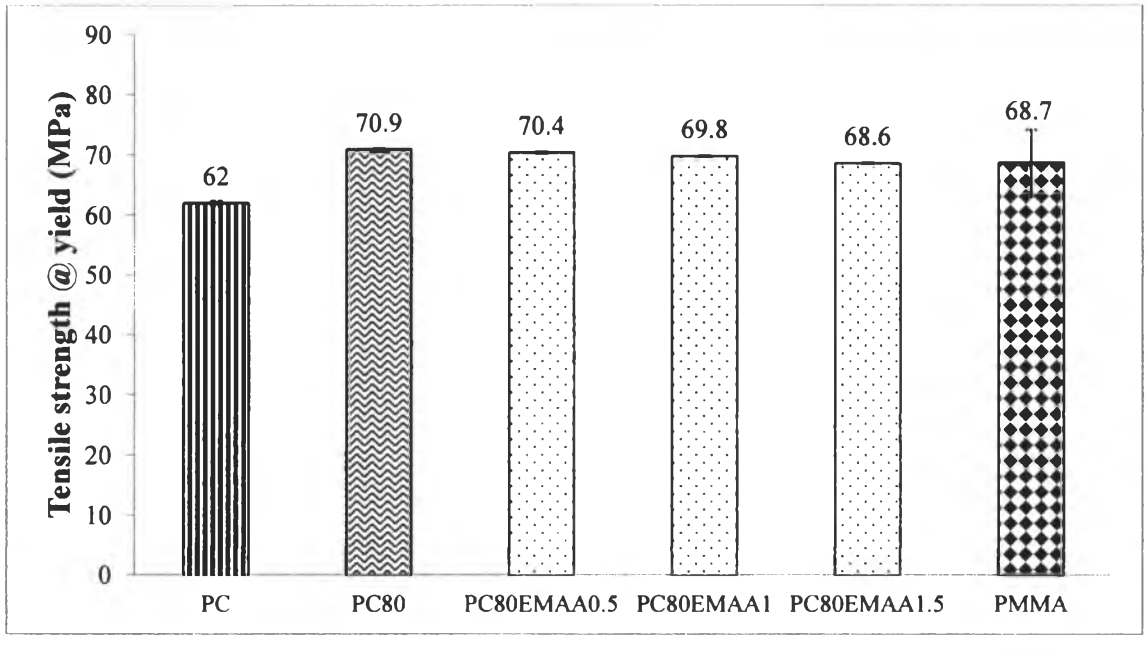

Figure 4.22 Tensile strength at yield of PC, PMMA, and PC80/EMAA alloys.

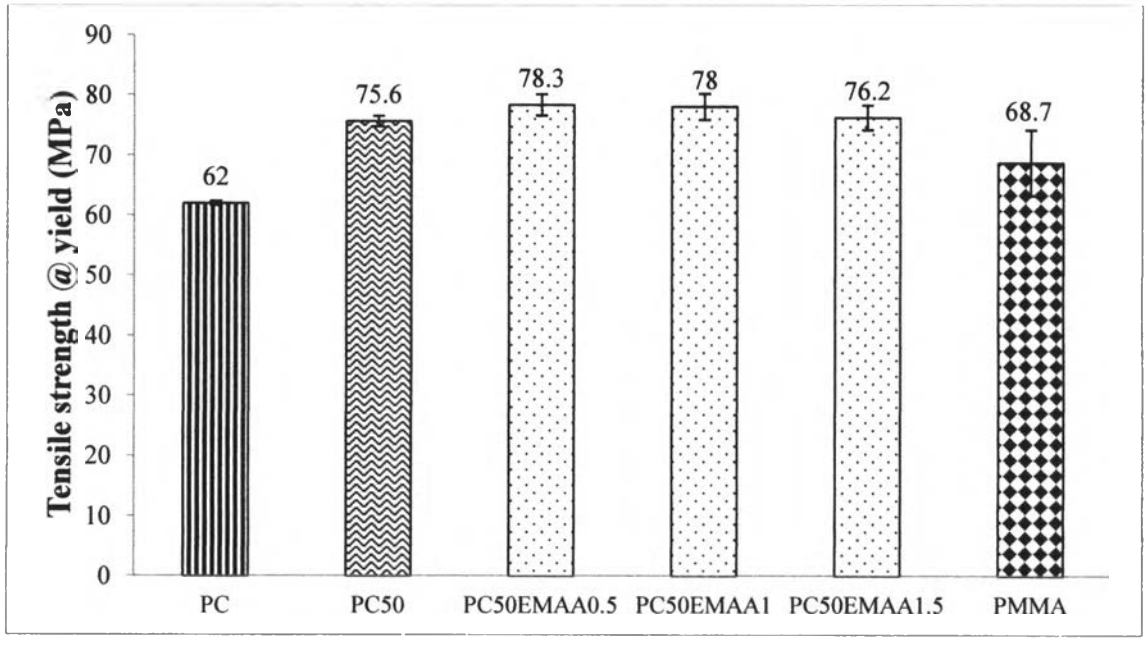

Figure 4.23 Tensile strength at yield of PC, PMMA, and PC50/EMAA alloys.

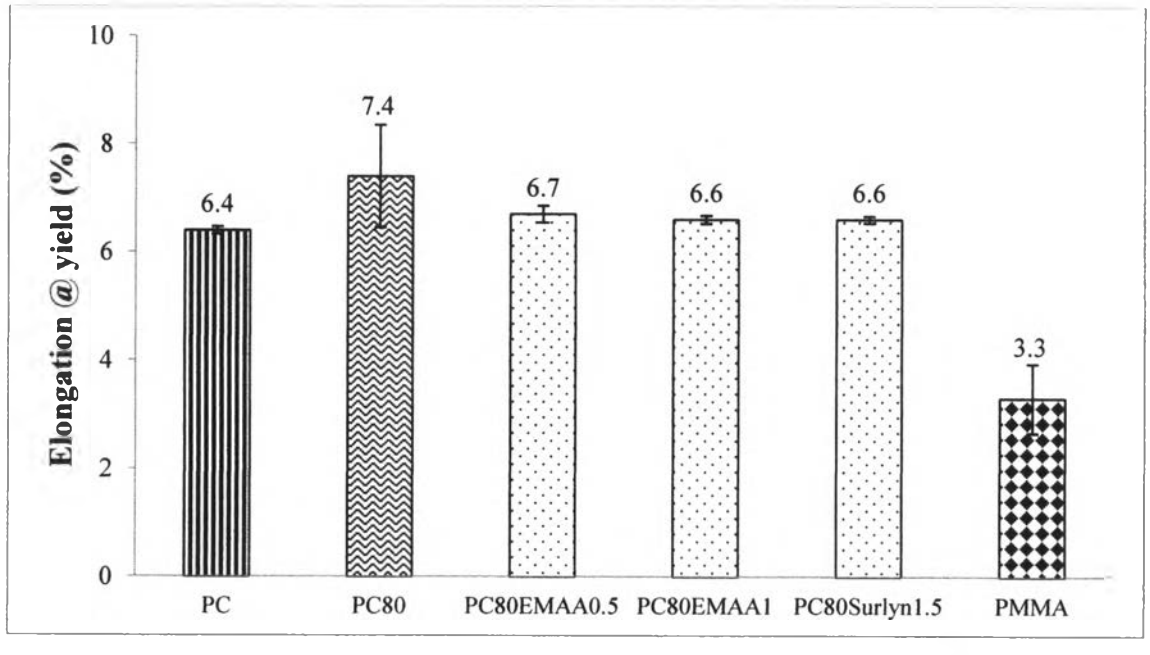

Figure 4.24 Elongation at yield of PC, PMMA, and PC80/EMAA alloys.

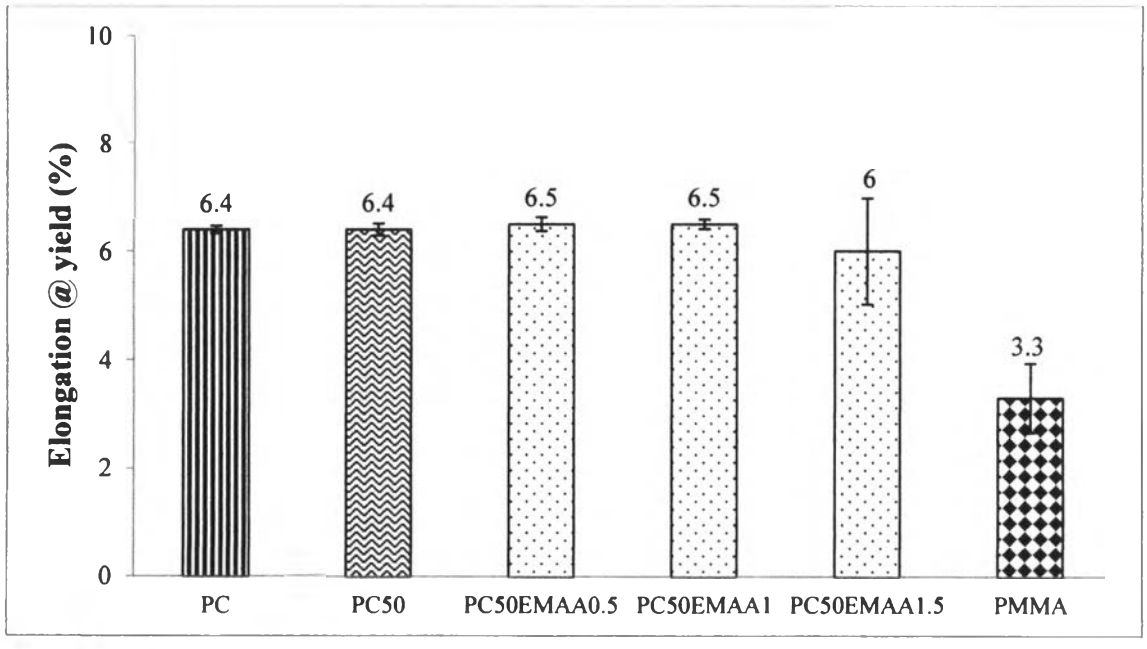

Figure 4.25 Elongation at yield of PC, PMMA, and PC50/EMAA alloys.

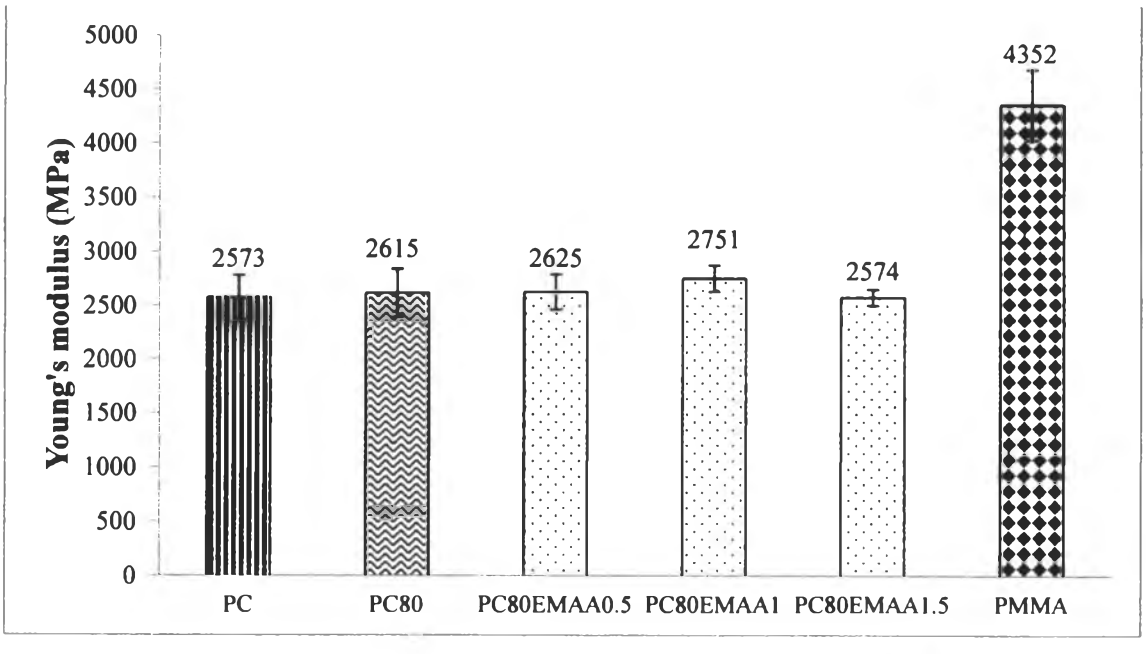

Figure 4.26 Young's modulus of PC, PMMA, and PC80/EMAA alloys.

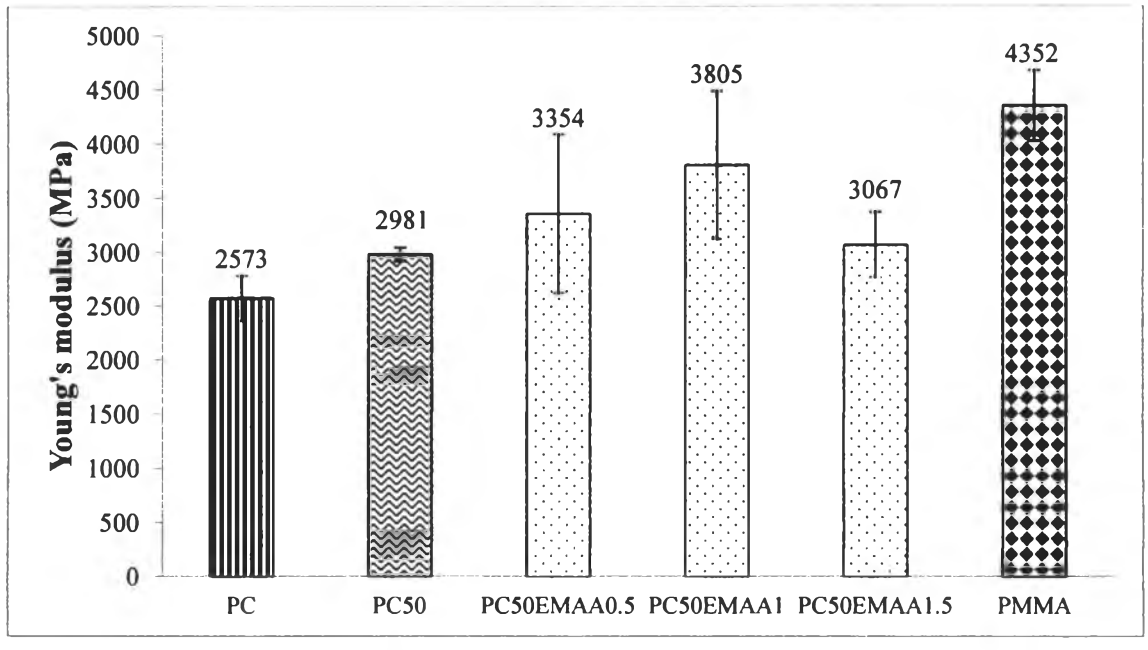

Figure 4.27 Young's modulus of PC, PMMA, and PC50/EMAA alloys.

4.2.4.2 Flexural properties

Figure 4.28-4.31 presented the flexural strength and flexural modulus of PC/PMMA alloys with EMAA. The flexural strength and flexural modulus of PC/PMMA alloys in the presence of EMAA seemed to be the same as uncompatibilized system. Then, it can be indicated that the addition of EMAA into PC/PMMA alloys did not influence to the flexural properties.

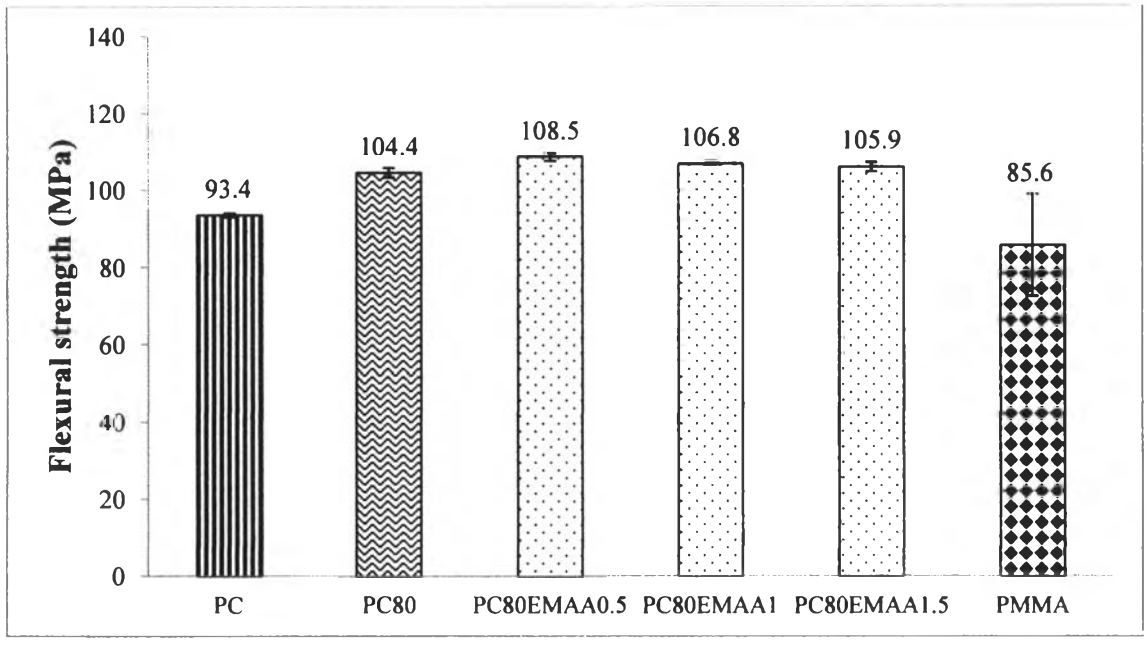

Figure 4.28 Flexural strength of PC, PMMA, and PC80/EMAA alloys.

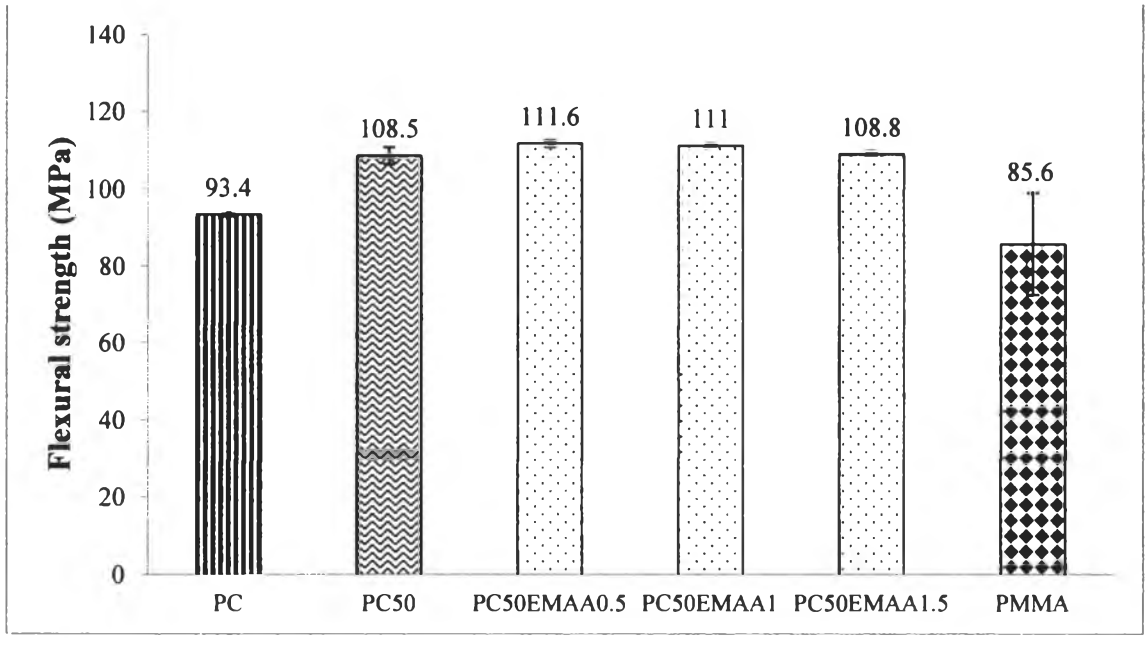

Figure 4.29 Flexural strength of PC, PMMA, and PC50/EMAA alloys.

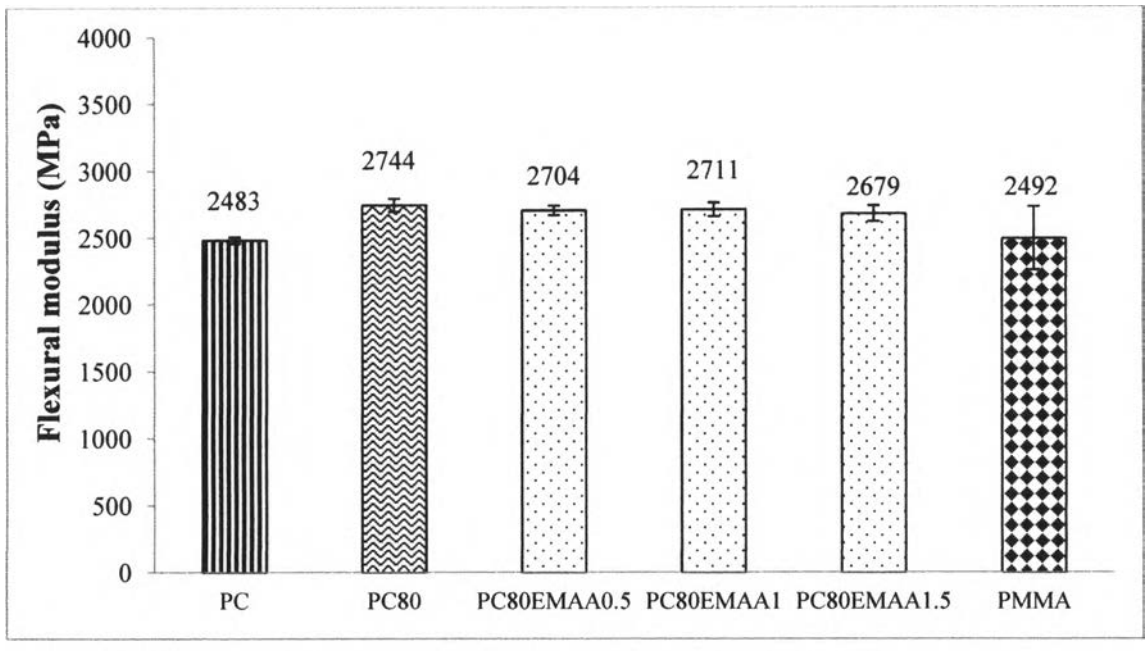

Figure 4.30 Flexural modulus of PC, PMMA, and PC80/EMAA alloys.

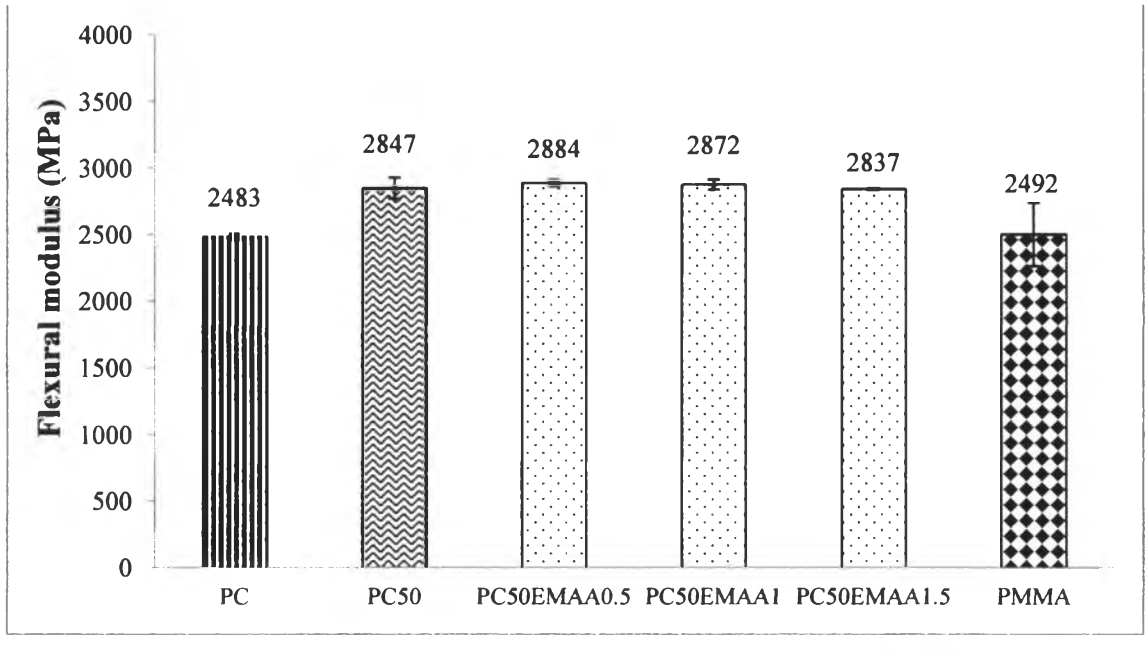

Figure 4.31 Flexural modulus of PC, PMMA, and PC50/EMAA alloys.

4.2.4.3 Notched Izod Impact properties

The addition of EMAA into the system did not improve the impact strength of the alloys. As can be seen in Figure 4.32 and 4.33, the impact strength of PC/PMMA was slightly lower than uncompatibilized PC/PMMA. Even though carboxylic group of EMAA can react with carbonate group of PC and ester group of PMMA for generating the copolymer, it also lacked of long flexible chains part to absorb large amount of energy. To obtain high-impact strength alloys, they had to have the balance of toughness and stiffness to absorb and dissipate energy. In addition, sodium salt of EMAA also can cleave the chain at carbonate group in PC and ester group in PMMA led the molecular weight of alloys to decrease which resulted in the drastically drop in impact strength.

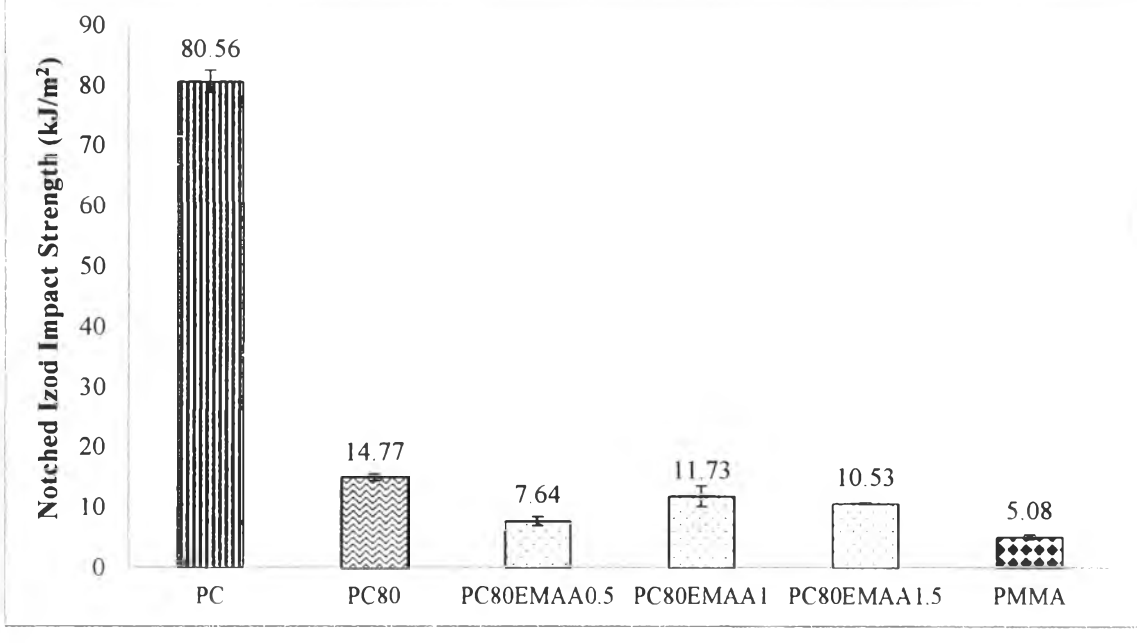

Figure 4.32 Notched izod impact strength of PC, PMMA and PC80/EMAA alloys.

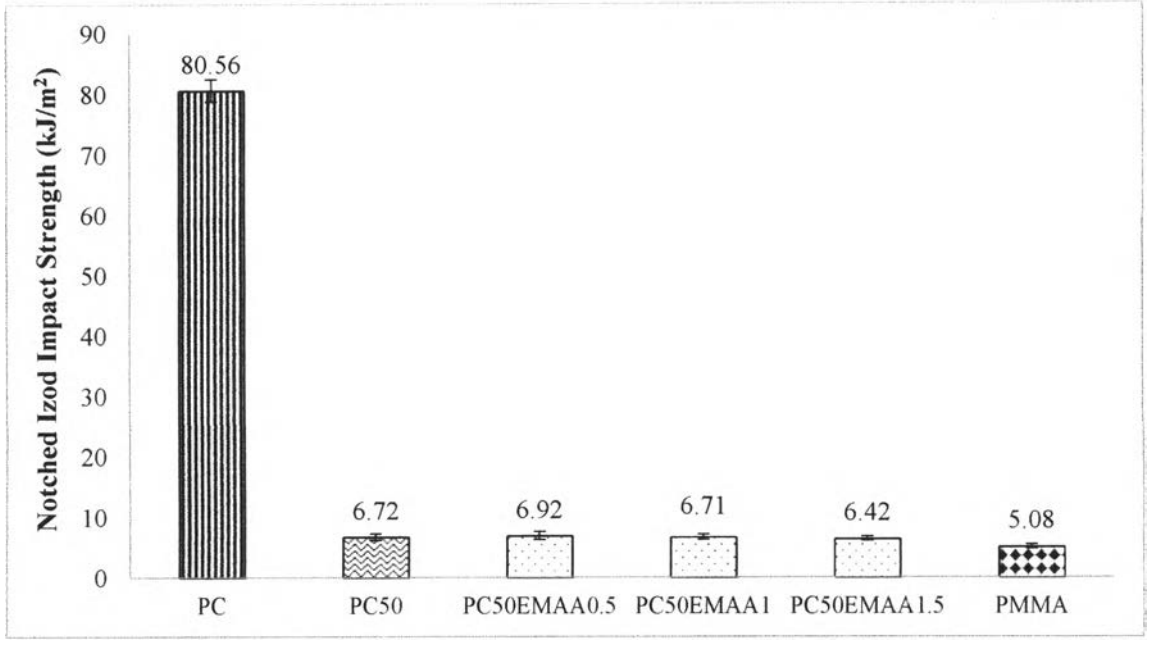

Figure 4.33 Notched izod impact strength of PC, PMMA and PC50/EMAA alloys.

4.3 Compatibilized PC/PMMA Alloys with Ethylene Methyl Acrylate Copolymer (EMA)

4.3.1 Physical properties

4.3.1.1 Rheological properties

MFI measurement can point to the rheological behavior of materials. The MFI of PC/PMMA alloys were shown in Figure 4.34 and 4.35. The addition of EMA has no effect on MFI when compared with uncompatibilized PC/PMMA. It was obviously that the content of EMA at 1 and 5 phr did not affect to the flowability of the alloys.

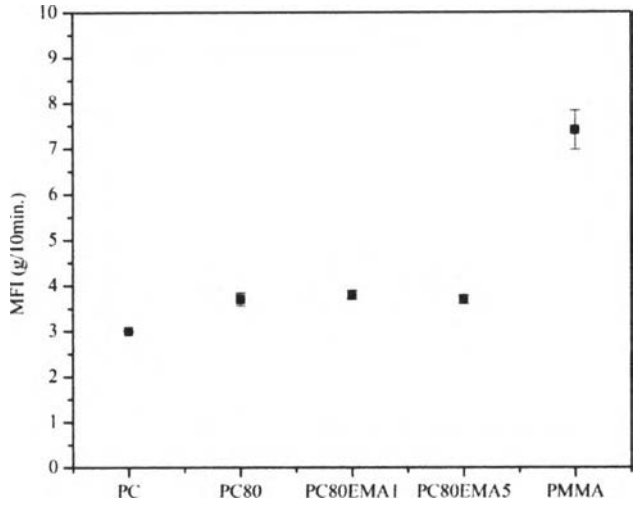

Figure 4.34 Melt Flow Index of PC, PMMA and PC80/EMA alloys.

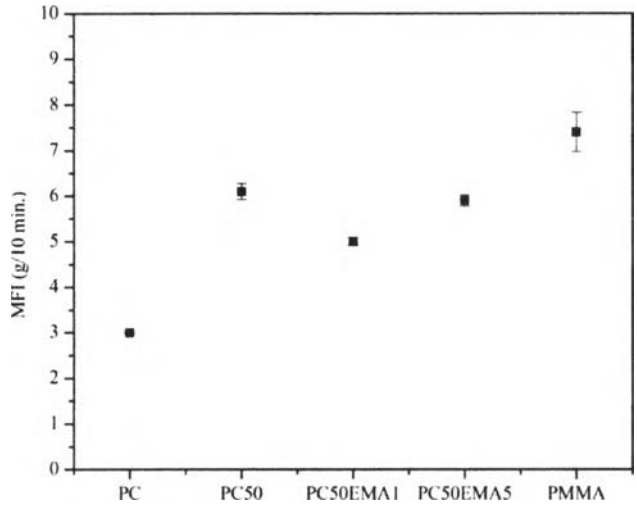

Figure 4.35 Melt Flow Index of PC, PMMA and PC50/EMA alloys.

4.3.2 Thermal properties

4.3.2.1 Temperature decomposition characterization

Figure 4.36-4.37 exhibit the onset degradation temperature of PC80 and PC50 with EMA, respectively. The addition of EMA led the degradation temperature (T_d) of PC80/PMMA20 to increase while the percentage weight loss slightly decreased. Conversely, the T_d of PC50 slightly decreased but the percentage weight loss tended to increase after adding EMA. It was evident that the addition of EMA into PC/PMMA alloys enhanced the thermal stability for only the PC80/PMMA20 composition. This characteristic implied that the obtained properties of the alloys depended on the ratio between polymer matrix and compatibilizer.

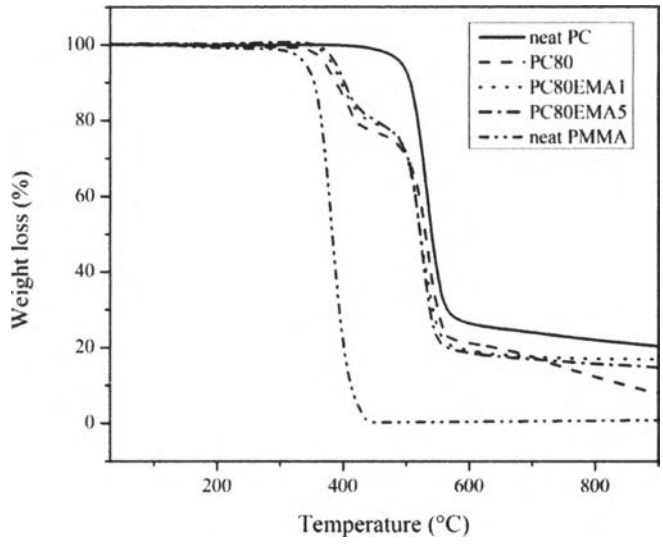

Figure 4.36 TGA plots of PC, PMMA and PC80/EMA alloys.

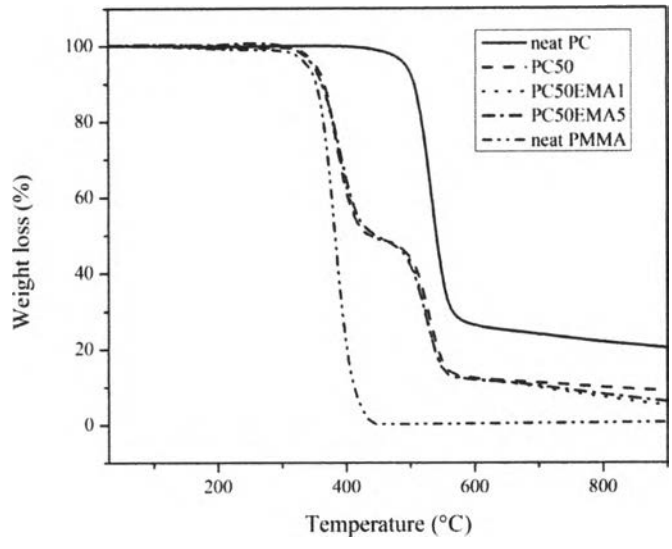

Figure 4.37 TGA plots of PC, PMMA and PC80/EMA alloys.

4.3.3 Miscibility

4.3.3.1 Glass transition temperature observation

From Figure 4.38-4.39, DSC thermograms displayed the glass transition temperature (T_g) of PC/PMMA alloys containing EMA. As it had been mentioned before that uncompatibilized PC80/PMMA20 showed single T_g (T_g of PC rich phase) because the content of disperse phase (PMMA) was not high enough for the detection limit of equipment and T_g of PMMA was noticeable when the PMMA content increased as can be seen in uncompatibilized PC50/PMMA50. Then, the T_g of PC80/PMMA20 alloy with EMA still exhibited single T_g and did not differ from uncompatibilized PC80/PMMA20. The T_g of PC50/PMMA50 composition in the presence of EMA also showed two distinct T_gs which T_g values were the same as uncompatibilized PC50/PMMA50. Then, it could be noted that the addition of EMA did not improve the miscibility of the alloys when compared with uncompatibilized PC/PMMA alloys.

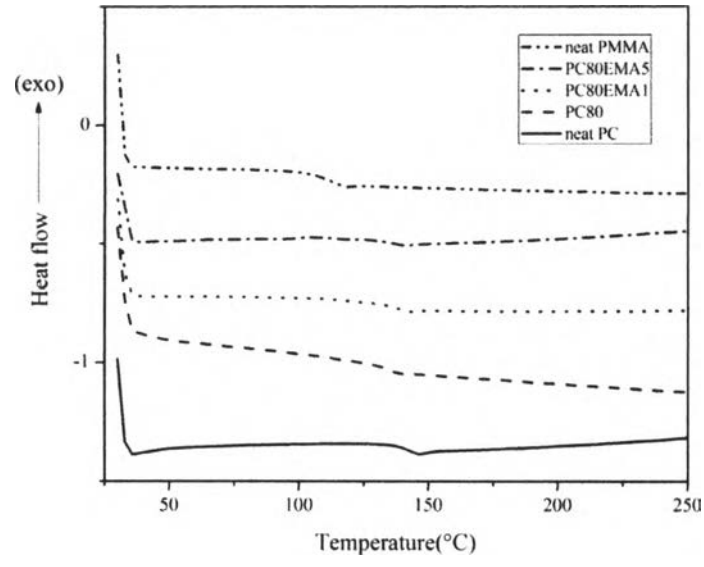

Figure 4.38 DSC plots (second heating) of PC, PMMA and PC80/EMA alloys.

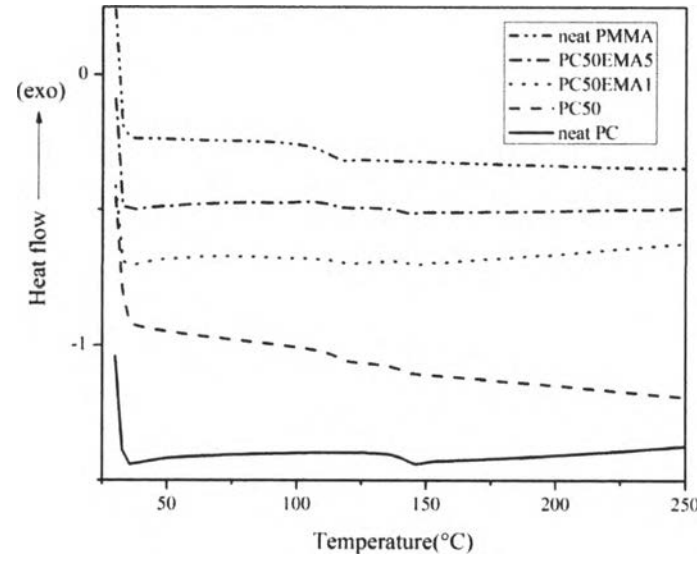

Figure 4.39 DSC plots (second heating) of PC, PMMA and PC50/EMA alloys.

In this study, DMA was used to determine the glass transition temperature (T_g) of PC/PMMA with EMA which this T_g was indicated by the tan δ peak. Figure 4.40 and 4.41 exhibit the T_g of PC80/EMA and PC50/EMA alloys, respectively. It showed the single T_g at all compositions. The T_g of the alloys seemed to increase when EMA content increased. From this result, it could be noted that the addition of EMA into the system could not improve the miscibility of the alloys. This result was related to DSC measurement as aforementioned.

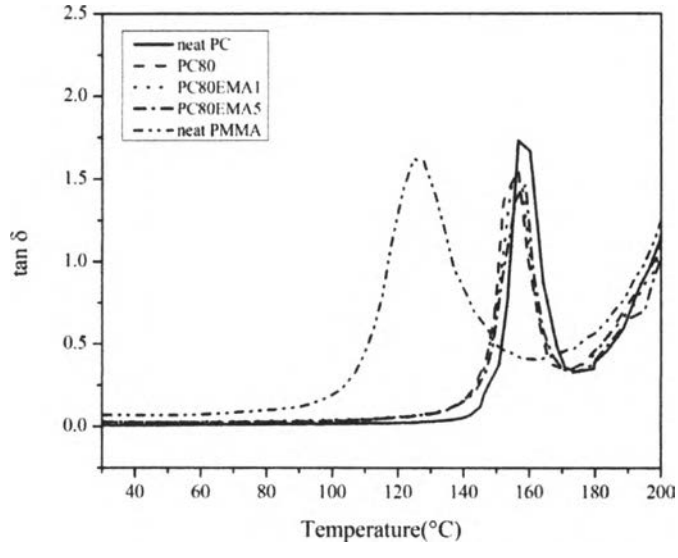

Figure 4.40 DMA plots of PC, PMMA and PC80/EMA alloys.

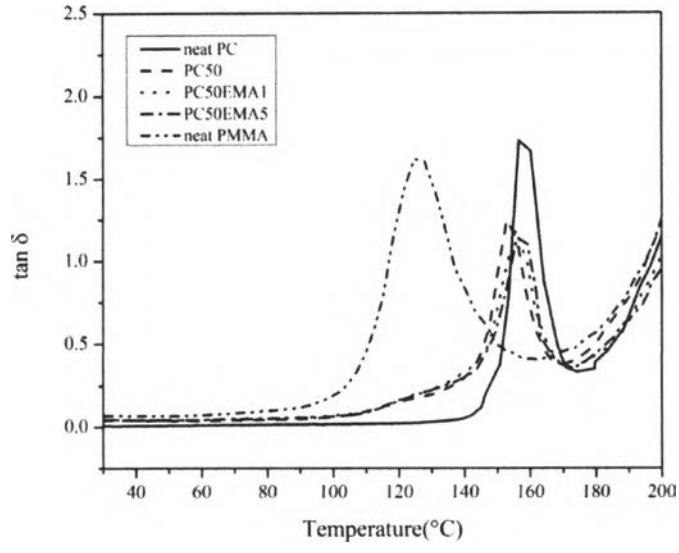

Figure 4.41 DMA plots of PC, PMMA and PC50/EMA alloys.

4.3.3.2 Morphological temperature observation

SEM was used to observe the morphology of the impact-fractured surface of the PC/PMMA alloys in the presence of EMA with and without etching as shown in Figure 4.42 and 4.43. Dimethylacetamide was used as a solvent to etch out PC domain and the surface was immersed in solvent for 3 minutes. The size of PC domains (the etched component) was smaller than uncompatibilized PC/PMMA when EMA was added and the dispersion of this etched component was more uniform. Thus, it could be seen that the addition of EMA could be improved the adhesion between PC and PMMA and also enhanced the dispersion of the minor phases (PMMA) in the alloys. In addition, the toughness of these alloys could be confirmed from the unetched images. All the impact-fractured surface of the PC/PMMA alloys were more rough after adding EMA, but only the SEM image of PC80/PMMA50 with 5 phr of EMA composition having high impact strength differed from the others. Its impact-fractured surface showed the certain craze direction with tearing lines and its phase was more elongated when compared with the others. Furthermore, This PC80/PMMA20 with 5phr EMA was the only one composition that did not completely break (the picture was not shown in this

report). From these reasons, it could be concluded that the addition of EMA could improve the dispersion of the system and the impact strength of the alloys particularly in PC80/PMMA20 in the presence of 5 phr of EMA.

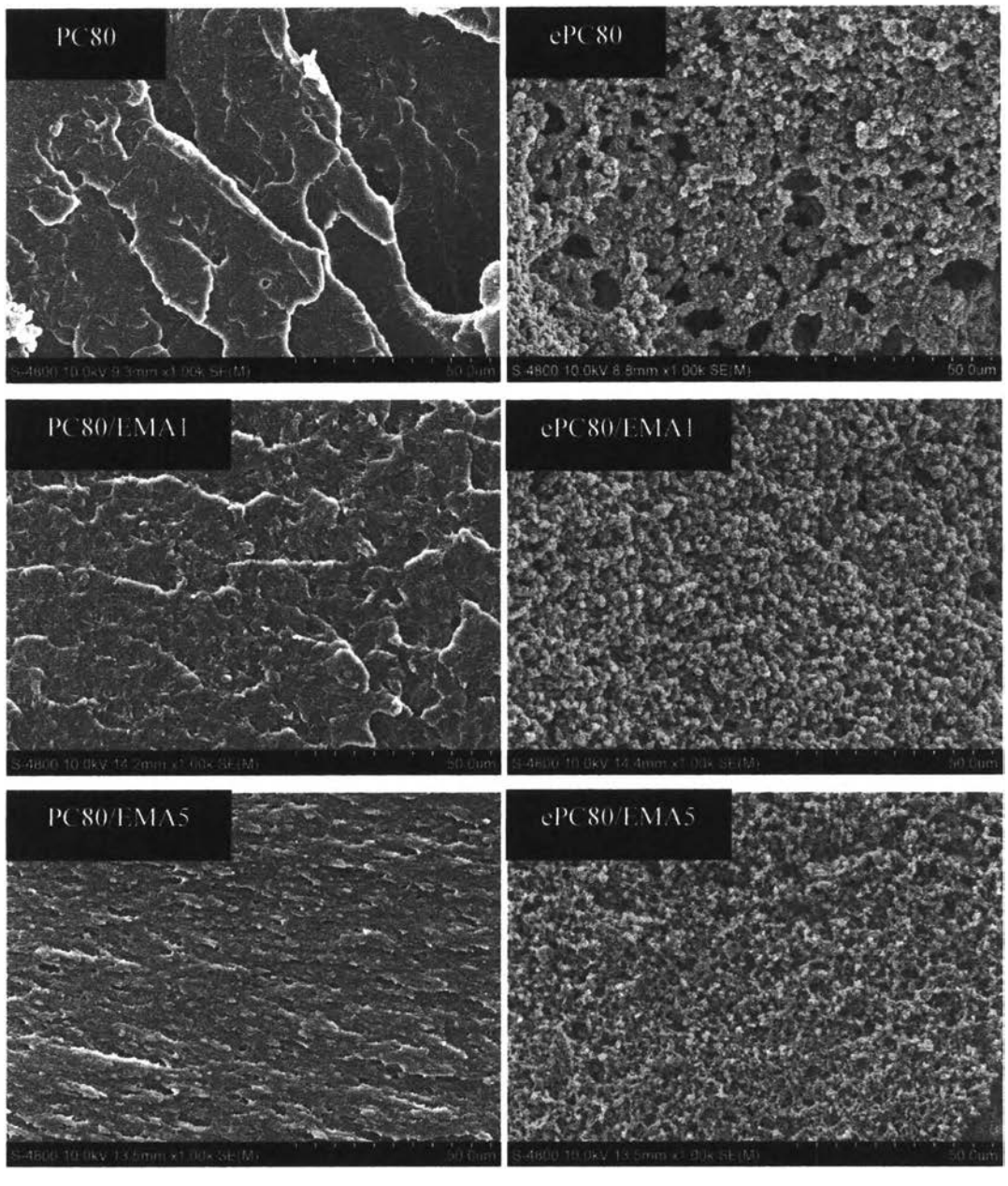

Figure 4.42 SEM micrographs of fracture surface of PC80/EMA alloys (etching (ePCXX) and no etching (PCXX)).

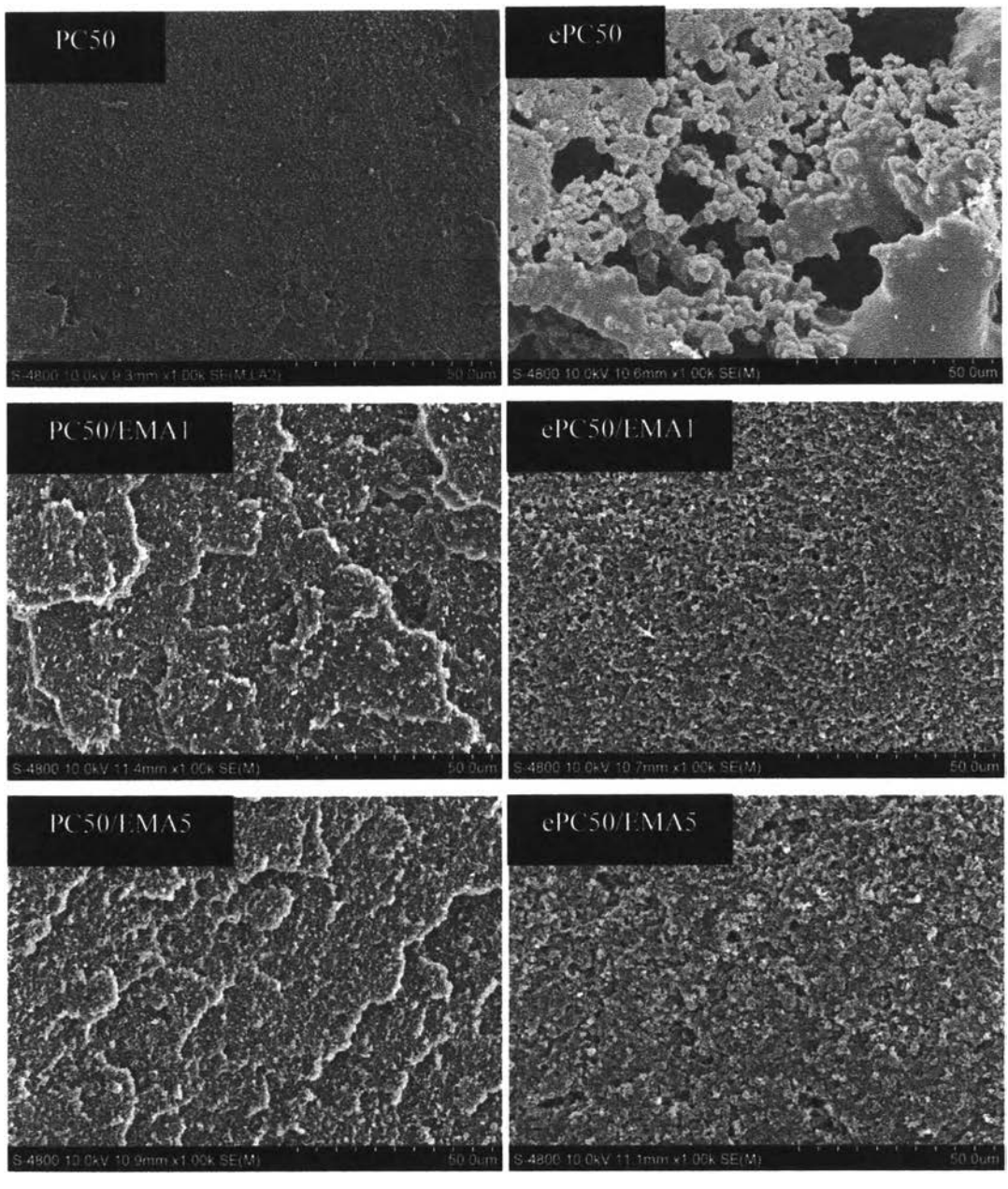

Figure 4.43 SEM micrographs of fracture surface of PC50/EMA alloys (etching (ePCXX) and no etching (PCXX)).

4.3.4 Mechanical properties

4.3.4.1 Tensile properties

The tensile strength at yield, elongation at yield and Young's modulus of PC/PMMA alloys with EMA were shown in Figure 4.44-4.49. The tensile

strength of PC80/PMMA20 composition slightly increased when the amount of EMA increased. It was because the addition of EMA in the range of 1-5 phr into PC80/PMMA20 composition was suitable for improving the adhesion between PC and PMMA which caused the better stress transfer between of each component. In contrast with PC50/PMMA50 composition, adding more amount of EMA was likely to obtain poor tensile strength. For the elongation of PC/PMMA alloys with EMA as increase in the EMA content, the elongation was prone to increase which was owing to the effect of the soft elastomeric EMA induced more elongated of the alloys. From the tensile strength and the elongation of the alloys results, the variation of Young's modulus of PC80/PMMA20 composition was insignificant whereas it was inclined to decrease for PC50/PMMA50 composition.

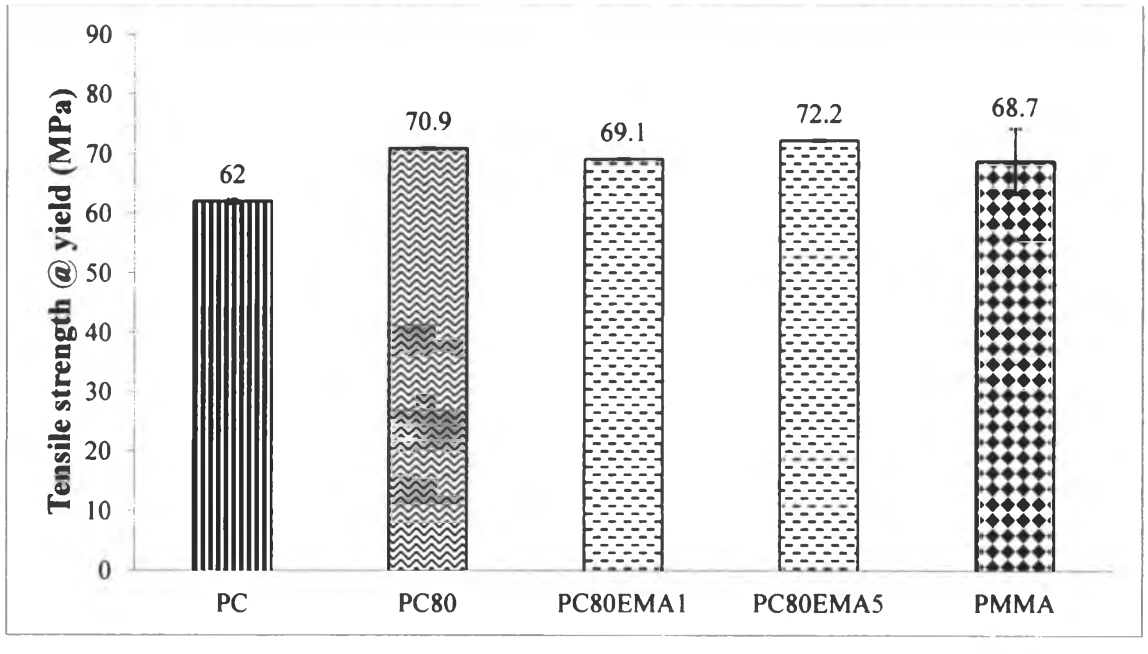

Figure 4.44 Tensile strength at yield of PC, PMMA, and PC80/EMA alloys.

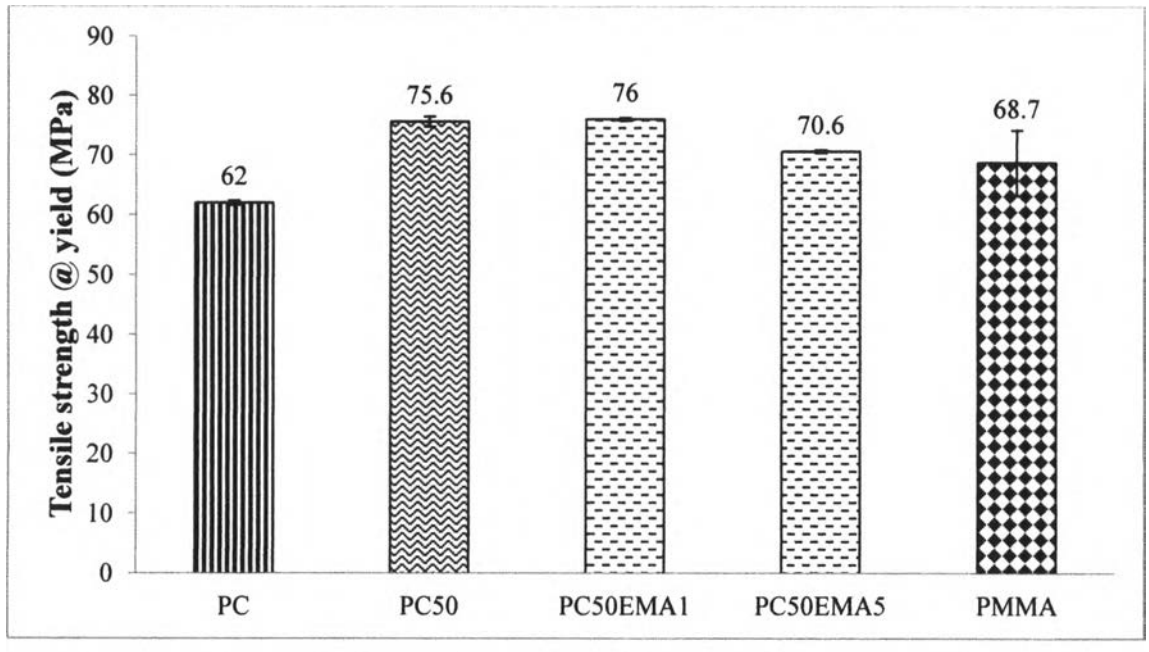

Figure 4.45 Tensile strength at yield of PC, PMMA, and PC50/EMA alloys.

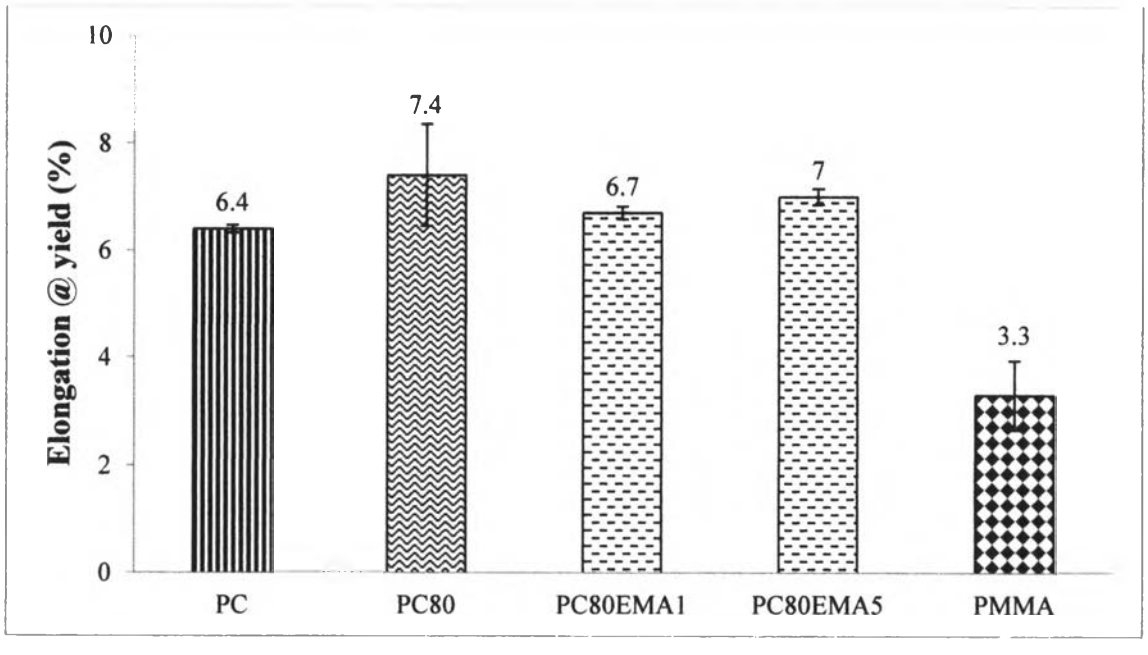

Figure 4.46 Elongation at yield of PC, PMMA, and PC80/EMA alloys.

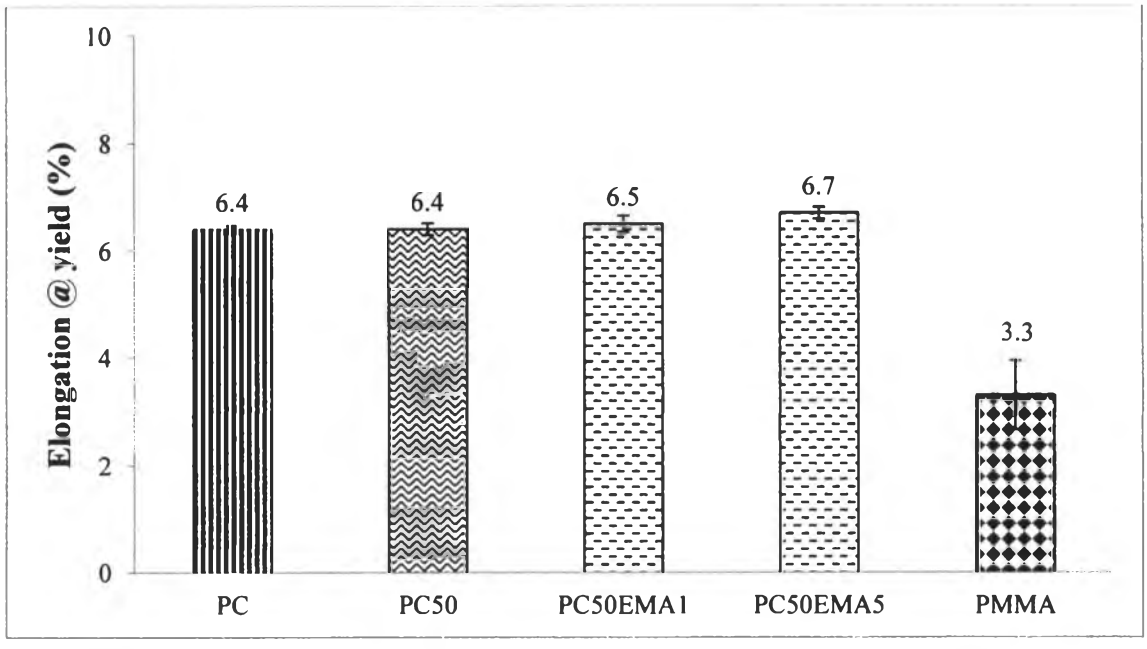

Figure 4.47 Elongation at yield of PC, PMMA, and PC50/EMA alloys.

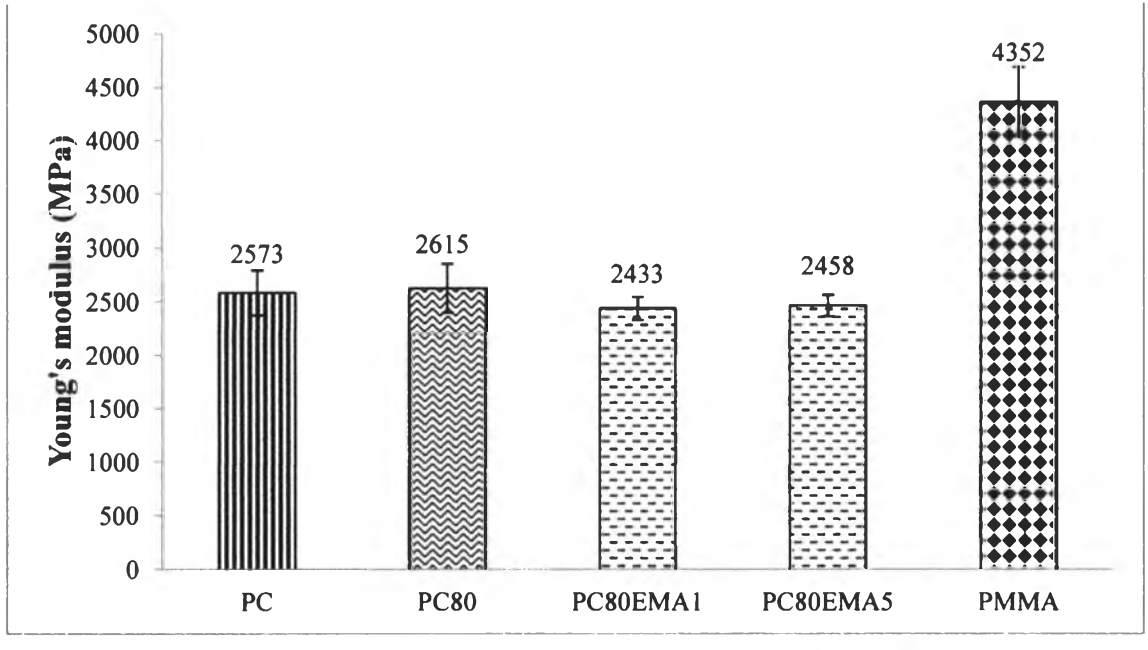

Figure 4.48 Young's modulus of PC, PMMA, and PC80/EMA alloys.

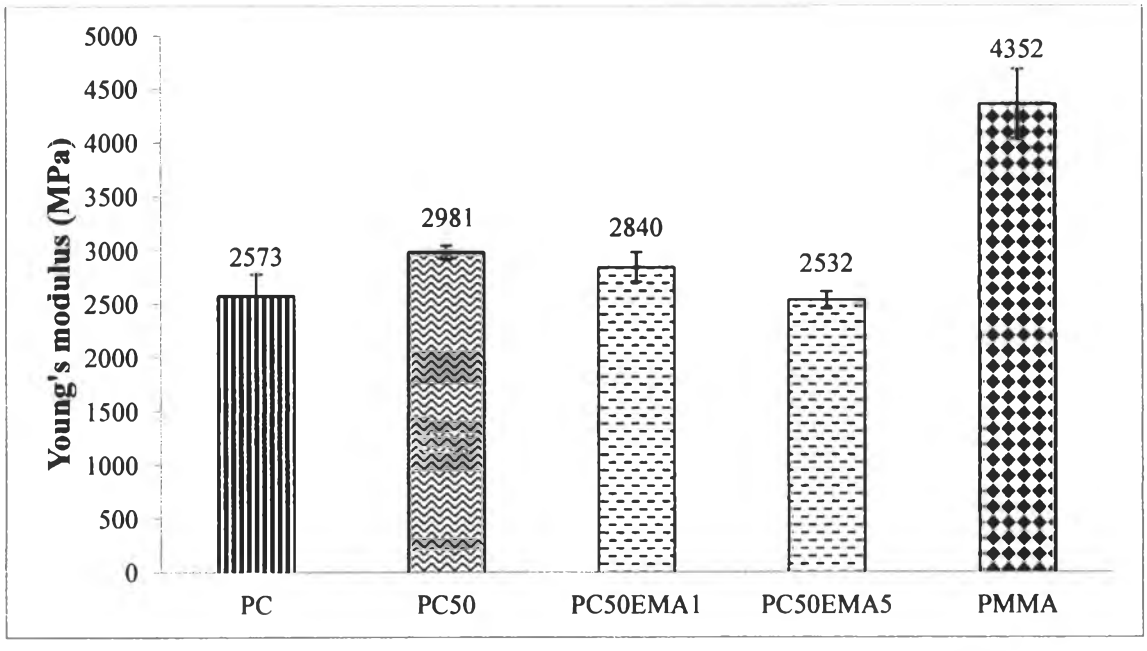

Figure 4.49 Young's modulus of PC, PMMA, and PC50/EMA alloys.

4.3.4.2 Flexural properties

Figure 4.50-4.53 exhibit the flexural strength and flexural modulus of PC/PMMA alloys with EMA. According to this result, both of flexural strength and flexural modulus tended to decrease when increased the EMA content. It was due to the soft segment of EMA phases inside the PC/PMMA that led to the lower rigidity of the alloys.

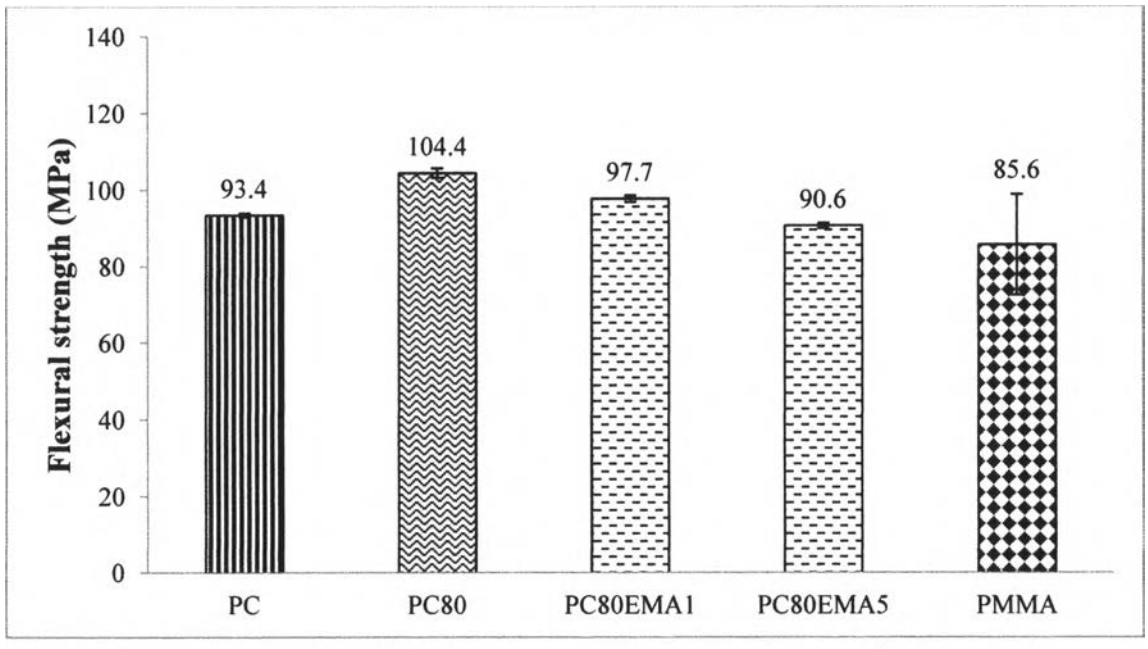

Figure 4.50 Flexural strength of PC, PMMA, and PC80/EMA alloys.

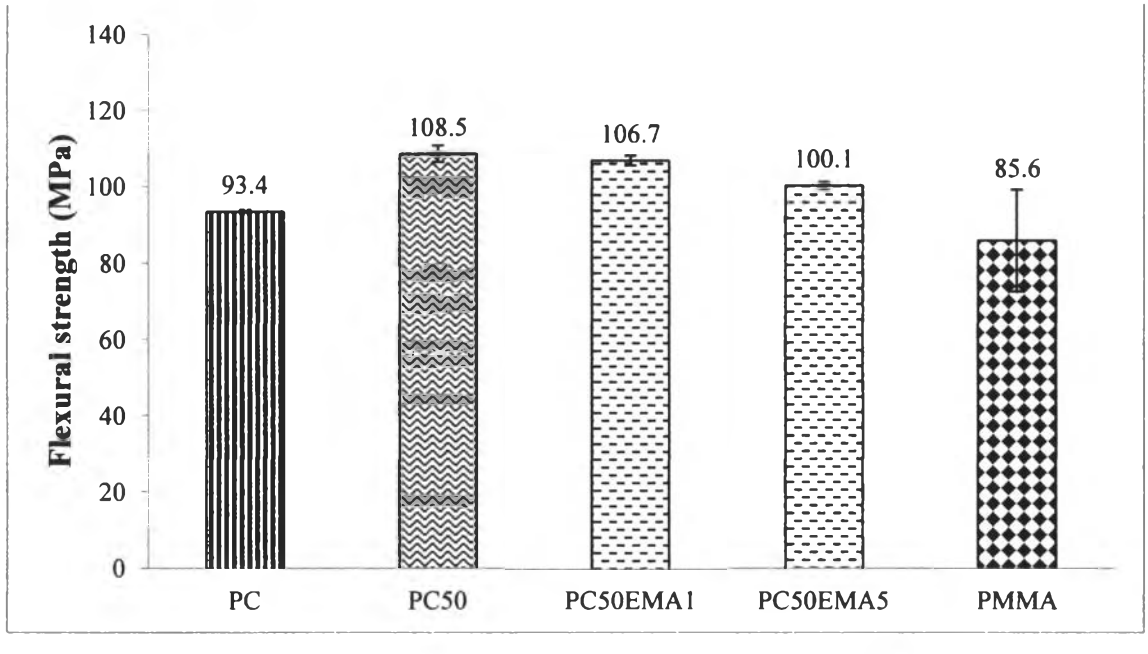

Figure 4.51 Flexural strength of PC, PMMA, and PC50/EMA alloys.

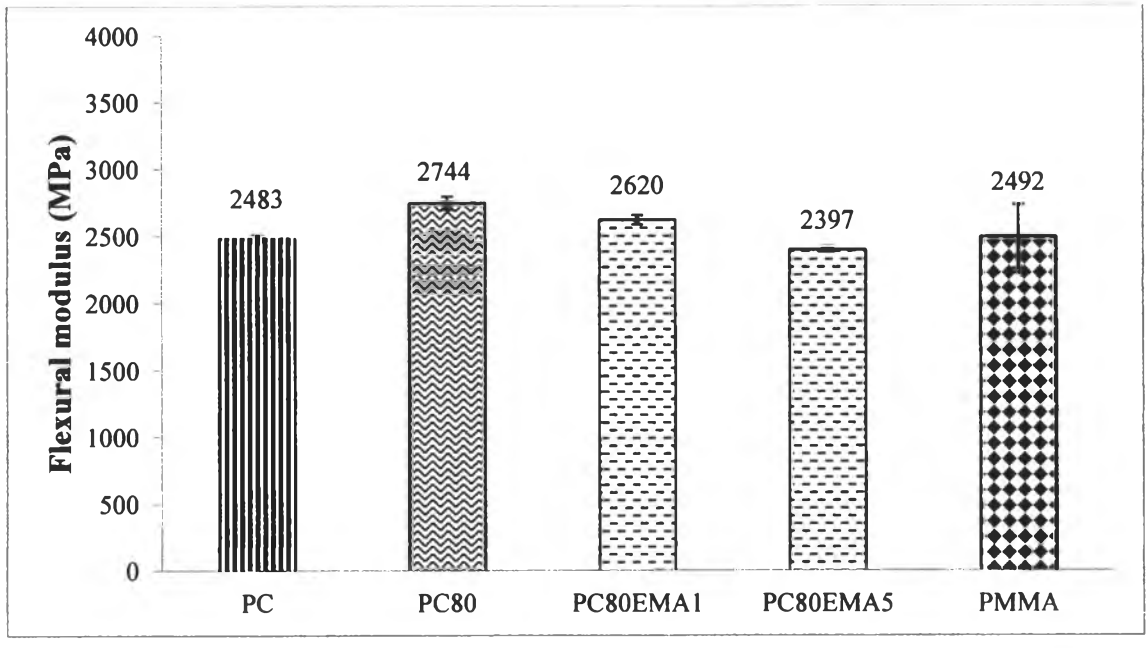

Figure 4.52 Flexural modulus of PC, PMMA, and PC80/EMA alloys.

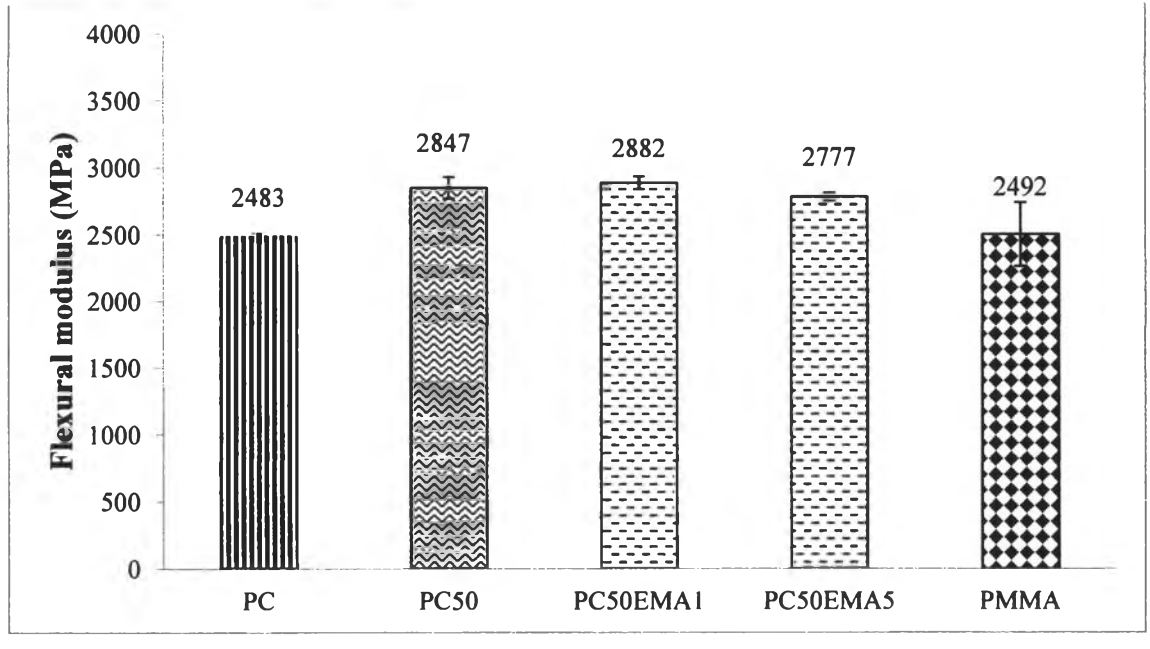

Figure 4.53 Flexural modulus of PC, PMMA, and PC50/EMA alloys.

4.3.4.3 Notched Izod Impact properties

Figure 4.54 and 4.55 show the notched izod impact strengths of PC/PMMA alloys after adding EMA. It was found that the inclination of impact strengths of PC80/PMMA20 with elastomer, EMA, increased with increasing the amount of EMA. The composition of PC80 with 5 phr EMA gave the best impact strength which closed to neat PC. The reason was the effect of elastomeric phase, EMA, in the PC/PMMA. The soft segment of EMA was able to reduce the stiffness and increased the toughness of the alloys which resulted in the improvement in impact strength of the alloys. In contrast, the addition of EMA into PC50/PMMA50 system did not change the impact strength of alloys significantly. This might be possible to the ratio of EMA to PMMA was not adequate for PC50/PMMA50 composition.

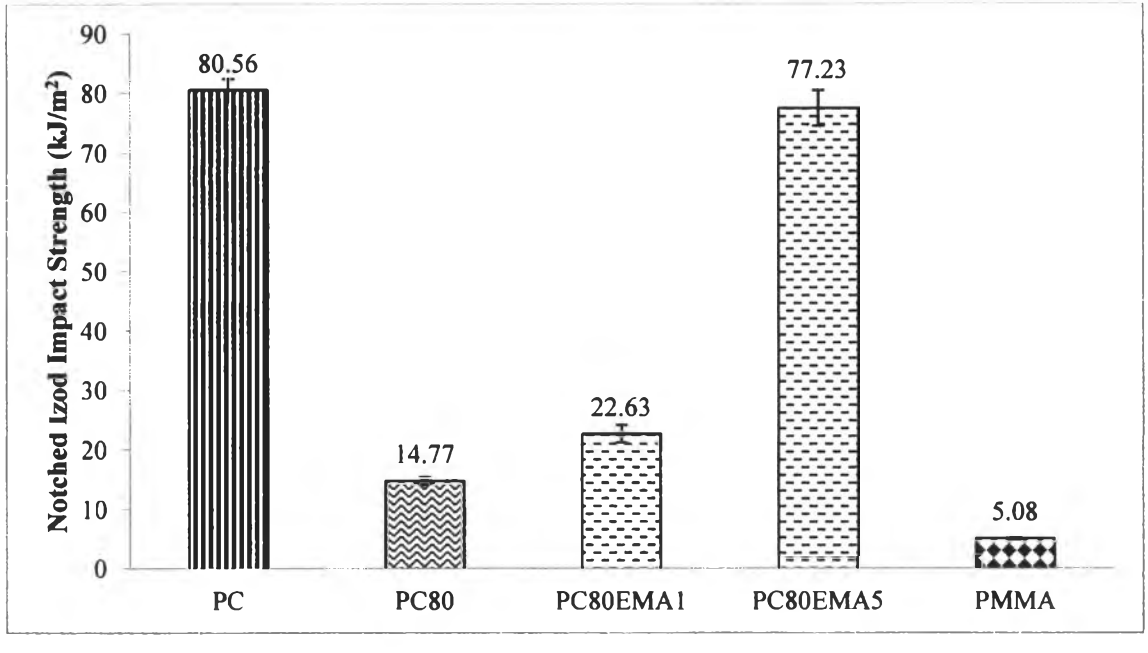

Figure 4.54 Notched izod impact strength of PC, PMMA and PC80/EMA alloys.

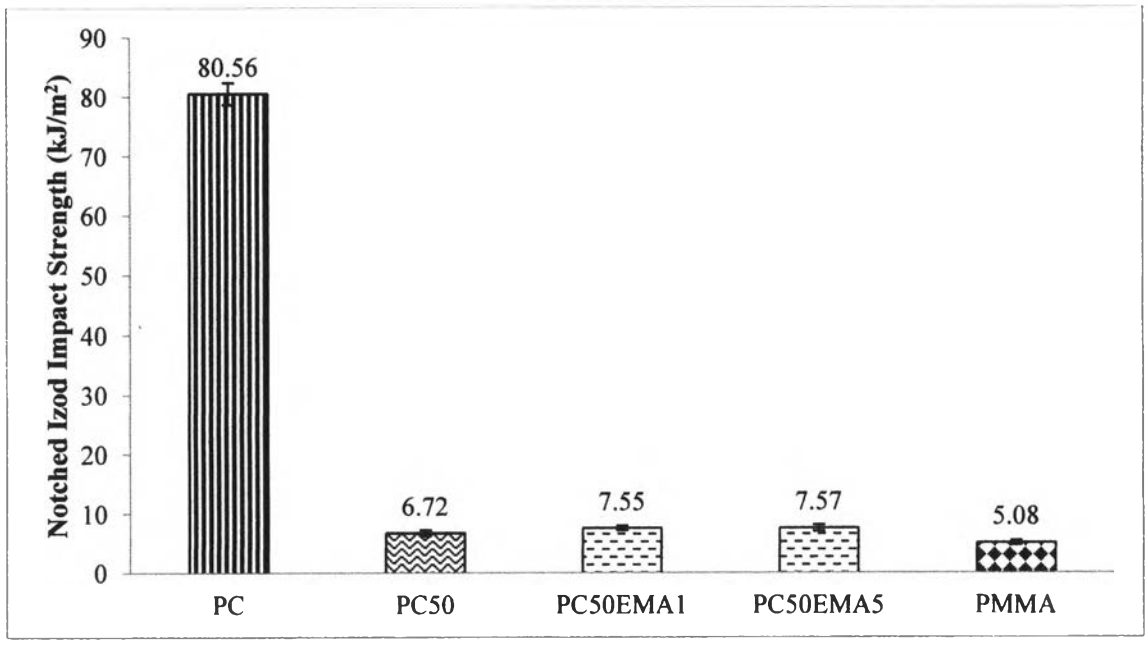

Figure 4.55 Notched izod impact strength of PC, PMMA and PC50/EMA alloys.

4.3.5 Scratch resistance

4.3.5.1 The pencil hardness test

Table 4.1 The pencil hardness grade of PC,PMMA and PC/PMMA/EMA alloys

Formulas	Pencil hardness grade
PC	F
PC80	3H
PC80EMA5	2H
PC50	4H
PC50EMA5	3H
PMMA	7H

The pencil hardness test is one of the simple and effective techniques to evaluate the surface hardness of the materials which is determined by

pencil grades as can be seen in Scheme 2. The hardest and softest are 9H and 9B, respectively. The middle of the hardness scale is F. Table 4.1 reports the pencil hardness grade of surface hardness of PC, PMMA, uncompatibilized PC/PMMA alloys and PC/PMMA/EMA alloys. It is indicate that PC has lower scratch resistance than PMMA and the surface hardness increase with increasing in PMMA content. In addition, the addition of EMA into PC/PMMA alloys can cause the surface hardness of the alloys become softer. Thus it can be note that EMA can as a softener for PC/PMMA alloys.

Softest ←																		→ Hardest
9B	8B	7B	6B	5B	4B	3B	2B	B	HB	F	H	2H	3H	4H	5H	6H	7H	8H	9H

Scheme 2. The pencil hardness scale.

4.4 Compatibilized PC/PMMA Alloys with Ethylene/Methyl acrylate/Glycidyl methacrylate terpolymer (EMG)

4.4.1 Physical properties

4.4.1.1 Rheological properties

The flowability was determined by MFI of the materials. Figure 4.56 and 4.57 present the MFI of PC, PMMA and PC/PMMA alloys in the presence of EMG. The inclination of MFI of uncompatibilized PC/PMMA alloys increased with increasing in PMMA content because PMMA has lower thermal stability and easy to flow at high temperature when compared with PC. However, the MFI of PC/PMMA alloys slightly decresased after adding EMG. The reason is the reaction of glycidyl group of EMG and hydroxyl group at the chain end of PC and methyl acrylate part of EMG also can be compatible with PMMA. Thus, the addition of EMG at 1 and 3 phr into PC80 and PC50 exhibited insignificant changing in MFI.

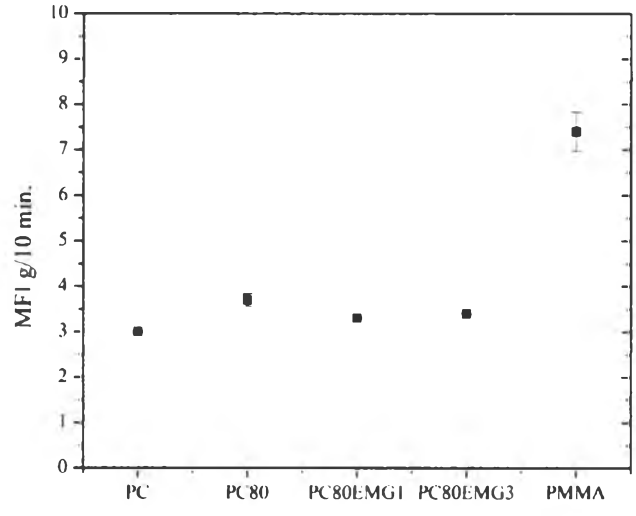

Figure 4.56 Melt Flow Index of PC, PMMA and PC80/EMG alloys.

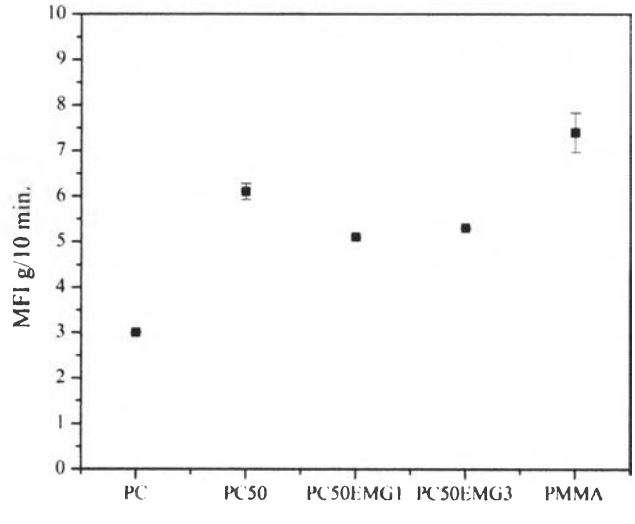

Figure 4.57 Melt Flow Index of PC, PMMA and PC50/EMG alloys.

4.4.2 Thermal properties

4.4.2.1 Temperature decomposition characterization

Thermal stability of alloys was studied by using TGA. Figure 4.58 and 4.59 exhibit the onset degradation temperature of PC80 and PC50 with EMG, respectively. The degradation temperature (T_d) of PC80/PMMA20 containing EMG gradually increased with increasing EMG content while the percentage weight loss tended to decrease. In the case of PC50, the addition of EMG did not affect to both of T_d and percentage weight loss of the alloys. They showed indifferent from uncompatbilized system. It was indicated that the addition of EMG into PC/PMMA alloys improved the thermal stability for only the PC80/PMMA20 composition. This characteristic implied that the obtained properties of the alloys were related to the ratio between polymer matrix and compatibilizer.

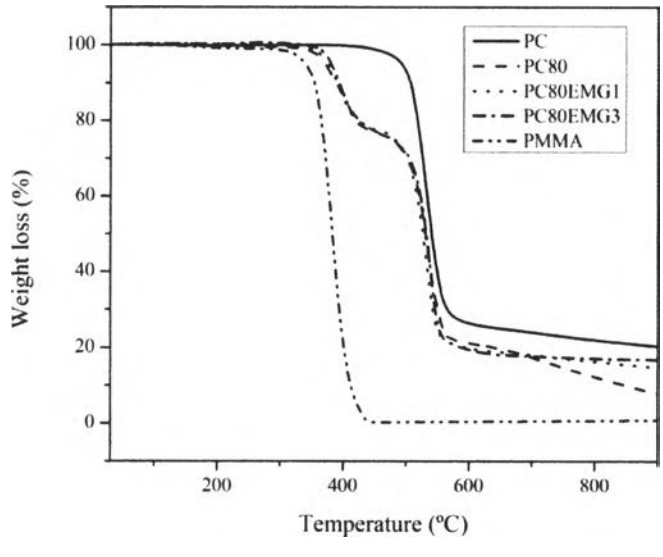

Figure 4.58 TGA plots of PC, PMMA and PC80/EMG alloys.

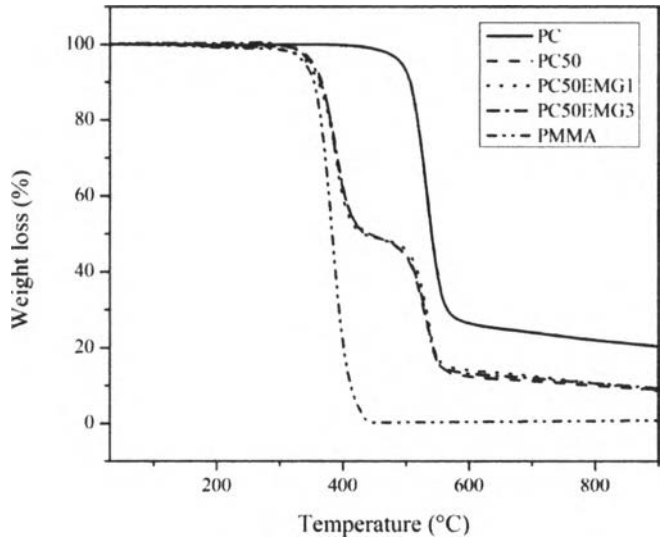

Figure 4.59 TGA plots of PC, PMMA and PC50/EMG alloys.

4.4.3 Miscibility

4.4.3.1 Glass transition temperature observation

The glass transition temperature (T_g) of PC/PMMA alloys with various EMG contents was observed by DSC. Figure 4.60 and 4.61 show the second heating of DSC thermograms of PC,PMMA and PC/PMMA alloys with EMG. According to this result, the glass transition temperature of PC and PMMA is approximately 139.1 and 107.1, respectively. Due to the entrapment of minor phase (PMMA), the uncompatibilized PC80/PMMA20 exhibited single T_g corresponding to PC-rich phase. When adding EMG into the system, the single T_g of alloys tend to increase when the amount of EMG increased. In the case of PC50, the two distinct T_gs was observed and still did not shift inward after adding EMG. Then, it can be noted that the addition of EMG did not improve the miscibility of the alloys.

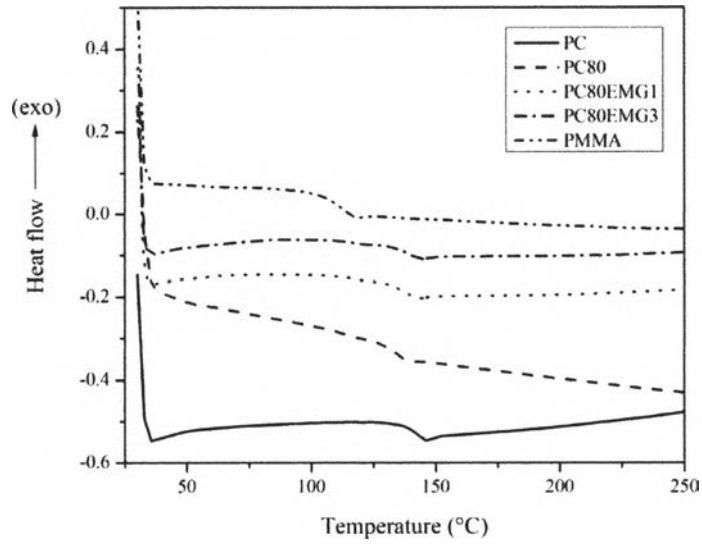

Figure 4.60 DSC plots (second heating) of PC, PMMA and PC80/EMG alloys.

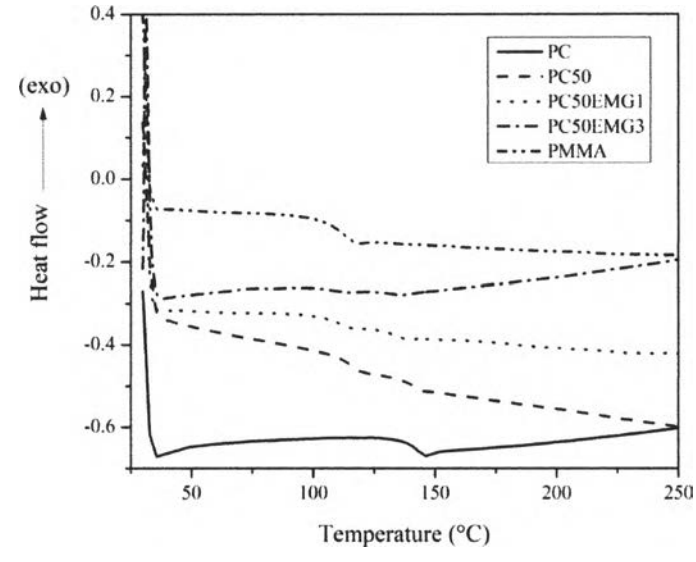

Figure 4.61 DSC plots (second heating) of PC, PMMA and PC50/EMG alloys.

The T_g observation can be evaluated by tan δ peak from DMA technique. Figure 4.62 and 4.63 exhibit the single T_g of PC80/EMG and PC50/EMG alloys, respectively. According to this result, the single Tg of PC80 having EMG was similar to the uncompatbilized system. However, the addition of EMG into the composition of PC50 led the T_g of alloys to increase. The reaction between hydroxyl group at the end chain of PC and glycidyl group of EMG can cause the higher molecular weight and the longer polymer chains resulted in the shift of T_g to higher temperature. It can be indicated that the obtained properties was based on the proportion of polymer matrix to compatibilizer and the miscibility of the alloys could not be improved by adding EMG.

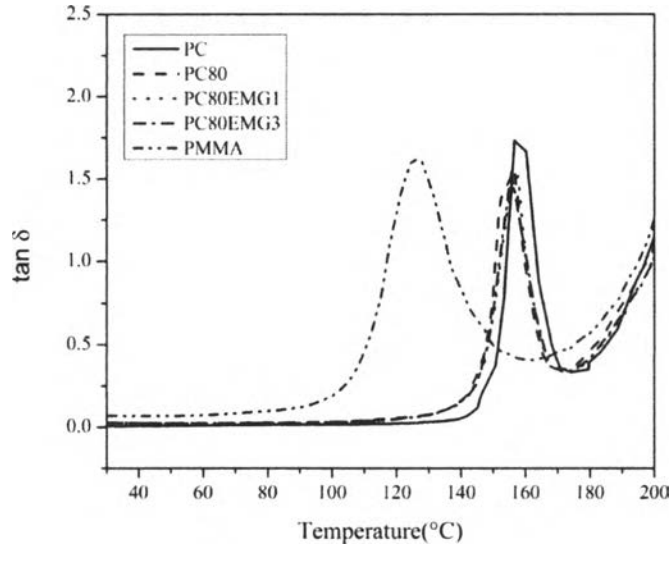

Figure 4.62 DMA plots of PC, PMMA and PC80/EMG alloys.

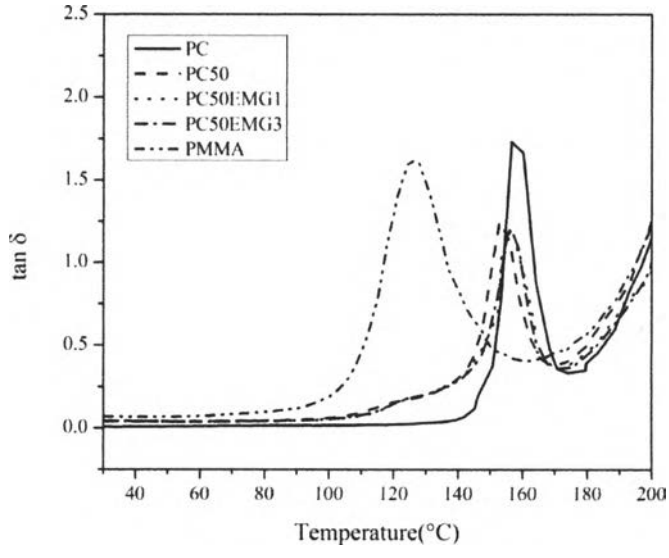

Figure 4.63 DMA plots of PC, PMMA and PC50/EMG alloys.

4.4.4 Mechanical properties

4.4.4.1 Tensile properties

The tensile strength at yield, elongation at yield and Young's modulus of PC/PMMA with EMG were shown in Figure 4.64-4.69. The inclination of tensile strength and Young's modulus of the alloys gradually decreased when increasing EMG content due to the incorporation of elastomeric EMG phase. The addition of EMG elastomer can reduce the stiffness of the alloys and increase the toughness of alloys. Additionally, since PC is a polymer matrix, the tensile elongation at yield results of alloys was in the same range of PC's elongation.

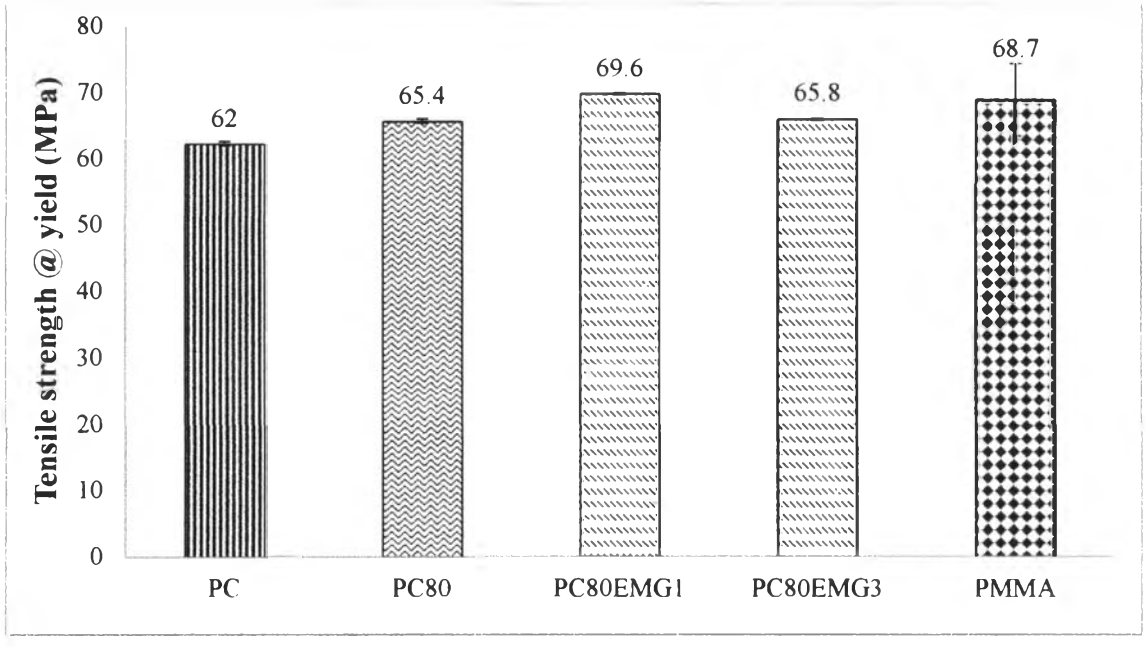

Figure 4.64 Tensile strength at yield of PC, PMMA, and PC80/EMG alloys.

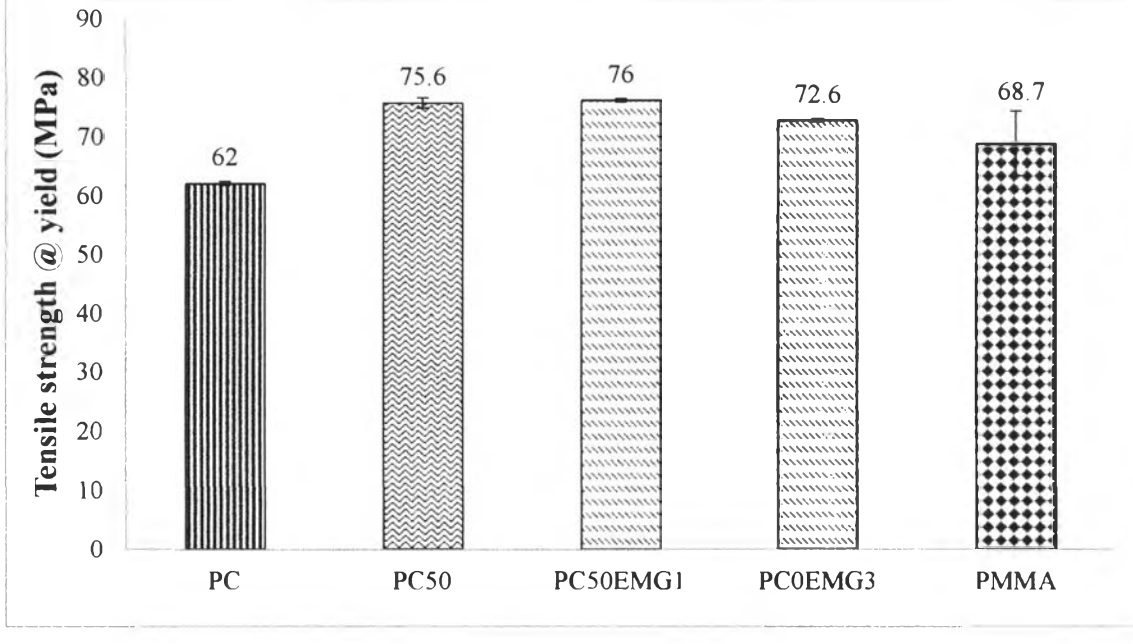

Figure 4.65 Tensile strength at yield of PC, PMMA, and PC50/EMG alloys.

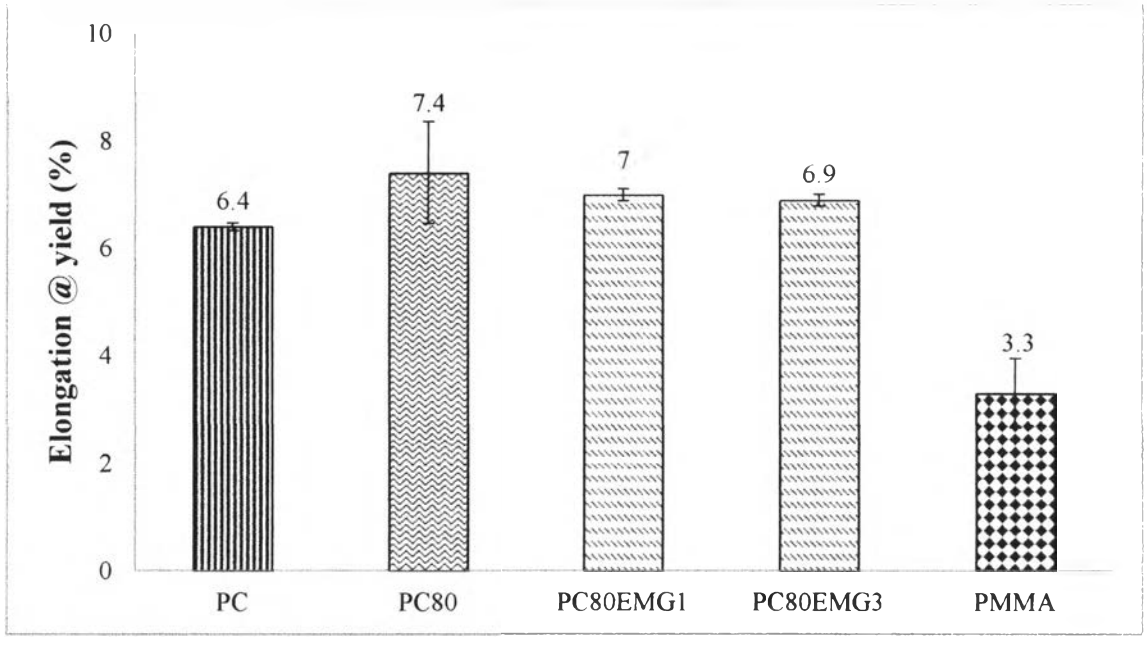

Figure 4.66 Elongation at yield of PC, PMMA, and PC80/EMG alloys.

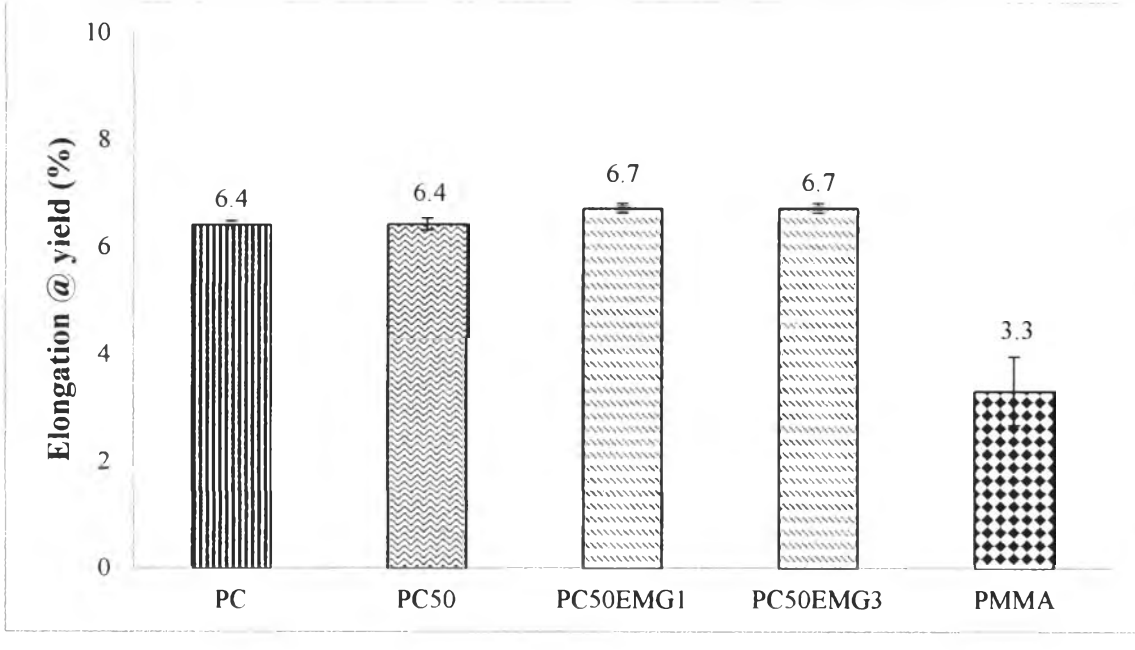

Figure 4.67 Elongation at yield of PC, PMMA, and PC50/EMG alloys.

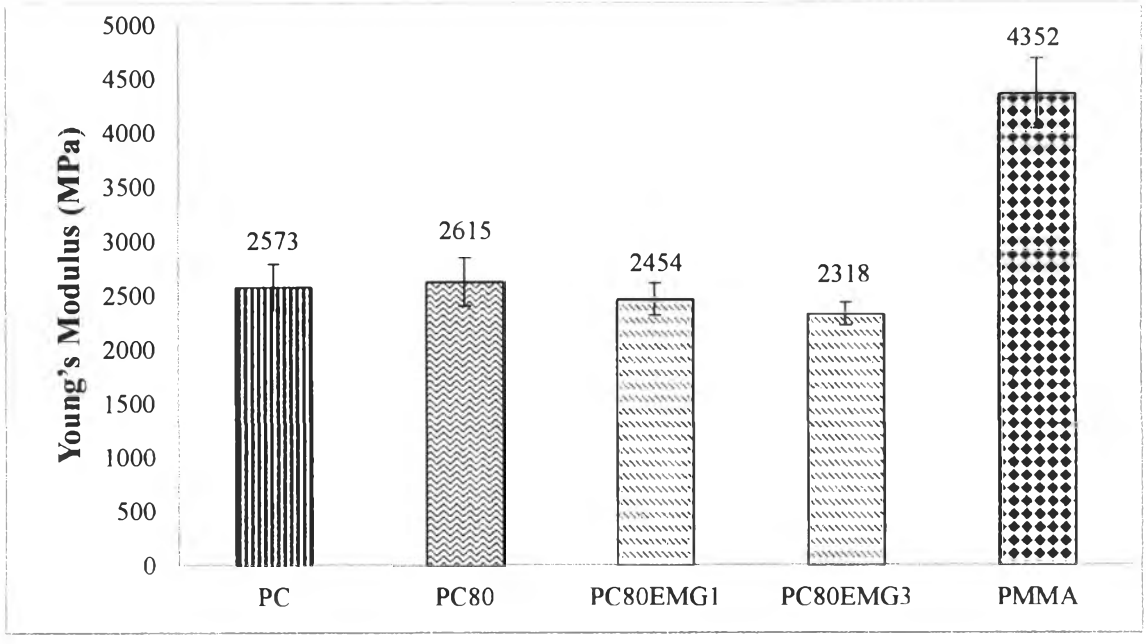

Figure 4.68 Young's modulus of PC, PMMA, and PC80/EMG alloys.

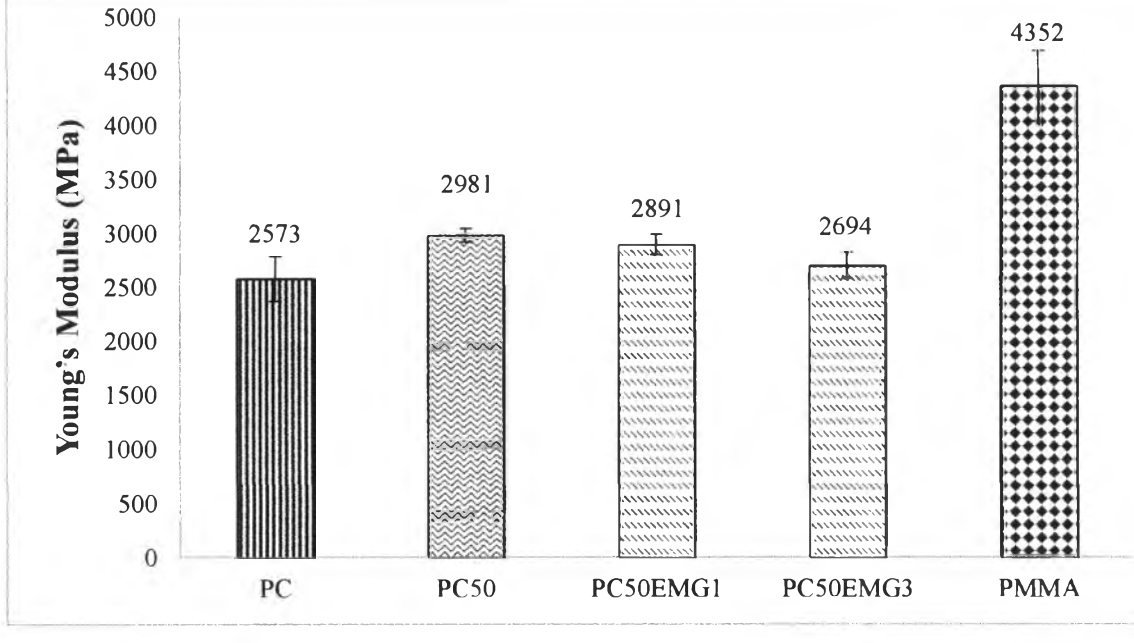

Figure 4.69 Young's modulus of PC, PMMA, and PC50/EMG alloys.

4.4.4.2 Flexural properties

The effect of EMG on the flexural strength and flexural modulus of PC/PMMA alloys were shown in Figure 4.70-4.73 It was found that the flexural strength and flexural modulus of PC/PMMA alloys with EMG tended to decrease with increasing the amount of EMG owing to the elastic property of soft segment of EMG.

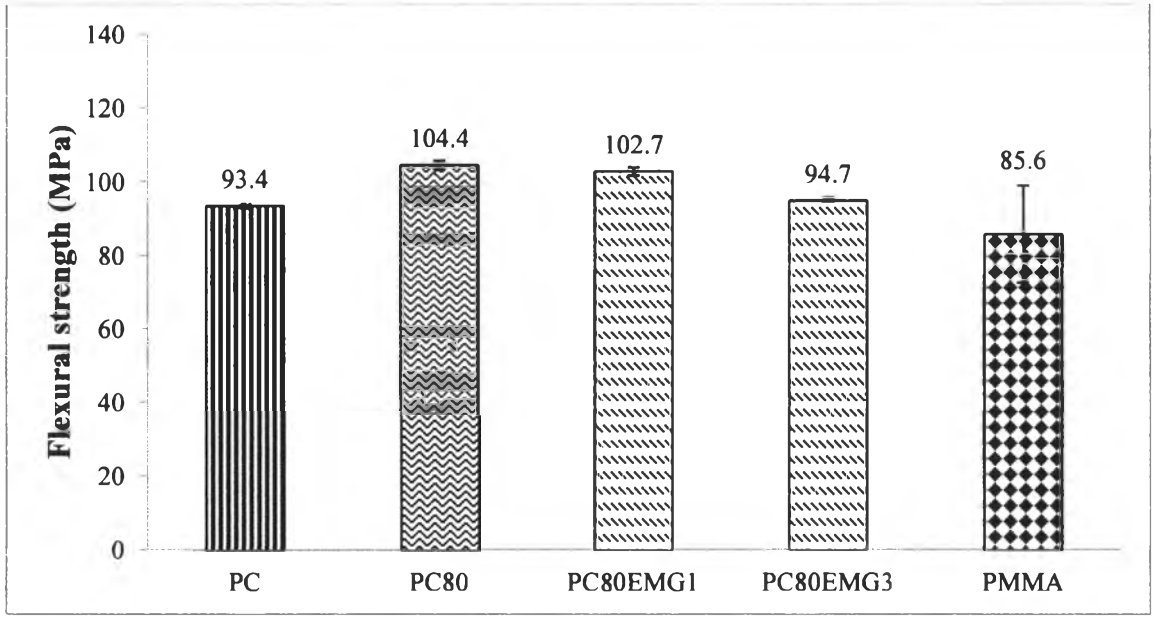

Figure 4.70 Flexural strength of PC, PMMA, and PC80/EMG alloys.

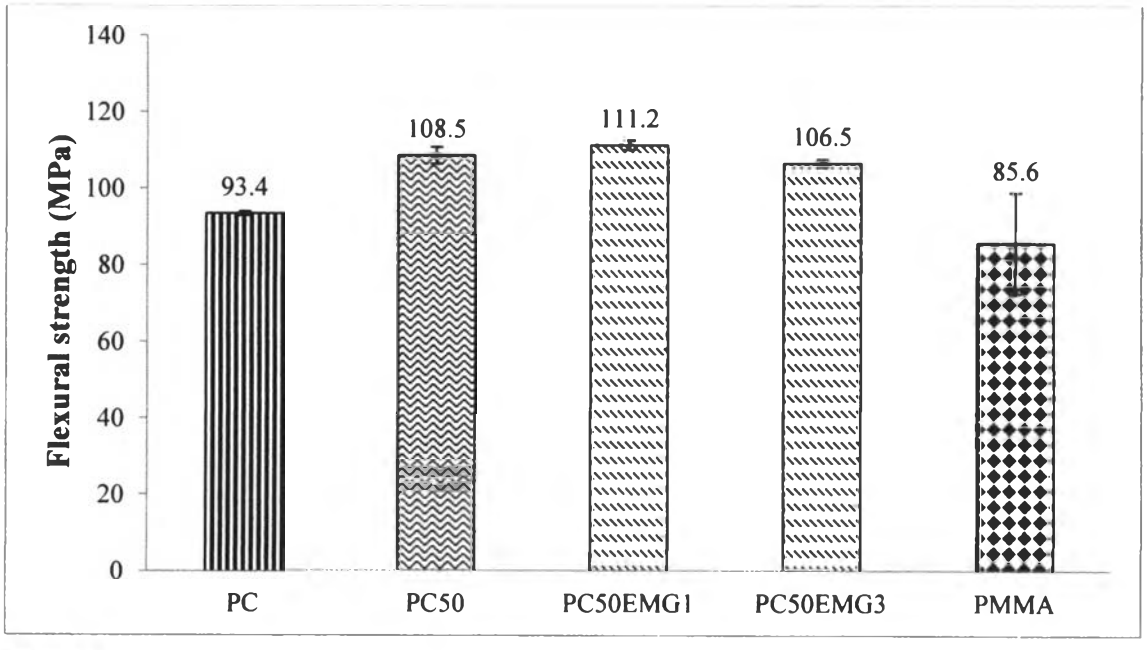

Figure 4.71 Flexural strength of PC, PMMA, and PC50/EMG alloys.

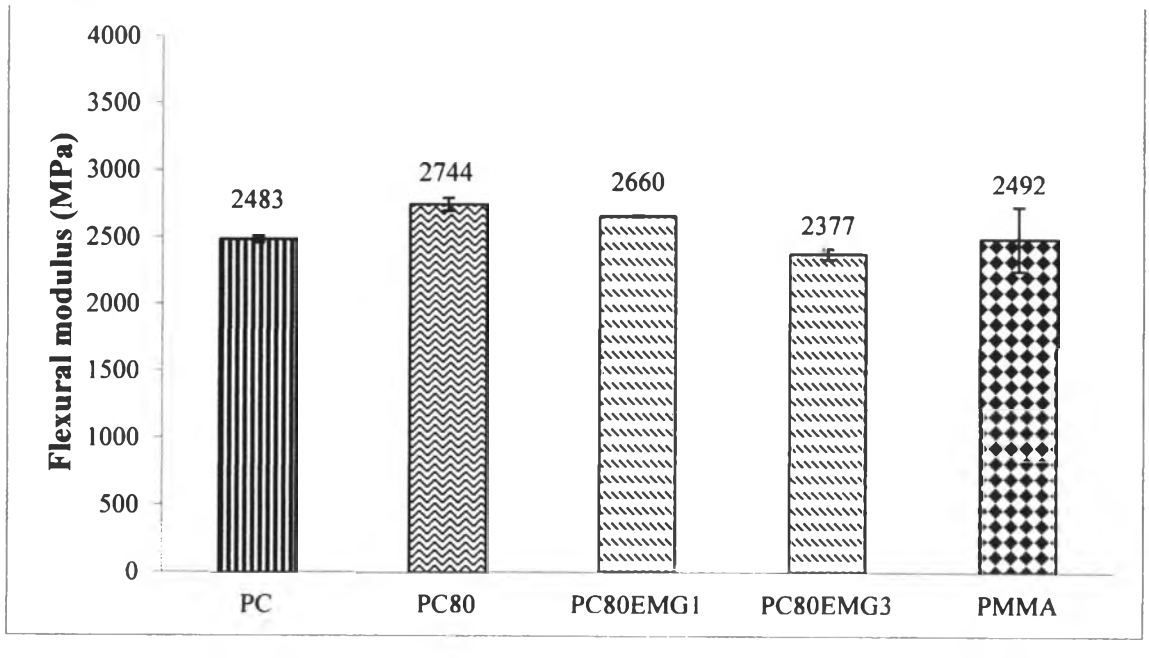

Figure 4.72 Flexural modulus of PC, PMMA, and PC80/EMG alloys.

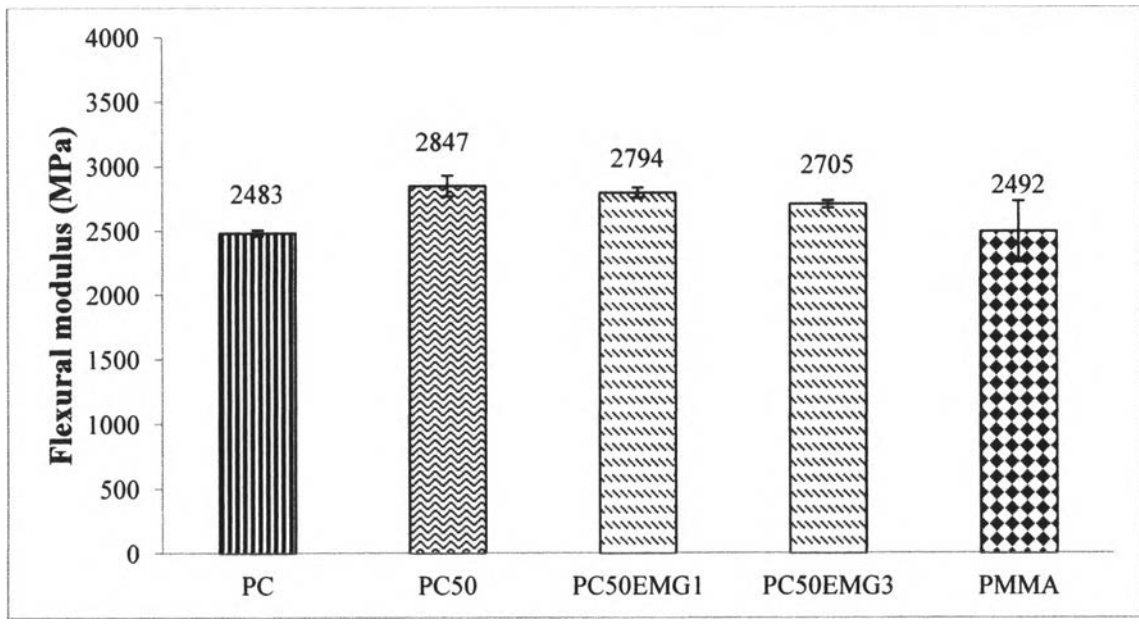

Figure 4.73 Flexural modulus of PC, PMMA, and PC50/EMG alloys.

4.4.4.3 Notched Izod Impact properties

Figure 4.74-4.75 show the notched izod impact strengths of PC/PMMA alloys with EMG. It was found that the impact strengths of PC80/PMMA20 with EMG abruptly increased when 1 phr of EMG was added and the impact strength of this composition was higher than PC. The reason was the effect of elastomeric phase, EMG, in the PC/PMMA. The soft segment of EMG was able to reduce the stiffness and increased the toughness of the alloys. However, the impact strength of PC80 was prone to decrease when the EMG content was more than 1 phr. It was possible due to the excess of EMG content. Then, the composition of PC80 with 1 phr EMG gave the best impact strength which resulted in the improvement in impact strength of the alloys. In the case of PC50, the addition of EMA into the alloys showed the insignificant change of the impact strength. This might be possible to the ratio of EMG to PMMA was not adequate for PC50/PMMA50 composition

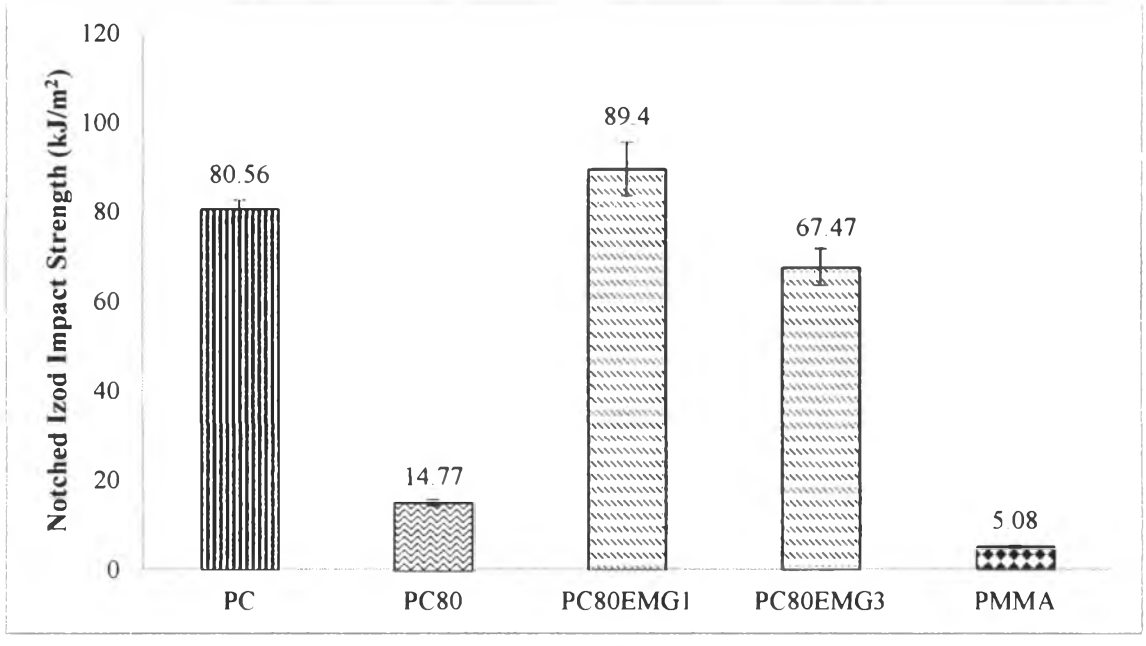

Figure 4.74 Notched izod impact strength of PC, PMMA and PC80/EMG alloys.

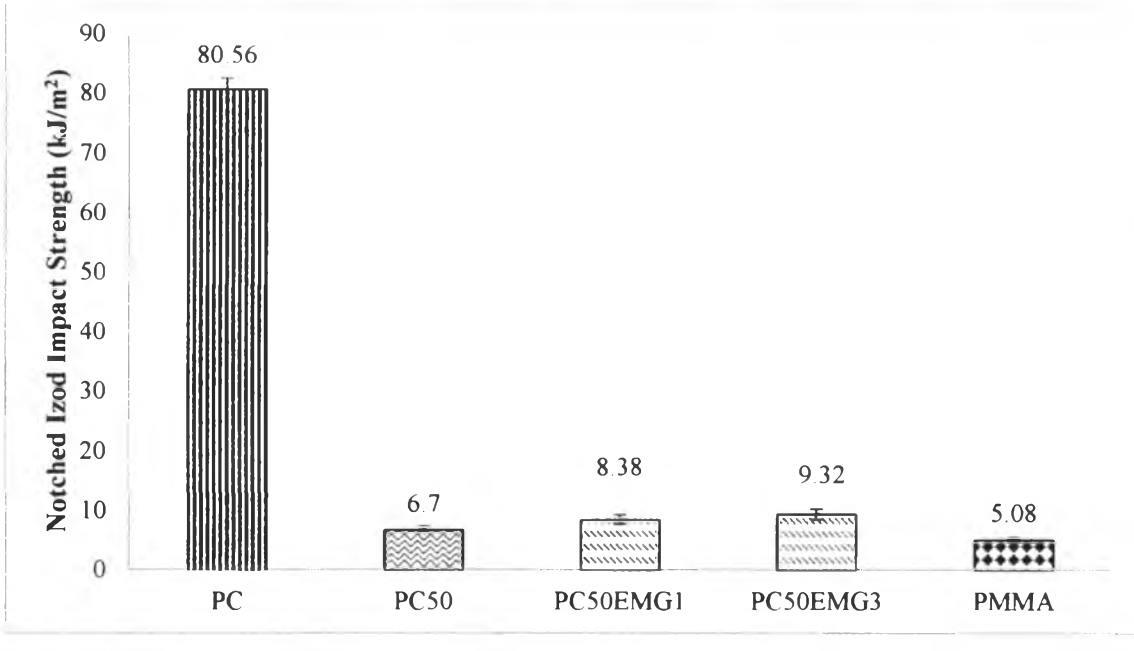

Figure 4.75 Notched izod impact strength of PC, PMMA and PC50/EMG alloys.

4.5 Compatibilized PC/PMMA Alloys with Poly(ethylene-*co*-methacrylic acid (EMAA(Zn))

4.5.1 Physical properties

4.5.1.1 Rheological properties

The flowability of PC/PMMA alloys were identified by melt flow index (MFI) measurement at 250°C with the hammer weighted 2.16 kg. For uncompatibilized system, MFI of alloys increased with increasing PMMA content. Figure 4.76-4.77 present MFI of PC, PMMA and PCPMMA alloys with EMAA(Zn). The addition of EMAA(Zn) into PC/PMMA system showed insignificant effect to the flowability of the compounds which their MFI did not differ from unconpatibilized system. It was likely to decrease when EMAA(Zn) was added as can be obviously seen in PC50/EMAA(Zn). The effect of EMAA(Zn), poly(ethylene-co-methacrylic acid) zinc salt, on the flowability was different from EMAA, poly(ethylene-co-methacrylic acid) sodium salt due to the different complex structure of each ionomer. For PC/PMMA/EMAA(Zn) system, the reaction between PC, PMMA and EMAA(Zn) can also take place as the pevious discussion (PC/PMMA alloys with EMAA). On the other hand, the zinc carboxylate groups of EMAA(Zn) was not active as sodium carboxylate groups of EMAA to induce the degradation reaction.

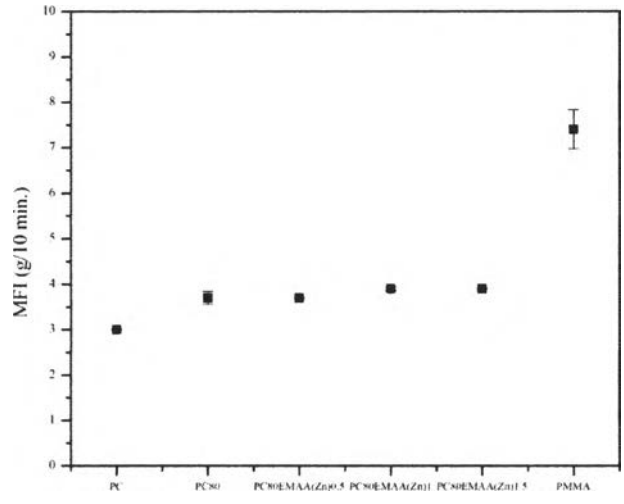

Figure 4.76 Melt Flow Index of PC, PMMA and PC80/EMAA(Zn) alloys.

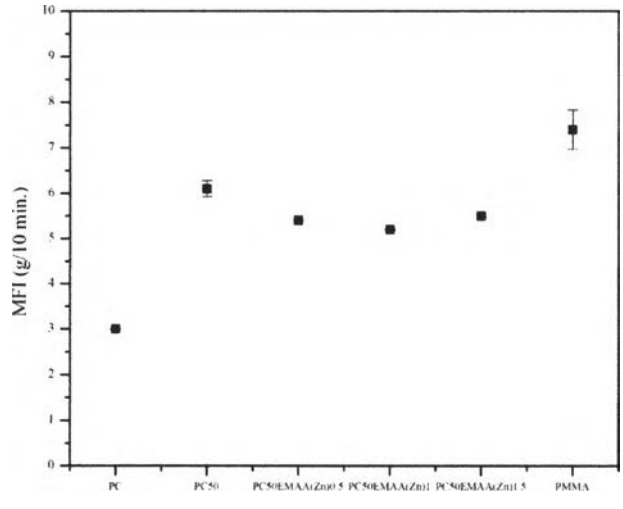

Figure 4.77 Melt Flow Index of PC, PMMA and PC50/EMAA(Zn) alloys.

4.5.2 Thermal properties

4.5.2.1 Temperature decomposition characterization

Figure 4.78-4.79 exhibit the onset degradation temperature of PC80 and PC50 with EMAA(Zn), respectively. The addition of EMAA(Zn) led the degradation temperature (T_d) of PC80/PMMA20 to increase while the percentage weight loss slightly decreased. In contrast, the T_d of PC50 slightly decreased but the percentage weight loss tended to increase after adding EMAA(Zn). It was noticeable that the addition of EMAA(Zn) into PC/PMMA alloys enhanced the thermal stability for only the PC80/PMMA20 composition. This characteristic implied that the obtained properties of the alloys depended on the ratio between polymers and compatibilizer.

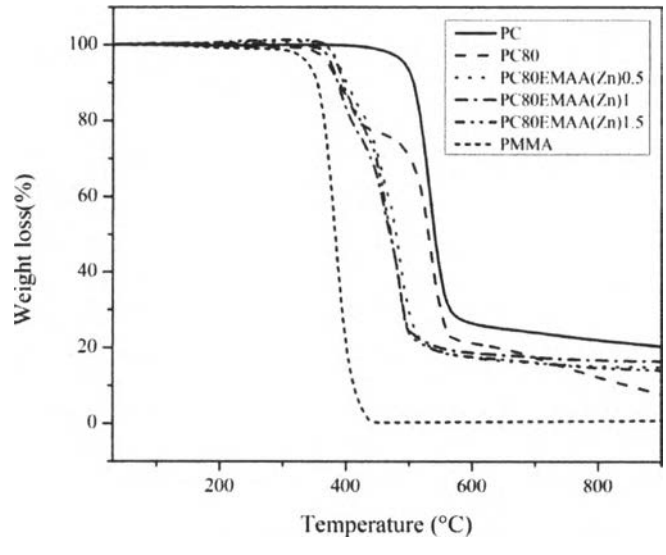

Figure 4.78 TGA plots of PC, PMMA and PC80/EMAA(Zn) alloys.

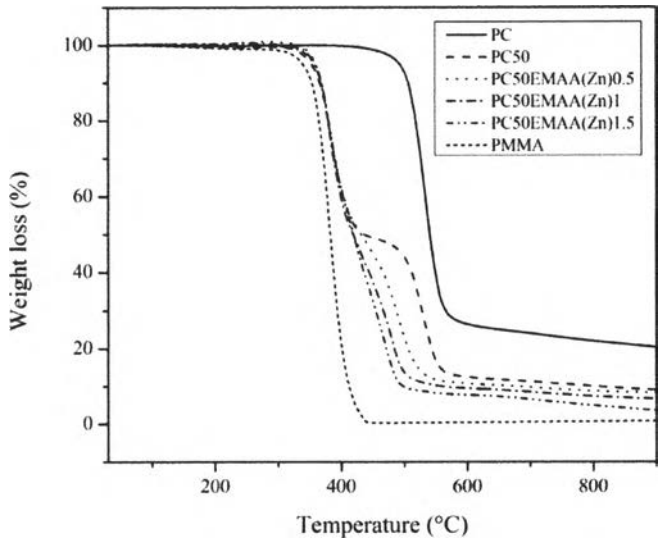

Figure 4.79 TGA plots of PC, PMMA and PC80/EMAA(Zn) alloys.

4.5.3 Miscibility

4.5.3.1 Glass transition temperature observation

Blending of PC and PMMA, the two distinct glass transition temperatures (2 T_gs) were clearly observed when PMMA content increased. Then, the combination of PC and PMMA showed the immiscible PC/PMMA alloys. In order to enhance the miscibility of these alloys, the compatibilizer was needed. For this section, EMAA(Zn) was use as a compatibilizer. DSC results (Figure 4.80 and 4.81) showed the single glass transition temperature (T_g) of alloys which was likely to increase after adding EMAA(Zn) For the case of PC50, the trend of T_g after adding EMAA(Zn) was opposite to PC80. It still showed two distinct T_g which slightly shift to lower temperature. This phenomenon was possible due to the plasticization effect of EMAA(Zn) resulting in the shifting of T_g to lower temperature. However, these two Tg did not shift inward. So the miscibility of PC/PMMA also was not improved by adding EMAA(Zn) From this result, it can be noted that the effect of EMAA(Zn) on the properties of alloys depend on the composition of polymers and the ratio of polymers to the compatibilizer.

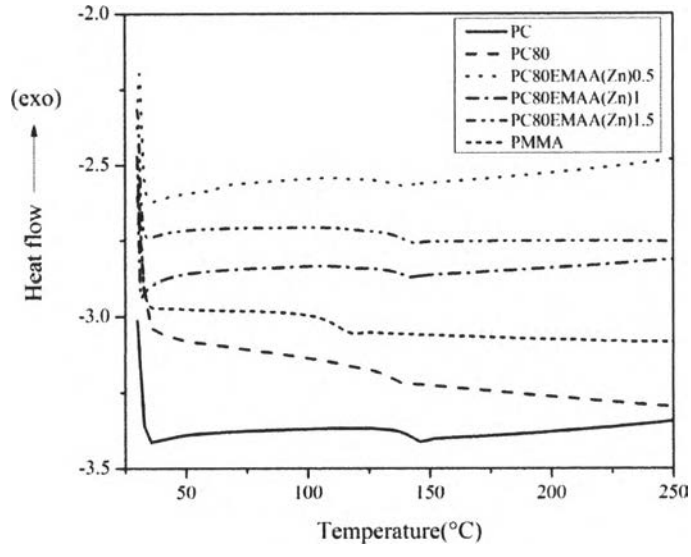

Figure 4.80 DSC plots (second heating) of PC, PMMA and PC80/EMAA(Zn) alloys.

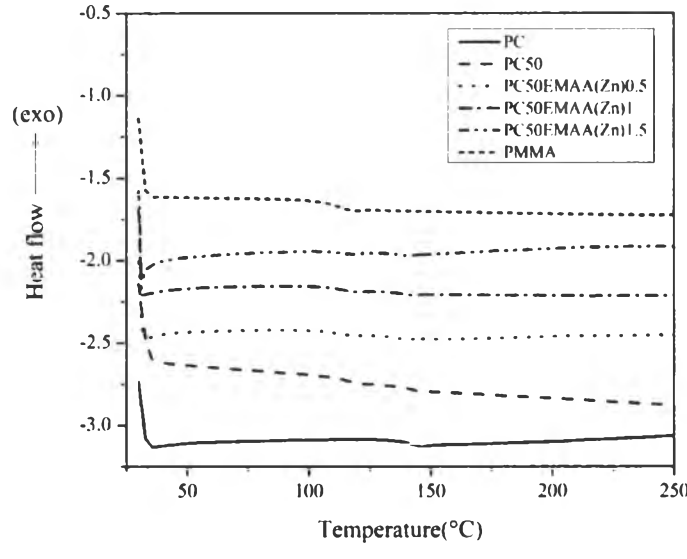

Figure 4.81 DSC plots (second heating) of PC, PMMA and PC50/EMAA(Zn) alloys

In this study, DMA was used to determine the glass transition temperature (T_g) of PC/PMMA with EMA which this T_g was indicated by the tan δ peak. Figure 4.82 and 4.83 exhibit the T_g of PC80/EMA and PC50/EMA alloys, respectively. The single T_g of the alloys was insignificant changing from uncompatibilized system. Based on this result, it could be noted that EMAA(Zn) could not enhance the miscibility of the alloys. This result was related to DSC measurement as mentioned before.

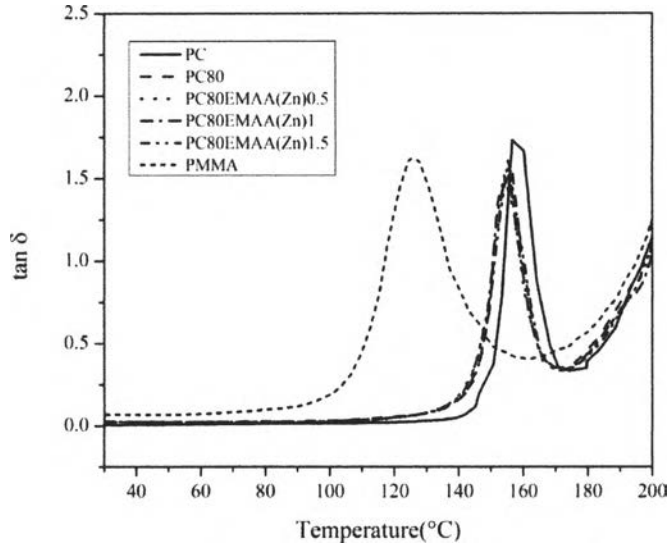

Figure 4.82 DMA plots of PC, PMMA and PC80/EMAA(Zn) alloys.

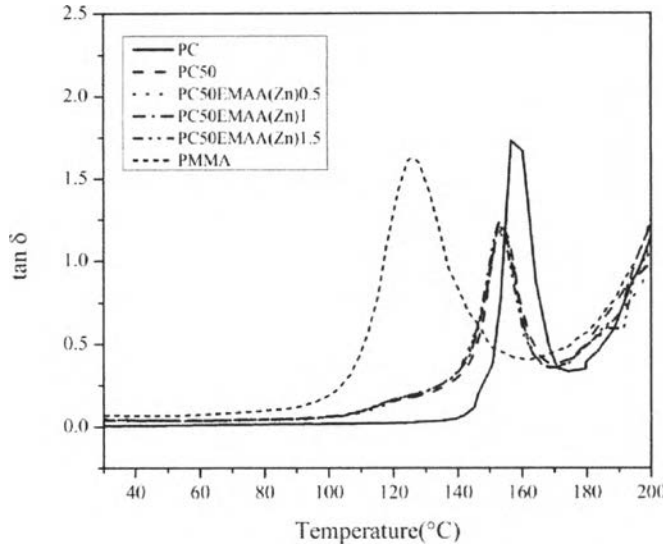

Figure 4.83 DMA plots of PC, PMMA and PC50/EMAA(Zn) alloys.

4.5.4 Mechanical properties

4.5.4.1 Tensile properties

The tensile strength at yield, elongation at yield and Young's modulus of PC/PMMA alloys with EMAA(Zn) is shown in Figure 4.84-4.89. The addition of EMAA(Zn) into PC/PMMA alloys did not significantly affect to the tensile properties. The tensile strength and elongation at yield were in the same range of uncompatibilized system. Additionally, Young's modulus of alloys slightly decrease with increasing EMAA(Zn) content as can be clearly seen in the composition of PC80.

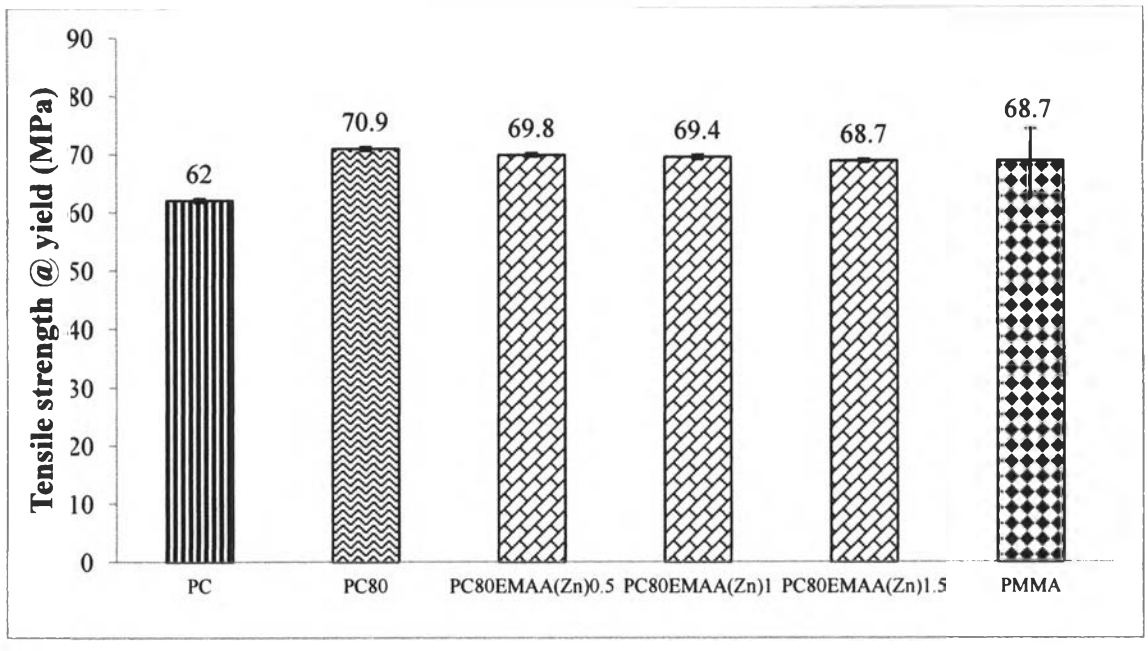

Figure 4.84 Tensile strength at yield of PC, PMMA, and PC80/EMAA(Zn) alloys.

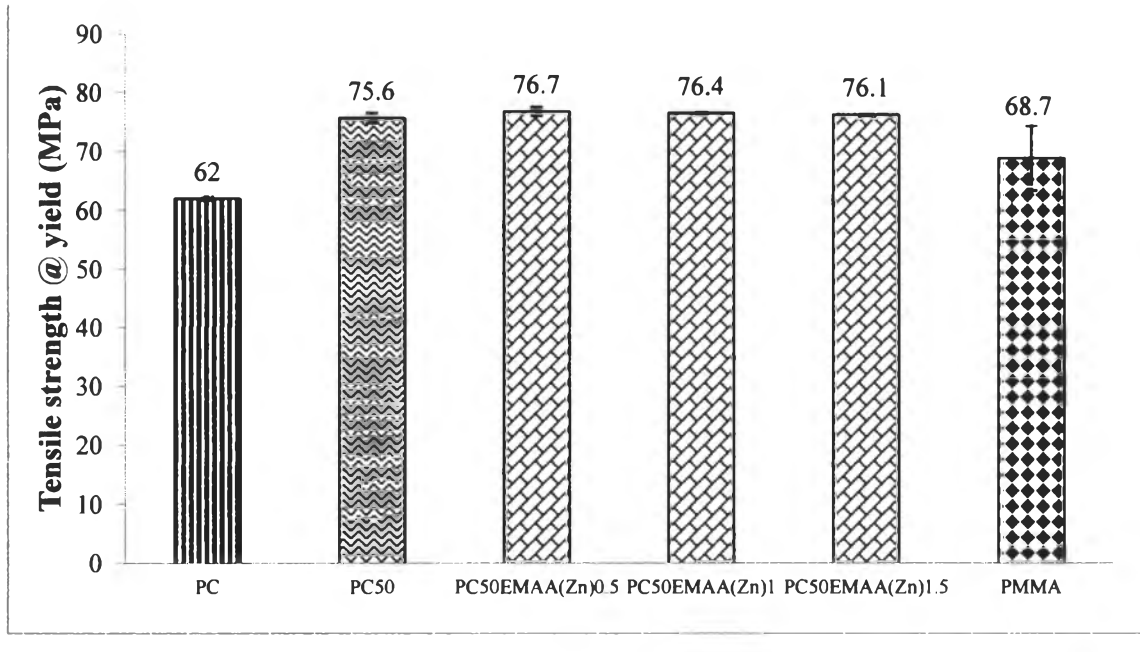

Figure 4.85 Tensile strength at yield of PC, PMMA, and PC50/EMAA(Zn) alloys.

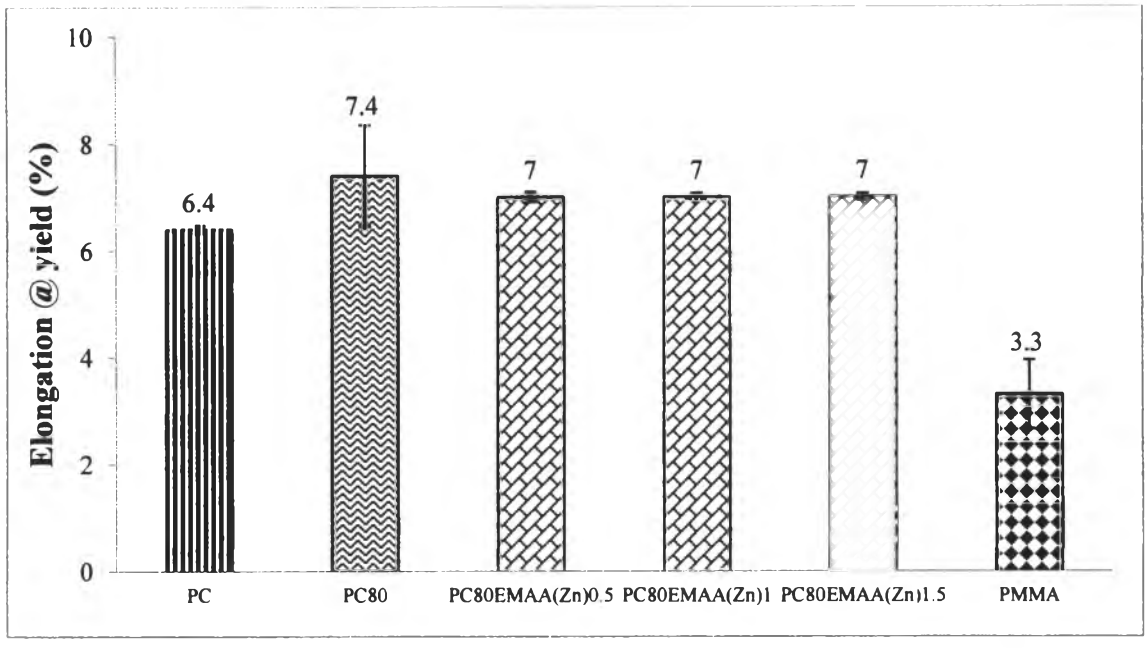

Figure 4.86 Elongation at yield of PC, PMMA, and PC80/EMAA(Zn) alloys.

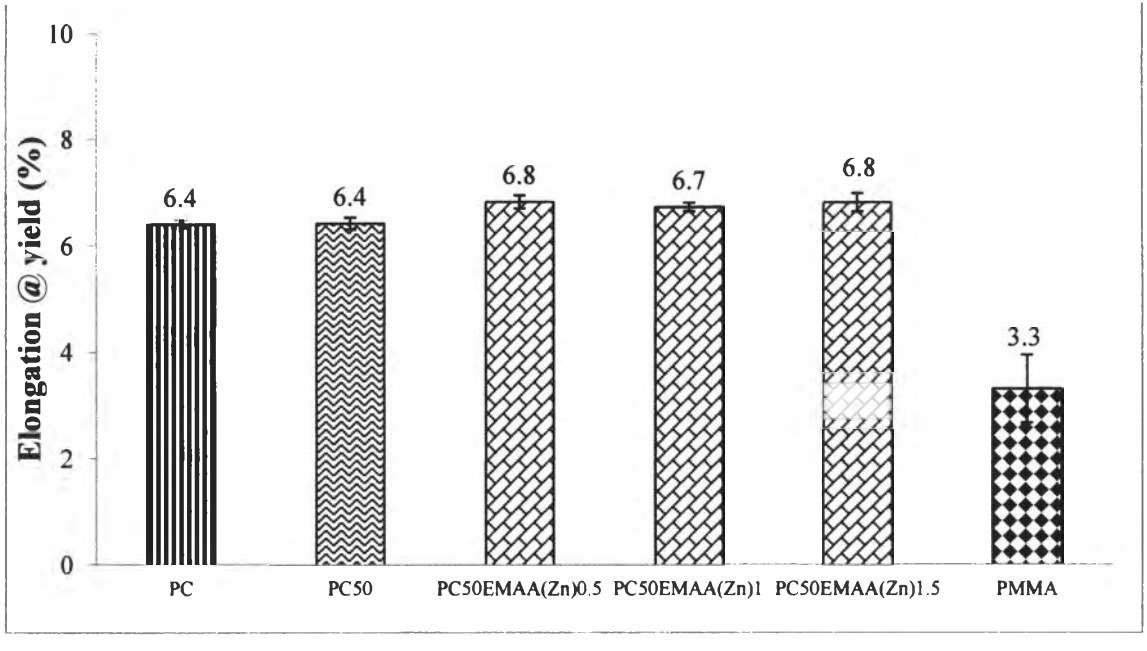

Figure 4.87 Elongation at yield of PC, PMMA, and PC50/EMAA(Zn) alloys.

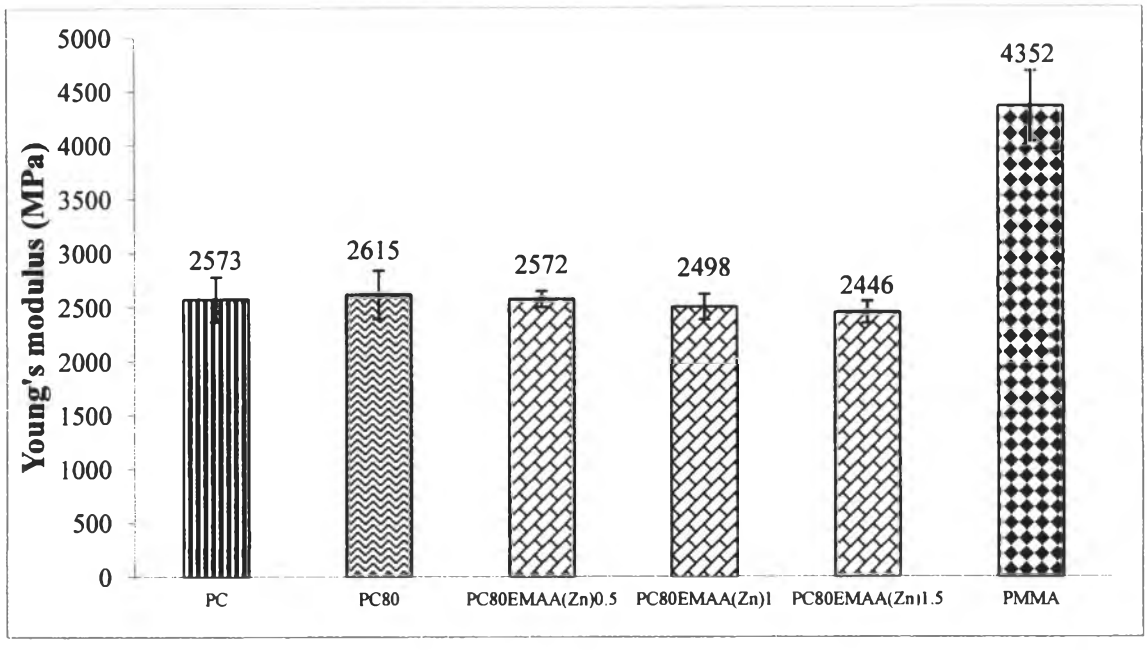

Figure 4.88 Young's modulus of PC, PMMA, and PC80/EMAA(Zn) alloys.

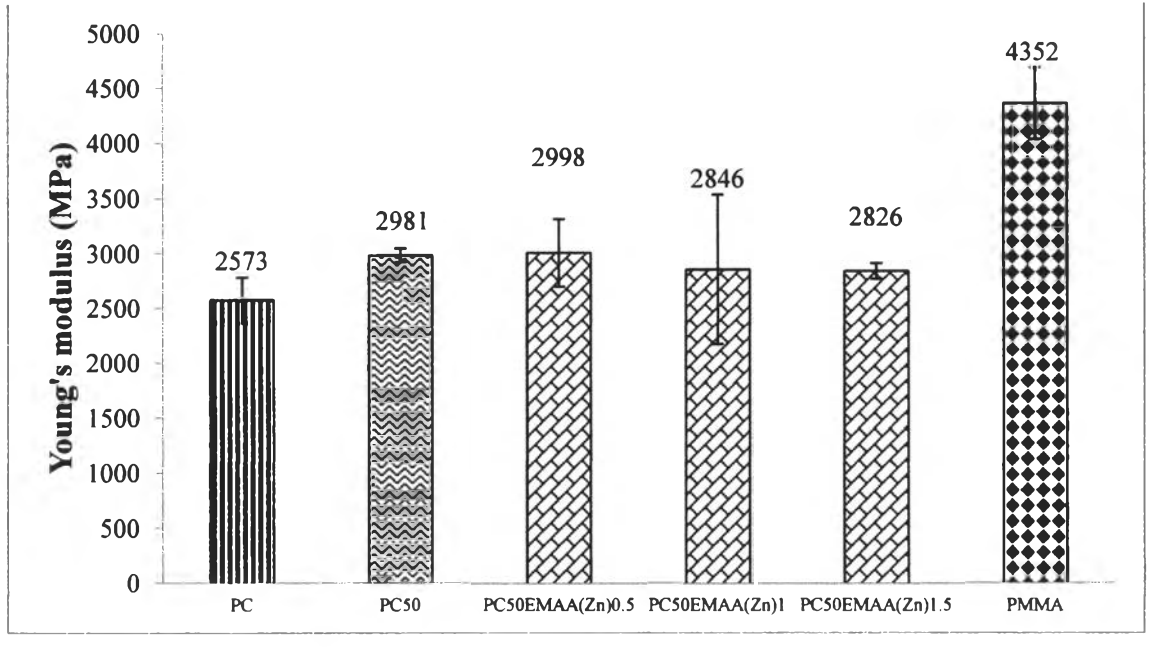

Figure 4.89 Young's modulus of PC, PMMA, and PC50/EMAA(Zn) alloys.

4.5.4.2 Flexural properties

Figure 4.90-4.93 exhibit the flexural strength and flexural modulus of PC/PMMA alloys with EMAA(Zn). According to this result, both of flexural strength and flexural modulus were in the same range of uncompatibilized PC/PMMA alloys. Although the reaction of PC, PMMA and EMAA(Zn) could be occurred, it showed insignificant effect on the tensile properties. So the addition of EMAA(Zn) in the range of 0.5-1.5 phr insignificantly enhanced the tensile properties.

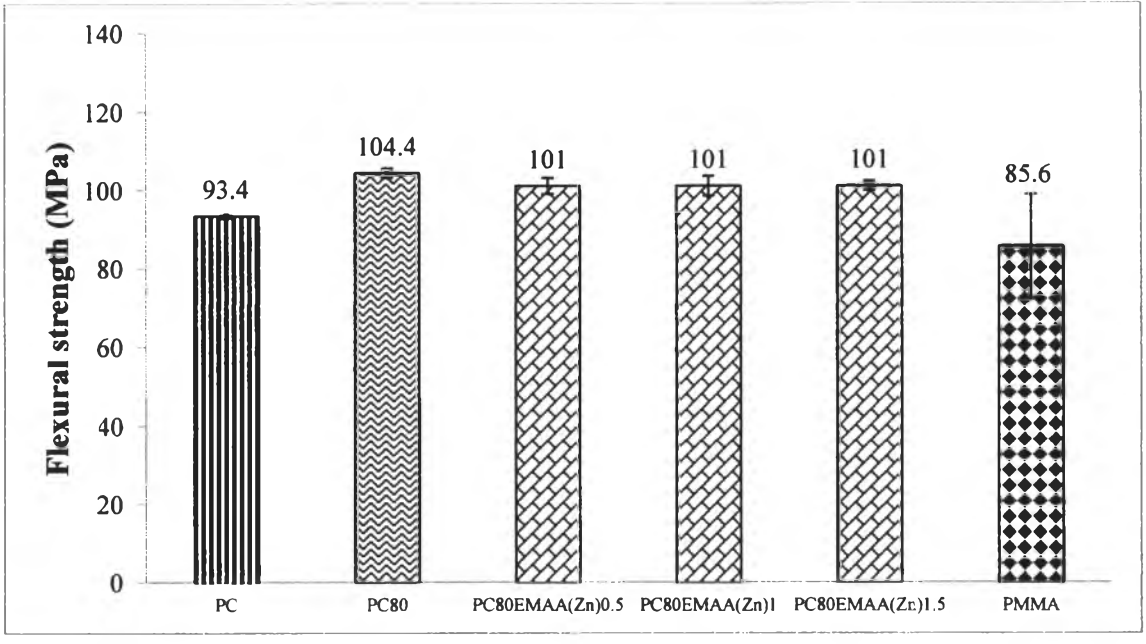

Figure 4.90 Flexural strength of PC, PMMA, and PC80/EMAA(Zn) alloys.

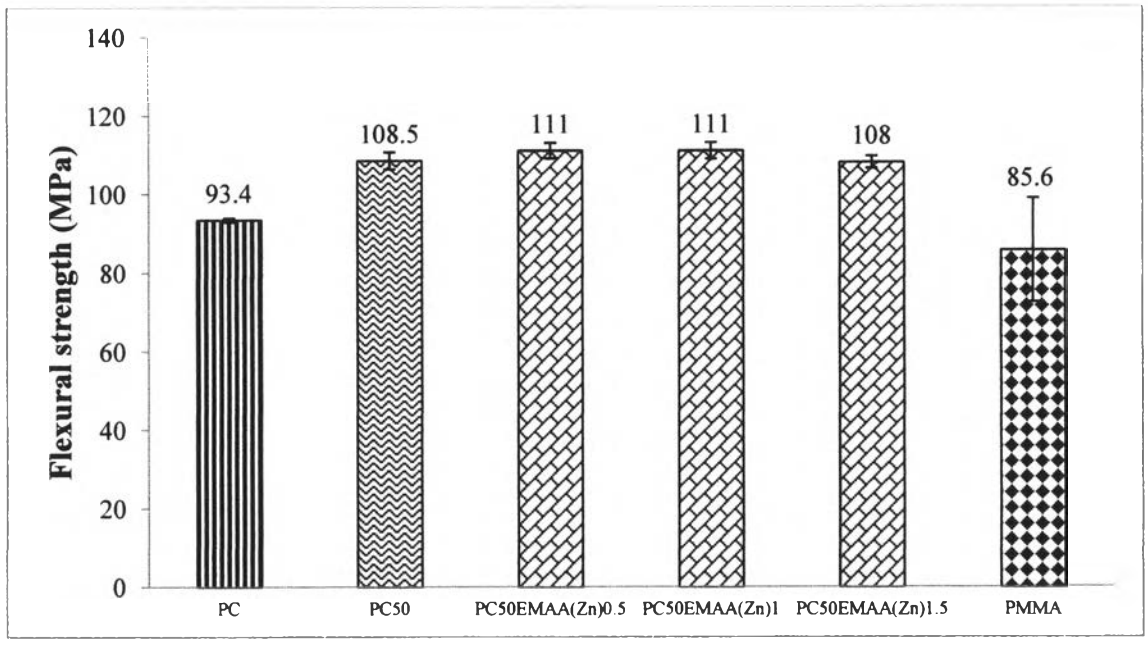

Figure 4.91 Flexural strength of PC, PMMA, and PC50/EMAA(Zn) alloys.

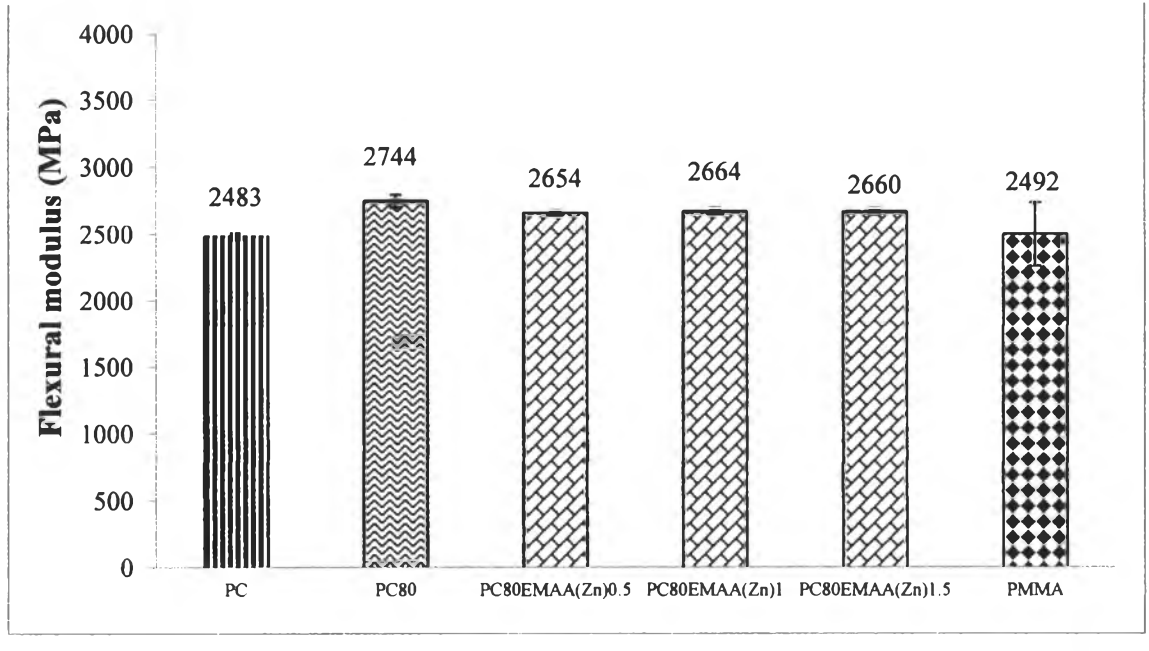

Figure 4.92 Flexural modulus of PC, PMMA, and PC80/EMAA(Zn) alloys.

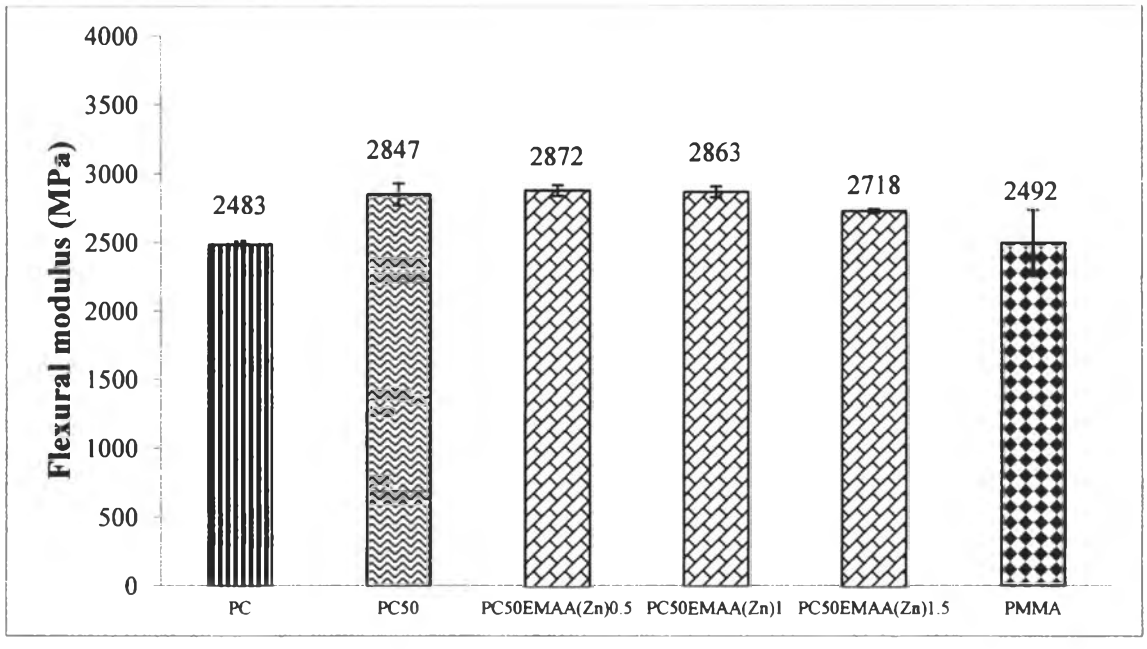

Figure 4.93 Flexural modulus of PC, PMMA, and PC50/EMAA(Zn) alloys.

4.5.4.3 Notched Izod Impact properties

Figure 4.94 and 4.95 present the impact strength of PC/PMMA alloy with EMAA(Zn). The addition of EMAA(Zn) into PC80/PMMA20 alloys demonstrated the fluctuation of impact strength due to the non-homogeneous dispersion of dispersed phased. However, the impact strength of PC50/EMAA(Zn) alloys was not significantly improve by adding EMAA(Zn). This might be due to the effect of the ionic domains of EMAA(Zn) which act as crosslinking sites that can restrict the movement of molecular chains. In addition, there are the interaction between the two base polymers and EMAA(Zn), which can also limit the movement of the molecular chains. So the energy dissipation of the system was restricted while the stress concentration was occurred which resulted in the drastically drop in impact strength.

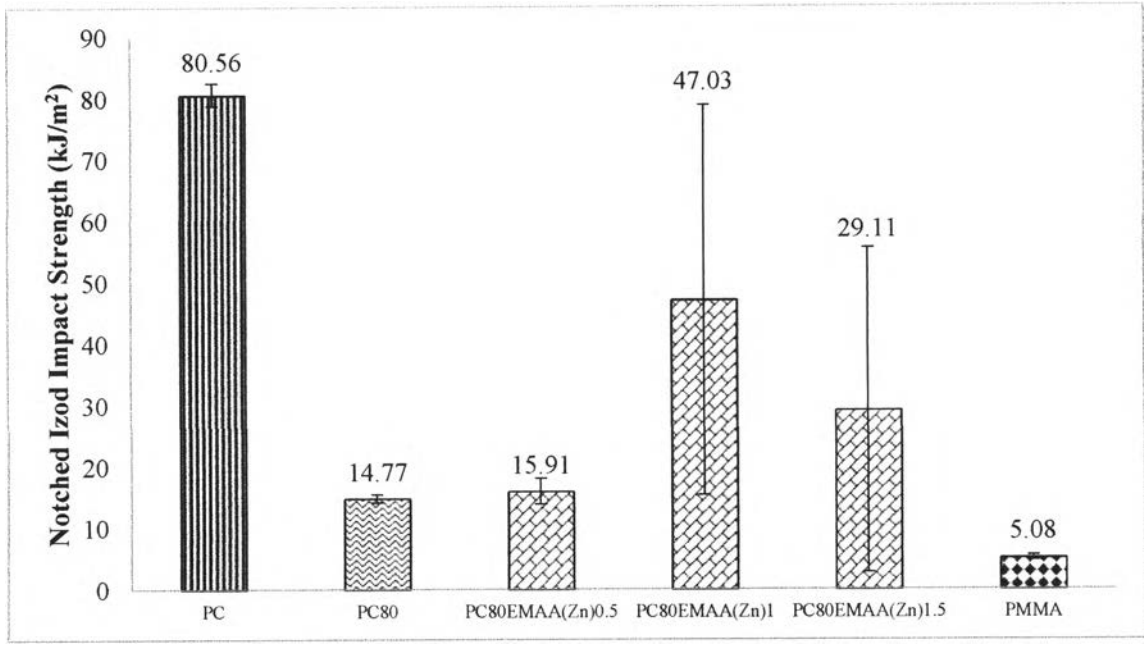

Figure 4.94 Notched izod impact strength of PC, PMMA and PC80/EMAA(Zn) alloys.

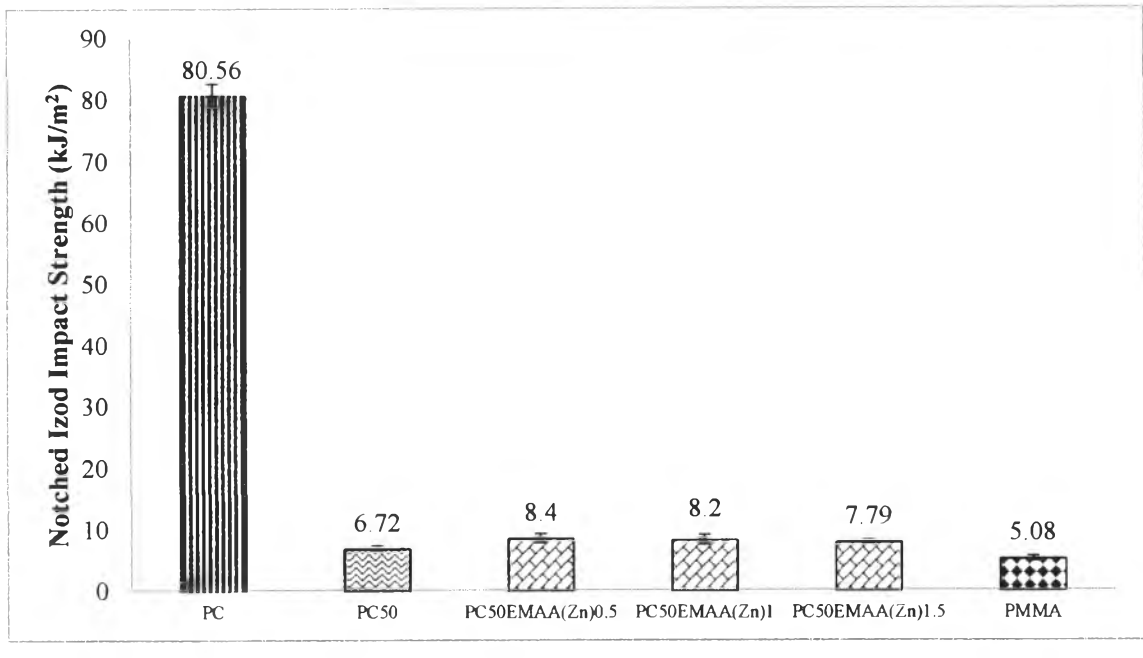

Figure 4.95 Notched izod impact strength of PC, PMMA and PC50/EMAA(Zn) alloys.

4.6 PC/PMMA Alloys with transesterification catalyst Samarium acetylacetonate hydrate (SMACA)

4.6.1 Physical properties

4.6.1.1 Rheological properties

MFI measurement can point to the rheological behavior of materials. The MFI of PC/PMMA alloys were shown in Figure 4.96 and 4.97. The inclination of the alloys containing SMACA increased when increased the amount of SMACA. It was because SMACA can activate the molecule of the polymer chain to move which made the flowability of alloys became easier. For PC80 containing SMACA 0.025 phr, its MFI was not been in line with the others. It was possible to be some errors occurred during the experimental process so this composition had to reproduce to make certain of the result.

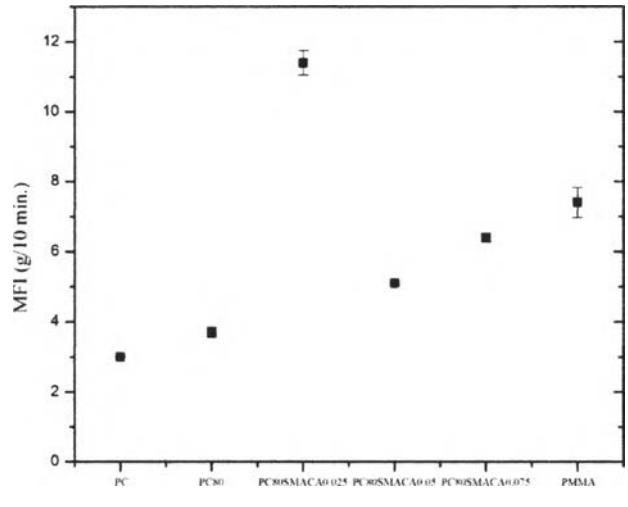

Figure 4.96 Melt Flow Index of PC, PMMA and PC80/SMACA alloys.

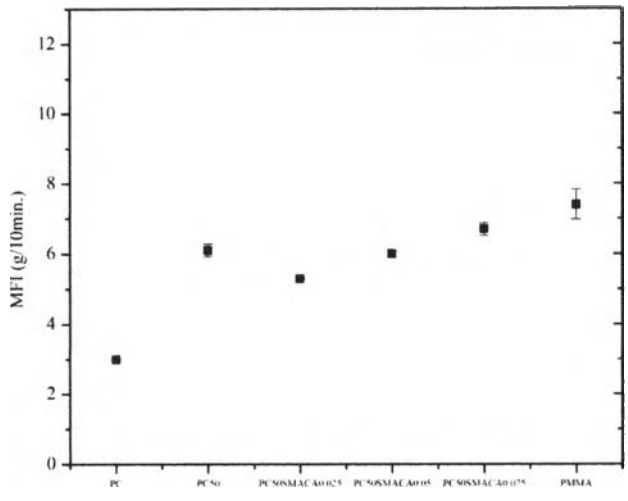

Figure 4.97 Melt Flow Index of PC, PMMA and PC50/SMACA alloys

4.6.2 Thermal properties

4.6.2.1 Temperature decomposition characterization

The onset decomposition temperature (Td) from TGA was used to evaluate the thermal stability of PC/PMMA alloys with SMACA as shown in Figure 4.98 and 4.99. There are the literatures reported that SMACA can be an efficient transesterification catalyst to promote copolymer of PC and PET for PC/PET blend resulting in the reduction of decomposition temperature of the blend. Because PMMA consist of ester group similarly to PET, PC/PMMA copolymer formation was expected to occur by using SMACA as a catalyst. However, the thermal stability of PC/PMMA alloys in the presence of SMACA did not be in line with the previous works. The decomposition of alloys with SMACA took place at slightly higher temperature than uncompatibilized PC/PMMA with two thermal degradation steps corresponding to PMMA and PC, respectively. There are no evidence has been found to explain or support the effect of SMACA on thermal degradation of PC/PMMA alloys contrasted with PC/PET alloys because it did not have the literature reported the effect of SMACA on the properties of PC/PMMA alloys before.

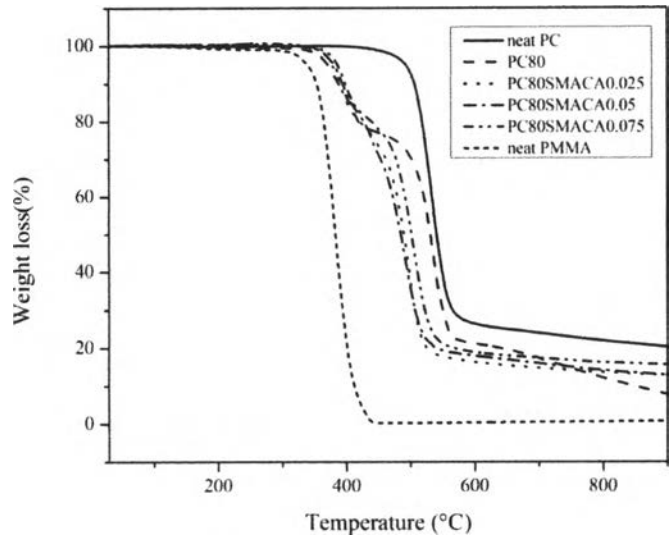

Figure 4.98 TGA plots of PC, PMMA and PC80/SMACA alloys.

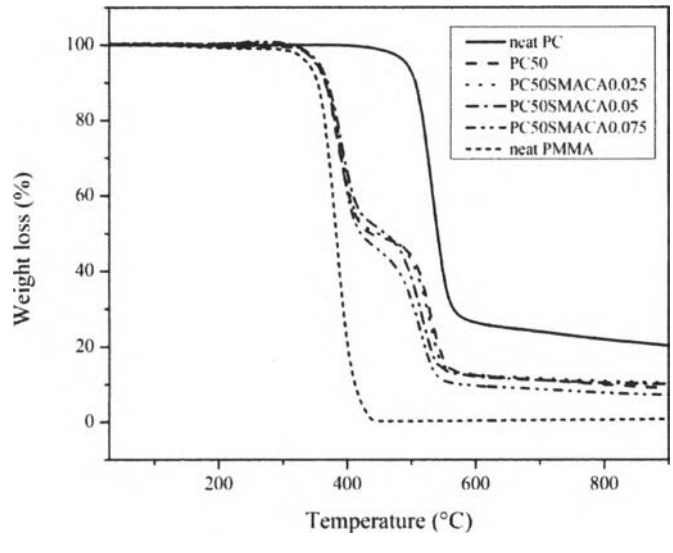

Figure 4.99 TGA plots of PC, PMMA and PC50/SMACA alloys.

4.3.3 Miscibility

4.3.3.1 Glass transition temperature observation

In this study, SMACA was selected to be a tranesterification catalyst for promoting PC-*g*-PMMA copolymer to be a compatibilizer for PC and PMMA components. In order to check the miscibility of alloys, DSC was used to observe the glass transition temperature (T_g) of alloys. Figure 4.100 and 4.101 exhibited the glass transition temperature of PC/PMMA alloys in the presence of SMACA. As mentioned earlier, the two distinct glass transition temperatures (2 T_gs) of PC/PMMA alloys without compatibilizer were obviously observed when PMMA content increased. According to DSC results, PC/PMMA alloys in the presence of SMACA showed the single T_g which was similar to uncompatibilized PC80. In addition, two distinct T_g of alloys still was noted with insignificant shifting inward although SMACA was added. From the T_g observation, it can be noted that the miscibility of PC/PMMA alloys did not improved by using SMACA as a transesterification catalyst.

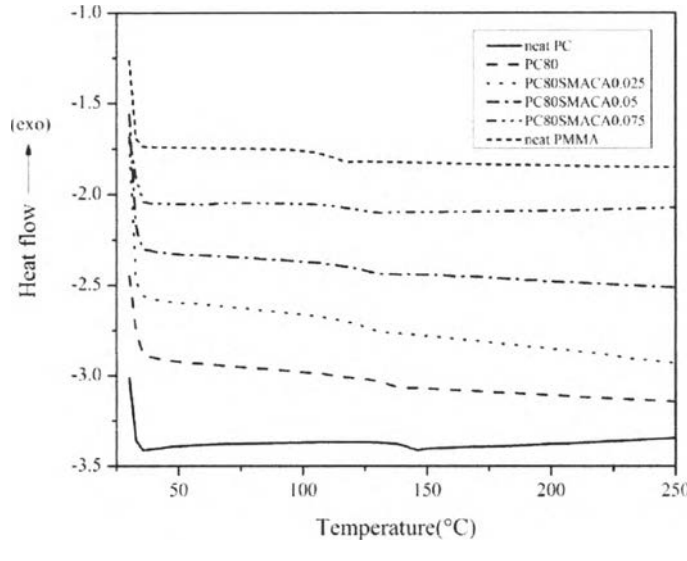

Figure 4.100 DSC plots (second heating) of PC, PMMA and PC80/SMACA alloys.

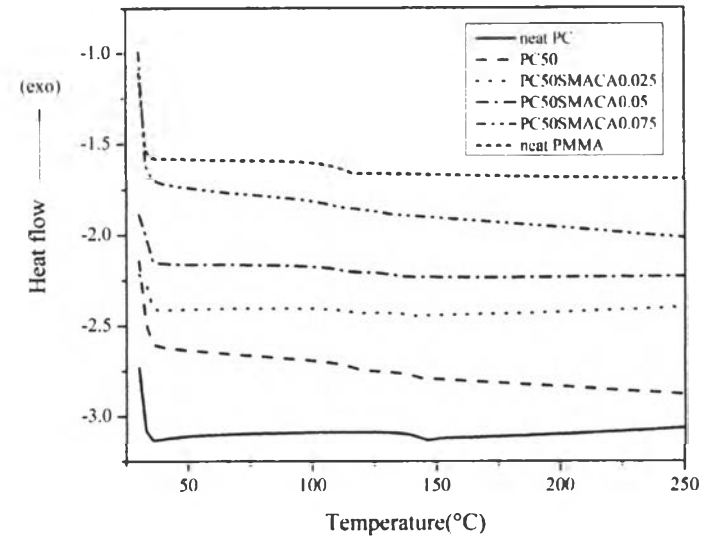

Figure 4.101 DSC plots (second heating) of PC, PMMA and PC50/SMACA alloys.

DMA is another technique used to observe the glass transition temperature (T_g) of polymer alloys. Figure 4.102-4.103 displayed the glass transition temperature of alloys with SMACA. Even though SMACA was inserted into PC/PMMA alloys to promote PC-*g*-PMMA copolymer for compatibilization, the glass transition temperature of alloy insignificantly shifted from the T_g of alloys in the absence of SMACA. Based on these results, the addition of SMACA did not enhance the miscibility of PC/PMMA alloys which related to the DSC results.

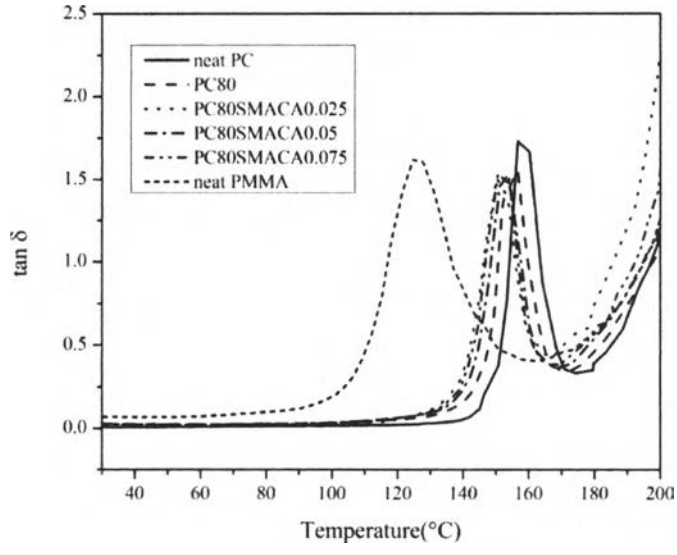

Figure 4.102 DMA plots of PC, PMMA and PC80/SMACA alloys.

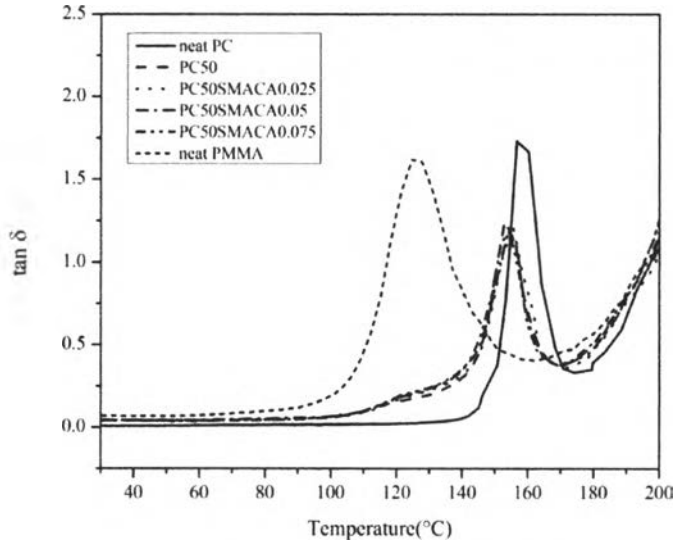

Figure 4.103 DMA plots of PC, PMMA and PC50/SMACA alloys.

4.6.4 Mechanical properties

4.6.4.1 Tensile properties

The addition of SMACA into PC/PMMA alloys did not significantly affect to the tensile properties as can be seen in Figure 4.104-4.109. The tensile strength at yield, elongation at yield and Young's modulus of alloys in the presence of SMACA seem to be identical as uncompatibilized system.

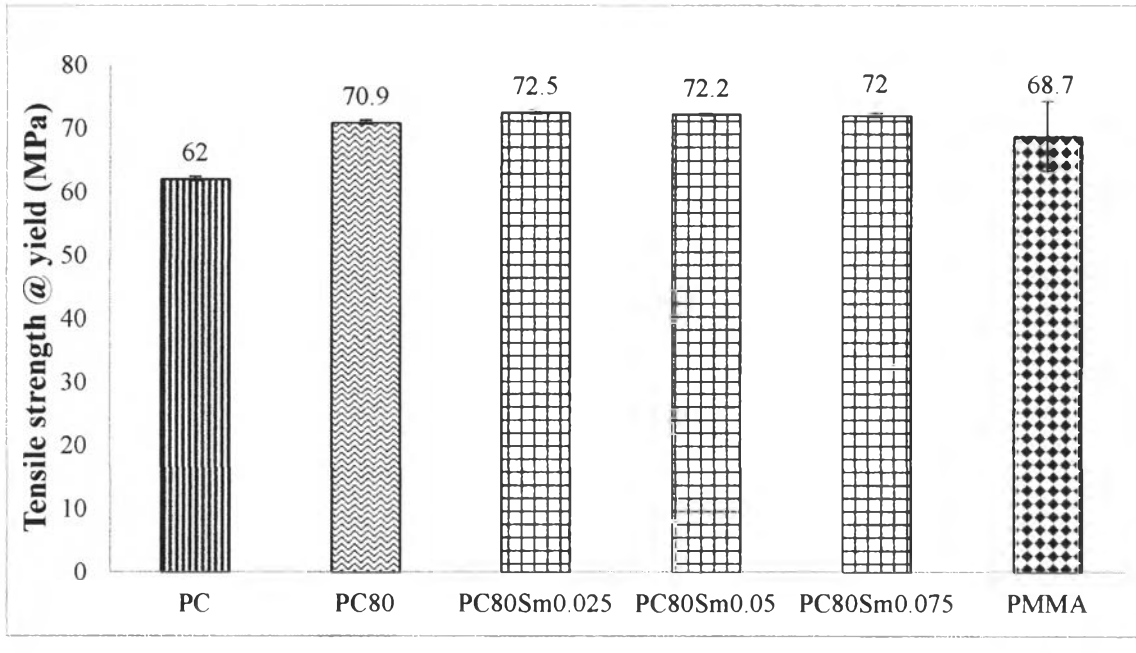

Figure 4.104 Tensile strength at yield of PC, PMMA, and PC80/SMACA alloys.

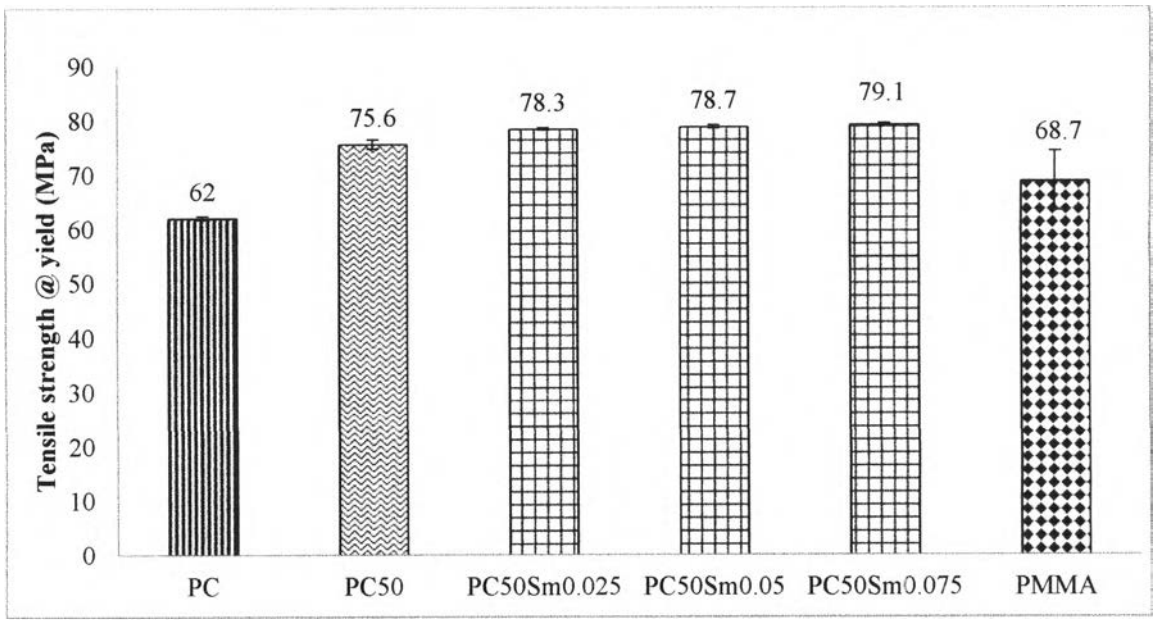

Figure 4.105 Tensile strength at yield of PC, PMMA, and PC50/SMACA alloys.

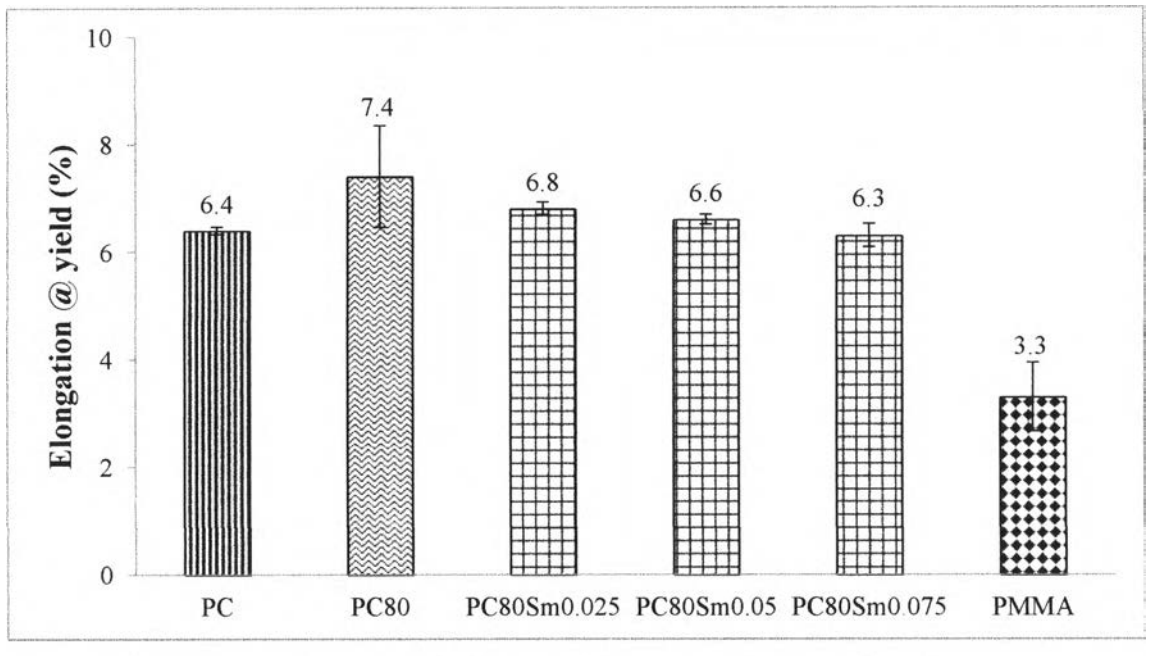

Figure 4.106 Elongation at yield of PC, PMMA, and PC80/SMACA alloys.

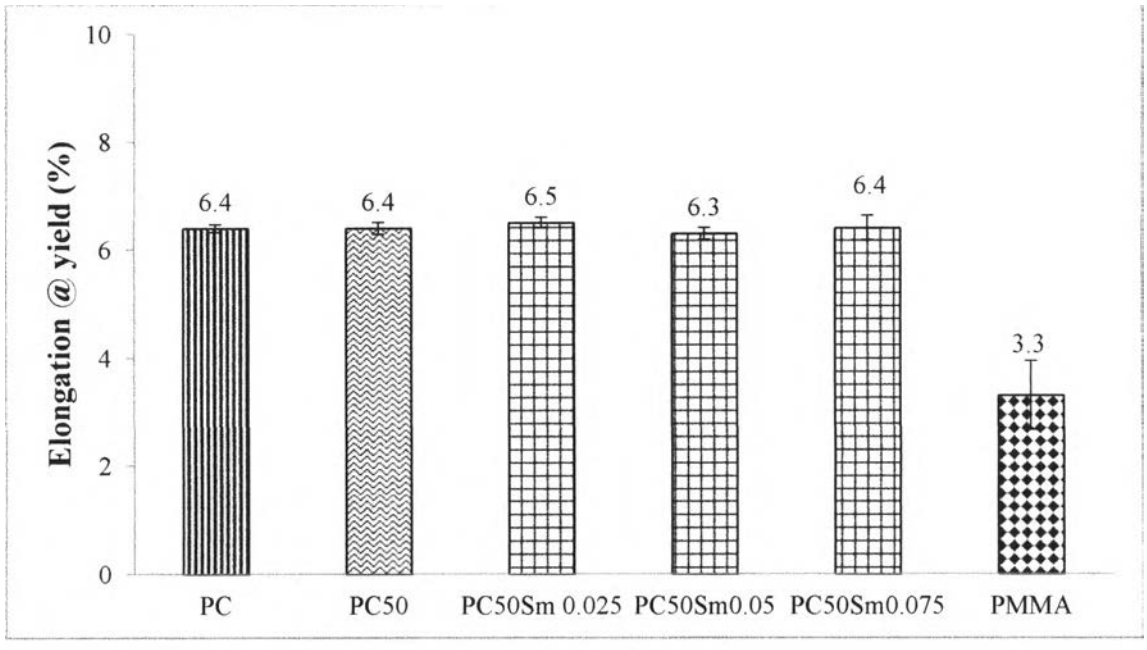

Figure 4.107 Elongation at yield of PC, PMMA, and PC50/SMACA alloys

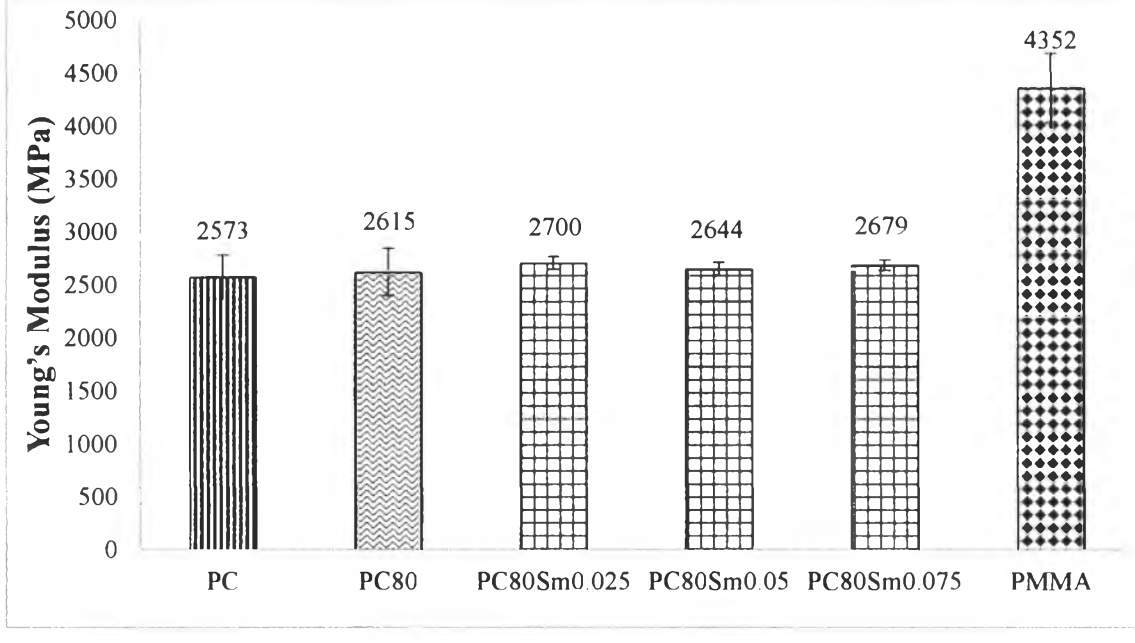

Figure 4.108 Young's modulus of PC, PMMA, and PC80/SMACA alloys.

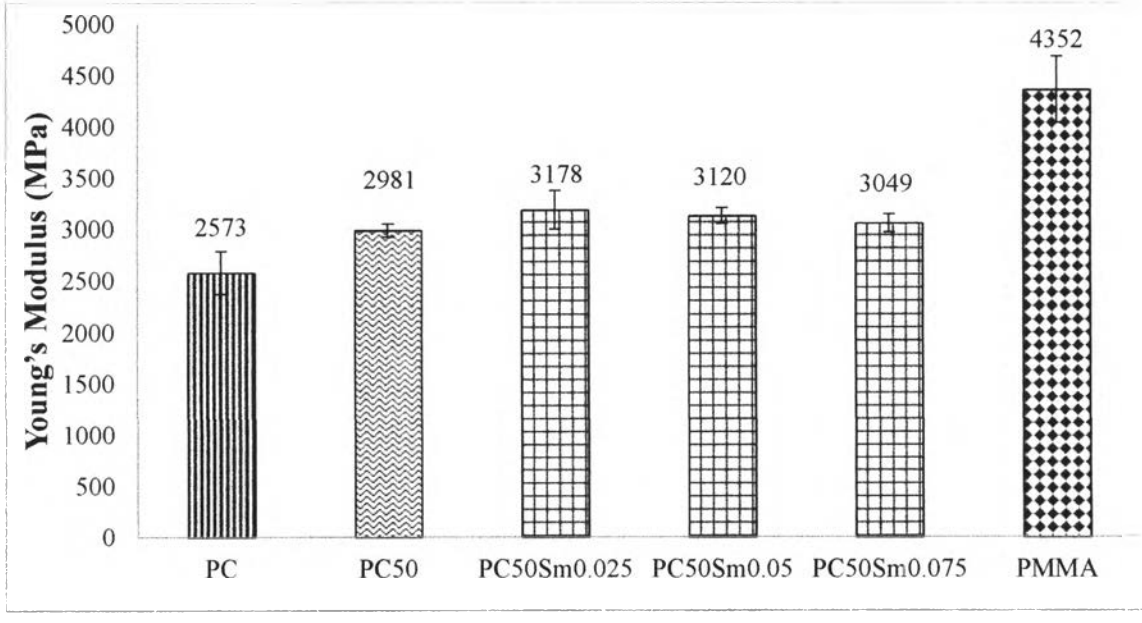

Figure 4.109 Young's modulus of PC, PMMA, and PC50/SMACA alloys.

4.6.3.3 Notched Izod Impact properties

Figure 4.110-4.111 exhibited the impact strength of PC/PMMA alloys in the presence of SMACA. The effect of SMACA on the impact strength of alloys was similar to the tensile properties. It showed insignificant improvement of impact strength.

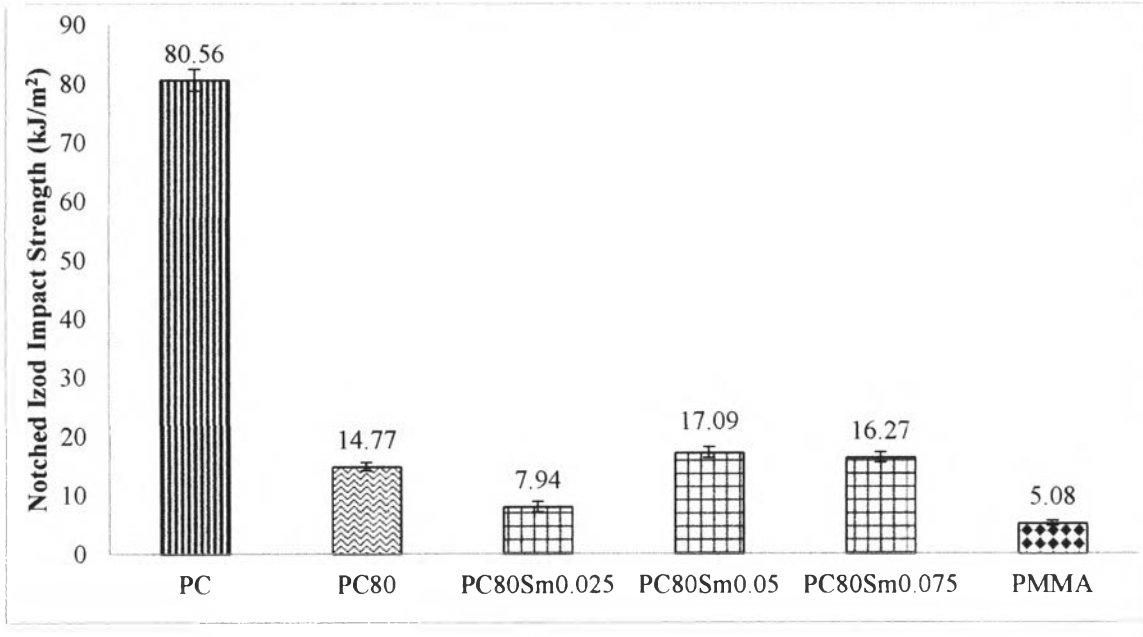

Figure 4.110 Notched izod impact strength of PC, PMMA and PC80/SMACA alloys.

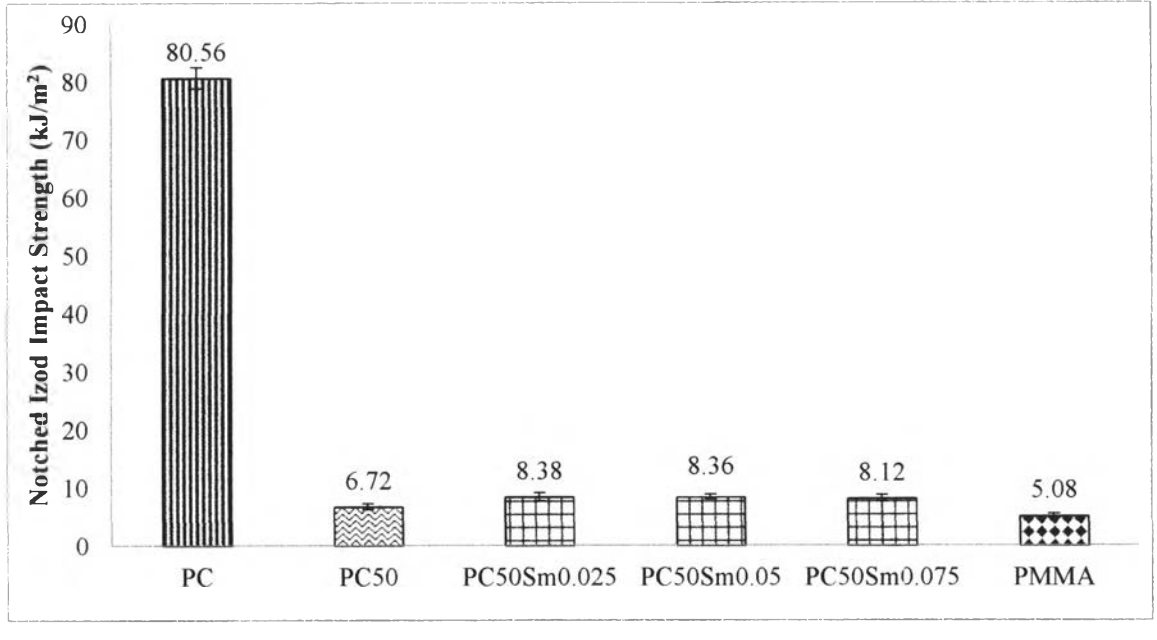

Figure 4.111 Notched izod impact strength of PC, PMMA and PC50/SMACA alloys.

4.6.5 Copolymer formation observation

In order to check the transesterification reaction between PC and PMMA, FTIR technique was used to evaluate the formation of PC-*g*-PMMA copolymer. Figure 4.112 display the FTIR spectra of PC, PMMA, PC80 and PC80/SMACA alloys. The spectrum of PC80 in the absence of SMACA showed two clear distinguishable carbonyl peaks at 1773 and 1733 cm-1 corresponding to the carbonyl group of PC and PMMA respectively(Singh, A. K. *et al.*, 2011). However, the FTIR spectra of PC80 in the presence of SMACA were similar to the spectrum of uncompatibilized PC80 with no shifting, overlapping and insignificant changing in the intensity of carbonyl peaks of PC and PMMA. According to FTIR result, the PC/PMMA graft copolymer was not occurred by using SMACA as a transesterification catalyst.

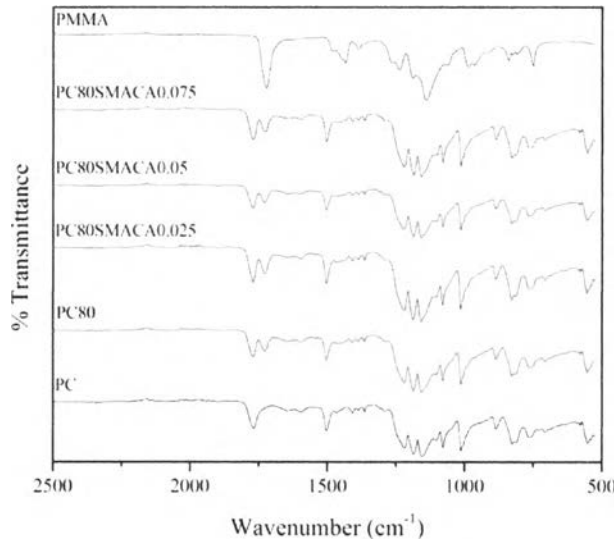

Figure 4.112 FTIR spectra of PC, PMMA and PC80/SMACA alloys.

4.7 PC/PMMA Alloys with transesterification catalyst Tin(II)chloride dihydtrate ($SnCl_2.2H_2O$)

4.7.1 Physical properties

4.7.1.1 Rheological properties

The rheology of alloys can be determined by MFI measurement. Figure 4.113 displays the melt flow indice (MFI) of PC/PMMA alloys in the presence of $SnCl_2.2H_2O$, the inclination of MFI of alloys abruptly increased when $SnCl_2.2H_2O$ was introduced. This was possible to be the ester-ester exchange reaction between PC and PMMA catalyzed by $SnCl_2.2H_2O$. Due to the transesterification reaction of PC and PMMA, the formation of PC/PMMA graft copolymer was occurred with reducing in molecular weight of alloys resulting in ease of flowability of alloys.

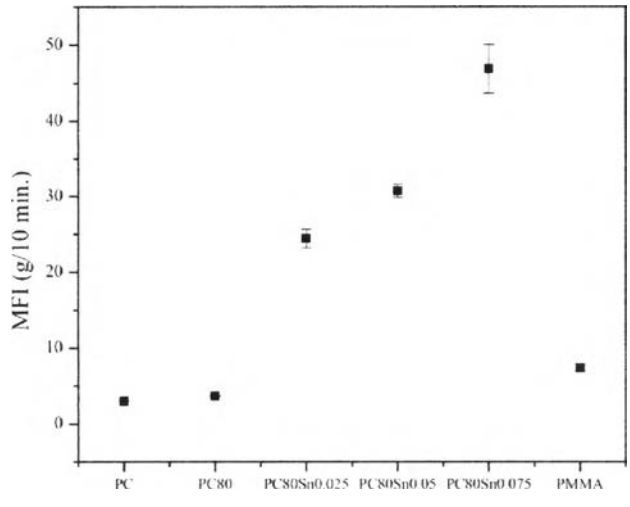

Figure 4.113 Melt Flow Index of PC, PMMA and PC80/ $SnCl_2.2H_2O$ alloys

4.7.2 Thermal properties

4.7.2.1 Temperature decomposition characterization

The thermal resistance was investigated by the onset decomposition temperature (T_d) from TGA. In general, catalyst was used to reduce the activation energy (E_a) which made the reaction occurred easily. There are many literature reported that the decomposition temperature of polymer blend in the presence of catalyst mostly shift to lower temperature caused by catalyst. However, this TGA results show the decomposition temperature of PC/PMMA alloys with $SnCl_2.2H_2O$ which is slightly higher than T_d of uncompatibilized system contrasted with the previous

works. In addition, The PC/PMMA alloys in the absence of EMAA exhibited two separate thermal degradation steps corresponding to PC and PMMA. However, the single step thermal degradation of these alloys containing $SnCl_2.2H_2O$ was observed. It was suggested that the $SnCl_2.2H_2O$ was an effective transesterification catalyst for promoting PC/PMMA graft copolymer. This copolymer can act as a compatibilizer for two components which could increase the homogeneity of the system resulting in the phases of PC and PMMA were likely compatible with each other.

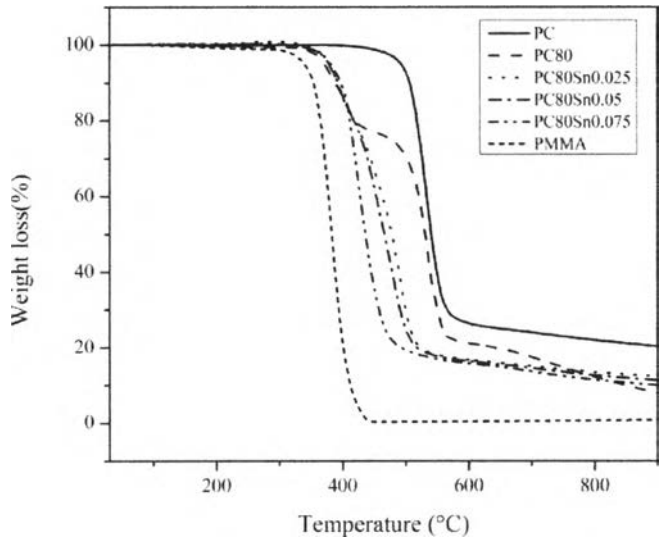

Figure 4.114 TGA plots of PC, PMMA and PC80/$SnCl_2.2H_2O$ alloys.

4.7.3 Miscibility

4.7.3.1 Glass transition temperature observation

In order to check the miscibility of alloys, DSC was used to observe the glass transition temperature of alloys. The glass transition temperature of PC/PMMA alloys in the presence of $SnCl_2.2H_2O$ was given in Figure 4.115 and 4.116. As a previous section, uncompatibilized PC80 and PC50 compositions showed the single T_g and two distinct T_g, respectively due to the immiscibility of these two components. After adding $SnCl_2.2H_2O$, the single T_g was observed at all compositions with shift to lower temperature. It was suggested that the miscibility of alloys was

improved by using $SnCl_2.2H_2O$ as a transesterification catalyst. $SnCl_2.2H_2O$ was an effective catalyst to induce the transesterification reaction between PC and PMMA. However, the chain scissions of PC could be occurred led to decreasing in molecular weight and shifting in T_g to lower temperature.

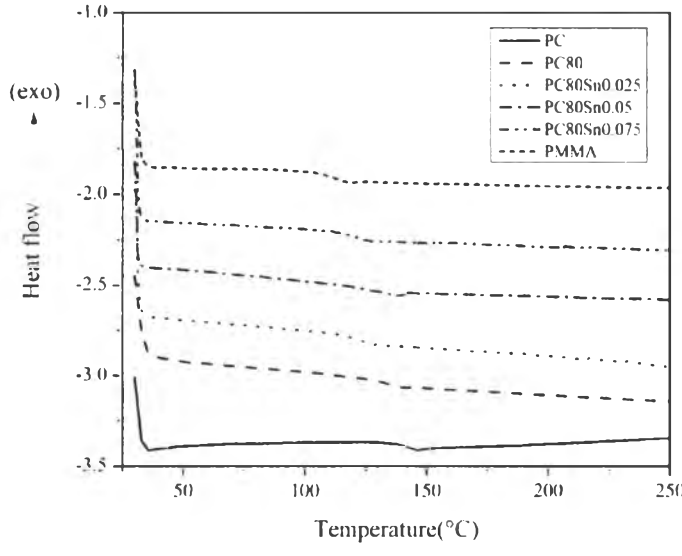

Figure 4.115 DSC plots (second heating) of PC, PMMA and PC80/$SnCl_2.2H_2O$ alloys.

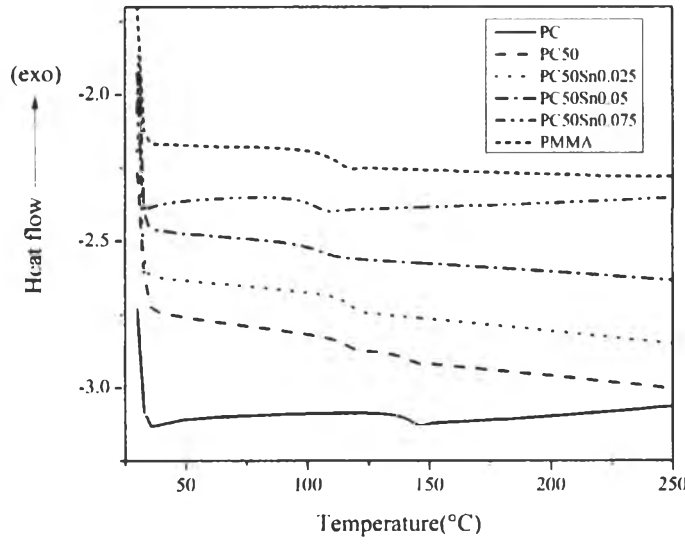

Figure 4.116 DSC plots (second heating) of PC, PMMA and PC50/$SnCl_2.2H_2O$ alloys.

4.7.4 Mechanical properties

4.7.4.1 Notched Izod Impact properties

The impact strength of PC/PMMA alloys in the presence of $SnCl_2.2H_2O$ was shown in Figure 4.117. A.K. Singh *et al.* suggested that the $SnCl_2.2H_2O$ was an effective transesterification catalyst in PC/PMMA blend for generating PC-*g*-PMMA copolymer. Even though the formation of PC/PMMA graft copolymer can improve the compatibility between PC and PMMA, the impact strength still severely dropped to lower than the impact strength of uncompatibilized PC80. In order to obtain the high impact strength material, it should have the right balance of toughness (long flexible chains) and stiffness (the obtained PC-*g*-PMMA copolymer) to absorb and dissipate energy, respectively. This PC/PMMA alloys in the presence of $SnCl_2.2H_2O$ lacked of the flexible parts to absorb energy. In addition, the chain scission reaction can occur led the molecular weight to decrease. Because of insufficient the flexible parts and the decrement of molecular weight resulting in drop in impact strength.

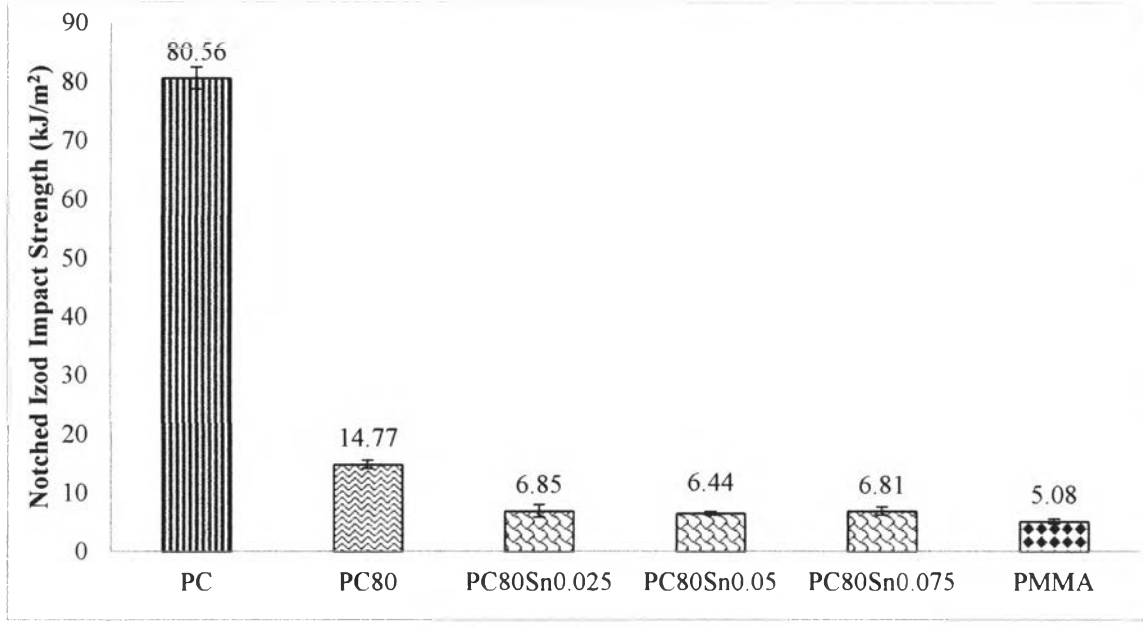

Figure 4.117 Notched izod impact strength of PC, PMMA and PC80/$SnCl_2.2H_2O$ alloys.

4.8 PC/PMMA Alloys compared with commercial grades

From overall results, PC80/PMMA20/EMA5 alloy and PC80/PMMA20/EMG1 alloy were selected to compared their properties with commercially available benchmarks including Wonderlite® PC-110 (Chi Mei Corporation), RTP 1800A TFE 15 (RTP Company), Infino PF-1035 (Samsung, a division of Cheil industries) and CYREX® 953 (Evonik CYRO LLC) because they presented the superior impact strength that can comparable to neat PC. Tables 4.2 reveal the comparison between the engineering properties of commercially available PC/PMMA alloys system and the selected PC/PMMA alloys. The PC80/PMMA20 in the presence of 5 phr of EMA and 1 phr of EMG provided the better mechanical properties than commercially available PC/PMMA product. In addition, the use of EMA and EMG proposed the significant improvement in impact strength of the alloys which also can be comparable to commercial PC and PC/PMMA.

Table 4.2 The properties of PC/PMMA alloys compared with commercial grades

Properties	PC	PC/PMMA (RTP 1800A TFE 15)	PC/PMMA (Infino PF-1035)	PC/PMMA (CYREX® 953)	PC80EMA5	PC80EMG1	PMMA	Unit
Melt Flow Rate (250°C/2.16 kg)	3	-	17 (250°C/ 10 kg)	1.9 (230°C/ 3.8 kg)	**3.7**	**3.3**	7	g/10 min.
Tensile Strength(yield)	61.7	44.8	61.0	54.2	**65.4**	**69.6**	63.2	MPa
Tensile Elongation(yield)	6.3	>10	-	4.2	**7**	**7**	2.7	%
Modulus	2366	2070	2100	2070	**2458**	**2454**	4027	MPa
Flexural Strength	92.9	82.7	80.0	86.2	**90.6**	**102.73**	72.4	MPa
Flexural Modulus	2459	2070	2100	2070	**2397**	**2664**	2255	MPa
Notched Izod Impact	78.7	36.3	60.8	137.3	**77.2**	**89.4**	4.7	kJ/m^2